# Induction of local DNA damage by focused visible light

## Applications in studies of DNA repair

Kamil Solarczyk

JAGIELLONIAN UNIVERSITY
IN KRAKÓW

Faculty of Biochemistry, Biophysics and Biotechnology
Department of Cell Biophysics

**Kamil Solarczyk**

# INDUCTION OF LOCAL DNA DAMAGE BY FOCUSED VISIBLE LIGHT APPLICATIONS IN STUDIES OF DNA REPAIR

PhD THESIS

Thesis Supervisor

**prof. dr hab. Jerzy Dobrucki**

Co-supervisor

**dr Mirosław Zarębski**

Kraków 2016

I would like to express my sincere gratitude to my Supervisor, **professor Jerzy Dobrucki**, for his continuous guidance, insightful comments and most of all, for fruitful discussions.

I wish to express my special thanks to **dr Mirosław Zarębski** for his support and advice during the research, which he offered from my very first days in the laboratory.

I would also like to thank all my Co-Workers at the Department of Cell Biophysics, especially **mgr Magdalena Kordon** and **mgr Oskar Szelest**.

My sincere and deepest thanks also goes to my **Parents, Joanna & Wiktor**, for EVERYTHING, but especially for trying to understand this passion and for giving me the opportunity to satisfy it.

Finally, I am immensely grateful to my **Wife, Ania** for her never ending support, patience during long, lonely evenings and particularly, for helping me to keep faith in the things that I do.

# Contents

# List of Figures

# List of Abbreviations

| | |
|---|---|
| 53BP1 | p53 binding protein 1 |
| 6-4PP | pyrimidine(6-4)pyrimidone photoproduct |
| 8-oxoG | 8-hydroxyguanine |
| $\gamma$H2AX | phosphorylated histone H2AX |
| A | adenine |
| AP | apurinic/apyrimidinic |
| APE1 | apurinic (AP) endonuclease |
| APTX | aprataxin |
| ATM | ataxia-telangiectasia mutated |
| ATR | ataxia-telangiectasia and Rad3-related |
| BaP | benzoapyrene |
| BER | Base Excision Repair |
| BLM | blood syndrome |
| BRCA1 | breast cancer 1 |
| BrdU | bromodeoxyuridine |
| C | cytosine |
| CAF1 | chromatin assembly factor 1 |
| CBS | Cockayne syndrome group B |
| CPD | cyclobutane pyrimidine dimer |
| CRISPR | Clustered Regularly Interspaced Short Palindromic Repeats |
| CSA | Cockayne syndrome group A |
| CtIP | CtBP-interacting protein |
| DDR | DNA Damage Response |
| DMS | dimethyl sulfonate |
| DNA | deoxyribonucleic acid |
| DNA2 | DNA replication helicase/nuclease 2 |
| DNA-PK | DNA-dependent protein kinase |
| DNMT1 | DNA (cytosine-5)-methyltransferase 1 |
| DPC | DNA-protein crosslink |
| DSB | double-strand break |
| dUTP | 2'-deoxyuridine 5'-triphosphate |
| EPR | enzymatic photoreactivation |
| ERCC1 | excision repair cross-complementation group 1 |
| EXO1 | exonuclease 1 |
| FapyGua | 2,6-diamino-5-formamidopyrimidine |
| FANC2 | Fanconi anemia group D2 protein |
| FEN1 | flap structure-specific endonuclease 1 |

| | |
|---|---|
| G | guanine |
| GFP | Green Fluorescent Protein |
| GG-NER | global genome NER |
| HMGN1 | high mobility group nucleosome-binding 1 |
| HP1 | heterochromatin protein 1 |
| HR | Homologous Recombination |
| IR | ionizing radiation |
| KAP-1 | KRAB-associated protein-1 |
| KR | Killer Red |
| LET | linear energy transfer |
| LigI | DNA ligase I |
| LigIII | DNA ligase III |
| LMDS | locally multiple damaged sites |
| LP-BER | long-patch BER |
| MDC1 | mediator of DNA damage checkpoint protein 1 |
| MGB | Minor Groove Binder |
| MMC | mitomycin C |
| MMR | Mismatch Repair |
| MMS | methyl methane sulfonate |
| MNNG | N-methyl-N'-nitro-N-nitrosoguanidine |
| MNU | N-methyl-N-nitrosourea |
| MRN | Mre11-Rad50-Nbs1 |
| Nbs1 | nibrin |
| NEIL2 | Nei-like DNA glycosylase 2 |
| NER | Nucleotide Excision Repair |
| NHEJ | Non-Homologous End Joining |
| N3-MeA | 3-methyladenine |
| N7-MeG | 7-methylguanine |
| O6-MeG | O6-methylguanine |
| OGG1 | 8-oxoguanine DNA glycosylase |
| PAH | polycyclic aromatic hydrocarbons |
| PAR | poly(ADP-ribose) |
| PARG | poly (ADP-ribose) glycohydrolase |
| PARP | poly (ADP-ribose) polymerase |
| PC4 | positive coactivator 4 |
| PCNA | proliferating cell nuclear antigen |
| PNK | polynucleotide kinase |
| PNKP | polynucleotide kinase 3'-phosphatase |
| Pol$\beta$ | DNA polymerase $\beta$ |
| RECQL | RecQ like helicase 5 |
| RFC | replication factor C |
| RFP | Red Fluorescent Protein |
| RNAPII | RNA polymerase II |
| ROS | reactive oxygen species |
| RPA | replication protein A |
| SAM | S-adenosylomethionine |
| SDSA | Synthesis-Dependent Strand Annealing |

| | |
|---|---|
| SMC1 | structrural maintenance of chromosomes 1 |
| SP-BER | short-patch BER |
| SSB | single-strand break |
| SSBR | Single-Strand Break Repair |
| ssDNA | single stranded DNA |
| T | thymine |
| TA | transcription activator |
| TDP1 | tyrosyl-DNA phosphodiesterase 1 |
| TdT | terminal deoxynucleotidyl transferase |
| TC-NER | transcription-coupled NER |
| tetR | tetracycline repressor |
| TFIIH | transcripction factor IIH |
| TFIIS | transcripction factor IIS |
| Topo | topoisomerase |
| TRF2 | Telomeric repeat binding factor 2 |
| TUNEL | TdT-mediated dUTP nick-end labeling |
| UDS | unscheduled DNA sythesis |
| UV | ultraviolet |
| UV-DDB | UV-damaged DNA-binding protein |
| WRN | Werner syndrome protein |
| XAB2 | XPA binding protein 2 |
| XPA | xeroderma pigmentosum complementation group A |
| XPE | xeroderma pigmentosum complementation group E |
| XPG | xeroderma pigmentosum complementation group G |
| XRCC1 | X-ray repair cross complementing protein 1 |

## Summary

The DNA is constantly modified and damaged due to the interaction with various endo- and exogenous factors. However, sophisticated repair processes assure that the majority of the induced lesions are rapidly eliminated. Unrepaired lesions halt basic cellular processes, such as DNA replication and might lead to chromosomal aberrations. The realization that DNA repair mechanisms are fundamental for genome integrity has led to a substantial boost in this field of research in recent years. The progress was mainly driven by the development of biochemical and biophysical methods, including several methods allowing for the induction of local DNA damage in nuclei of living cells and observation of the repair processes in situ, in fixed or living cells. This approach, based on advanced imaging techniques and fluorescent labelling, permits to study the behaviour of proteins engaged in the DNA repair processes and concomitant changes in the structure of chromatin. The most widely used group of methods takes advantage of the induction of local DNA damage by focused laser light and the observation of fusion proteins with fluorescent tags. Nevertheless, the existing methods possess several drawbacks, i.e. the induced damage is severe, sometimes lethal and consists of multiple types of DNA lesions. Moreover, these methods often require the presence of exogenous photosensitisers in cells.

The first goal of the studies described in this thesis was to develop a new method for local, controllable DNA damage induction, which would utilize visible light as the damaging agent. In PAPER 1 it was shown that visible laser light, typically employed in confocal microscopy, might be used for the induction of local, sublethal DNA damage in living HeLa cells in the absence of exogenous photosensitisers. Immunofluorescent detection of phosphorylated histone H2AX and several DNA repair factors engaged in different repair pathways has indicated that the induced damage consists of single and double-strand DNA breaks. The experiments have also shown that the number of induced lesions increases with the total dose of light delivered to the selected region of a nucleus. Cells locally damaged by blue laser light were able to divide, which indicates that the damage was sublethal and could be efficiently repaired.

The next step in the studies, described in PAPER 2, was to take advantage of the developed method and examine the behaviour of XRCC1, a protein engaged in the repair of single-strand DNA breaks. The conducted experiments have revealed that there are two stages of XRCC1 recruitment to the site of local DNA damage. Shortly after damage induction, the protein is homogenously distributed in the irradiated region. Within minutes after the insult, though, XRCC1 forms distinct foci containing multiple copies of this repair factor. The translocation from a cloud-like form to individual foci is usually completed within 5 minutes after damage induction. It was also observed that some foci are formed outside of the directly illuminated region. Moreover, some of these foci were shown to posses the ability to travel the distance of several micrometers within the nucleus. This behaviour, characteristic for nuclear bodies rather than sites of DNA repair, led us to a hypothesis that XRCC1 is not only recruited to DNA damage but also forms a type of stress bodies. Subsequent experiments confirmed this hypothesis. It was demonstrated that XRCC1 foci (bodies) are also formed after subjecting cells to a more general stress (heat shock) and that a subset of these foci

colocalises with Sp100, which is the major component of PML nuclear bodies. Furthermore, it was shown that Sp100 is recruited to sites of local DNA damage. This suggests an unknown role of Sp100 in DNA repair and constitutes a starting point for future studies.

In conclusion, this PhD thesis describes a new method of local DNA damage induction in living cells and proves that it can be successfully used in the studies of DNA repair processes. The major advantages of the proposed approach are its wide accessibility and a possibility to generate a sublethal, well-defined damage without introducing exogenous photosensitisers. In addition, the conducted experiments are among the first which point at a possibility of induction of DNA damage by visible light without the involvement of endogenous, cytosolic photosensitisers. The observations of the behaviour of XRCC1 after local damage induction, its involvement in the formation of stress bodies and the recruitment of Sp100 to sites of DNA damage not only confirm the usefulness of the new method, but also provide new insights into the mechanisms of DNA repair.

## Streszczenie

Poprzez oddziaływanie różnych, endo- oraz egzogennych czynników, nić DNA poddawana jest nieustannym modyfikacjom i uszkodzeniom. Dzięki wyrafinowanym procesom naprawczym, większość z powstających uszkodzeń jest szybko usuwana. Nienaprawione uszkodzenia blokują podstawowe procesy komórkowe, takie jak replikacja DNA, a część z nich może prowadzić do powstania aberracji chromosomowych. Mechanizmy naprawy DNA, ze względu na fundamentalne znaczenie dla zachowania integralności genomu, stały się zatem w ostatnich latach przedmiotem intensywnych badań. Postęp w badaniach naprawy DNA umożliwiony został m.in. poprzez rozwój biochemicznych oraz biofizycznych metod, w tym szeregu metod pozwalających na indukcję lokalnych uszkodzeń w jądrach żywych komórek oraz obserwację zjawisk naprawy in situ, w żywych komórkach. Takie podejście, wykorzystujące zaawansowane techniki obrazowania i znakowanie fluorescencyjne, pozwala na badanie zachowania białek uczestniczących w procesach naprawczych oraz na obserwację zmian struktury chromatyny, które tym procesom towarzyszą. Najpopularniejsza obecnie grupa metod opiera się na wykorzystaniu skupionego światła laserowego do indukcji lokalnego uszkodzenia DNA i obserwacji białek fuzyjnych z metką fluorescencyjną. Jednakże, istniejące techniki posiadają szereg wad. Powodują one jednoczesne wprowadzanie bardzo licznych, letalnych uszkodzeń DNA, zaliczających się do kilku typów (np. pęknięcia nici DNA i uszkodzenia oksydacyjne). W metodach tych konieczne jest użycie egzogennych fotouczulaczy.

Celem pierwszego etapu badań opisanych w niniejszej rozprawie było opracowanie nowej, wykorzystującej światło widzialne, techniki wprowadzania lokalnego uszkodzenia DNA. W pracy 1 pokazano, że światło laserowe z zakresu widzialnego, typowo wykorzystywane jako źródło światła w mikroskopii konfokalnej, może służyć do indukcji subletalnego, lokalnego uszkodzenia w żywych komórkach linii HeLa, bez udziału egzogennych fotouczulaczy. Poprzez detekcję immunofluorescencyjną ufosforylowanej formy histonu H2AX ($\gamma$H2AX) oraz szeregu czynników uczestniczących w różnych ścieżkach naprawy wykazano, że wprowadzone uszkodzenia to pojedyncze oraz podwójne pęknięcia nici DNA. Badania wykazały również, że liczba powstających uszkodzeń wzrasta wraz ze zwiększeniem całkowitej dawki światła dostarczonej do wybranego rejonu jądra komórkowego. Zaobserwowano, że indukowane uszkodzenie nie hamuje podziałów komórki, co świadczy o tym, że jest subletalne i może zostać skutecznie naprawione.

Kolejnym etapem badań, które opisane zostały w pracy 2, było wykorzystanie opracowanej metody wprowadzania lokalnego uszkodzenia DNA do badania zachowania białka XRCC1, uczestniczącego w naprawie pojedynczych pęknięć nici DNA. Przeprowadzone eksperymenty pokazały, że proces gromadzenia się białka XRCC1 w miejscu uszkodzenia przebiega dwuetapowo. W bardzo krótkim czasie po naświetlaniu wiązką laserową, zakumulowane białko jest rozłożone jednorodnie w obszarze poddanym działaniu światła. W ciągu kilku minut białko zmienia jednak swój rozkład przestrzenny, formując w miejscu naświetlanym wyraźne ogniska, zawierające bardzo wiele kopii obserwowanego czynnika naprawczego. Proces przechodzenia z formy jednorodnego rozkładu do ognisk zostaje zakończony około 5 minut po indukcji uszkodzenia. Zaobserwowano również powstawanie nielicznych ognisk poza miejscem bezpośrednio uszkodzonym. Co więcej, niektóre z tych ognisk wykazały zdolność do przemieszczania się

w jądrze komórkowym na odległość kilku mikrometrów. Takie zachowanie, charakterystyczne dla ciałek jądrowych, a nie dla miejsc naprawy DNA, pozwoliło wysunąć hipotezę, że białko XRCC1 gromadzi się nie tylko w miejscu uszkodzenia DNA, ale tworzy również rodzaj ciałek stresowych. Kolejne eksperymenty przemawiają na korzyść tej hipotezy. Wykazano, że ciałka XRCC1 tworzone są również w odpowiedzi na ogólny stres komórkowy (szok cieplny) oraz, że część ciałek XRCC1 kolokalizuje z białkiem Sp100, będącym głównym składnikiem ciałek jądrowych PML. Co więcej, zaobserwowano, że białko Sp100 również gromadzi się w miejscu lokalnego uszkodzenia DNA. Ten nieznany dotąd fakt może sugerować, że to białko także uczestniczy w naprawie DNA. Obserwacje te stanowią punkt wyjścia do dalszych badań.

Podsumowując, w przygotowywanej rozprawie doktorskiej opisano nową metodę generowania lokalnego uszkodzenia DNA w żywych komórkach oraz wykazano, że metoda ta może zostać z powodzeniem zastosowana w badaniach procesów naprawy DNA. Głównymi zaletami zaproponowanego podejścia są jego szeroka dostępność oraz możliwość indukcji subletalnego, dobrze zdefiniowanego uszkodzenia DNA bez wprowadzania egzogennych fotouczulaczy. Ponadto, przeprowadzone badania są jednymi z pierwszych, które wskazują na możliwość generowania uszkodzeń DNA poprzez światło widzialne o stosunkowo niewielkiej mocy, bez udziału endogennych, pozajądrowych fotouczulaczy. Zaobserwowane, nieopisane dotąd w literaturze zachowanie białka XRCC1 w odpowiedzi na lokalne uszkodzenie DNA, jego potencjalny udział w tworzeniu ciałek stresowych oraz gromadzenie białka Sp100 w miejscu uszkodzonym nie tylko potwierdzają przydatność zaproponowanej metody, ale również stanowią istotny wkład w poznanie mechanizmów naprawy DNA.

# Preface

DNA repair is a fascinating area of research. It is difficult not to be amazed by the idea that in a submicron scale, in the complex environment of the cell's nucleus, repair enzymes acting in an orchestrated fashion are able to detect and repair tiny modifications to DNA. If the repair fails, the consequences can be disastrous for a single cell or even for the whole organism. Although the fundamental steps of various DNA repair mechanisms were elucidated years ago, it was the advent of modern microscopic techniques coupled with the development of methods of localised DNA damage induction, that redefined the perception of these processes. The classic view of DNA repair as a sequence of enzymatic steps carried out by single proteins clashed with observations made in living cells. The massive and extremely rapid but also organised accumulation of repair factors at sites of DNA damage, accompanied and driven by histone modificiations and complex rearrangements of chromatin, have revealed the dynamic character of the repair processes. However, it was soon realized that the extent of damage generated by techniques of local DNA damage induction, although facilitating the detection of ongoing repair processes, raises concerns about its biological relevance and does not allow to disentangle different repair pathways. Today, 17 years after the most known histone modification, phosphorylation of histone H2AX, was demonstrated to occur at sites of laser microirradiation, researchers still seek selective and well characterised methods of inducing localised DNA lesions in the nuclei of living cells.

---

The aim of this doctoral thesis was to develop a new method of local DNA damage induction, based on the potential ability of focused visible light to generate DNA lesions in the absence of exogenous photosensitisers, and then to apply this new method in studies of the DNA repair processes.

---

In order to put the conducted research into context, I begin this thesis with a description of the basic facts regarding the possible types of DNA damage, physical and chemical agents leading to their formation and the repair processes which allow cells to eliminate DNA lesions (Chapters 1, 2, and 3). In the opening chapters, particular emphasis is placed on the possibility of induction of DNA damage by visible light, the methods of local DNA damage induction utilized in the studies of DNA repair and on the insights gained from these studies concerning the repair of single-strand DNA breaks. Discussion regarding these issues is further extended in Chapter 4.

# Theoretical Background

# Chapter 1

# TYPES OF DNA DAMAGE

It is now accepted that the DNA located within a cell's nucleus, a molecule once thought to be exceptionally stable, is constantly modified. Thousands of damage events occur in every cell per day, caused by the products of cellular metabolism or by environmental agents. However, despite the variety of mechanisms leading to DNA damage, DNA lesions can be classified into several major types.

## 1.1 Oxidative base modifications

Oxidation of DNA bases can be caused by the products of normal cellular metabolism [1] or by various exogenous physical or chemical agents, such as ionizing or ultraviolet radiation and many drugs [2]. Among all generated **reactive oxygen species (ROS)** the hydroxyl radical (*OH) is the most reactive and thus considered the most harmful. Hydroxyl radical reacts with DNA by addition to double bonds of DNA bases or by hydrogen abstraction from deoxyribose units and the methyl group of thymine [3].

The most common purine radicals formed by these mechanisms are C4-OH-, C5-OH- and C8-OH-adduct radicals of guanine and C4-OH- or C8-OH-adduct radicals of adenine [4,5]. Those radicals may be reduced or oxidized, depending on the redox environment and the redox properties of the radicals themselves [6]. One electron oxidation of C8-OH-adduct radicals of guanine and adenine leads to 8-hydroxypurines. Due to the low oxidation potential of guanine, **8-hydroxyguanine** (or its tautomer 7,8-dihydro-8-oxoguanine; **8-oxoG**), is the most frequent DNA base modification [7]. Apart from the hydroxyl radical mediated reaction, 8-oxoG was also shown to be formed by singlet oxygen [8], while 8-oxoA was detected after treating cells with $H_2O_2$ [9]. Both 8-oxoG and 8-oxoA are mutagenic and give rise to GC $\rightarrow$ TA [10] or AT $\rightarrow$ GC [11] transitions, respectively. The oxidation of C8-OH-adduct radicals competes with unimolecular opening of the imidazole ring, which can then be reduced to 2,6- or 4,6-diamino-5-formamidopyrimidine (FapyGua or FapyAde, respectively). FapyGua can lead to GC $\rightarrow$ CG transversions [12]. Alternatively, formamidopyrimidines may be formed from 7-hydro-8-hydroxypurines after one-electron reduction of C8-OH without ring opening.

Reaction of pyrimidines with (*OH) results in C5-OH and C6-OH-adduct radicals of cytosine and thymine, while abstraction of a hydrogen atom from the methyl group of thymine gives rise to an allyl radical [13]. Multiple products are formed from thymine

radicals under aerobic and anaerobic conditions, but two of them, thymidine glicol and 5-hydroxymethyluracil are produced in both environments [14, 15]. Addition of hydroxyl radicals to the double bond in cytosine results in unstable adduct radicals, which are prone to deamination and dehydratation [7]. For example, cytidine glycol, produced from the C5-OH-adduct radical of cytosine can give rise to 5-hydroxyuracyl or 5-hydroxycytosine - both these products have been detected in cells exposed to ionizing radiation [16,17]. In the absence of oxygen, the sequence of reduction, protonation and deamination of C5-OH adduct radical results in formation of 5-hydroxy-6-hydrouracil.

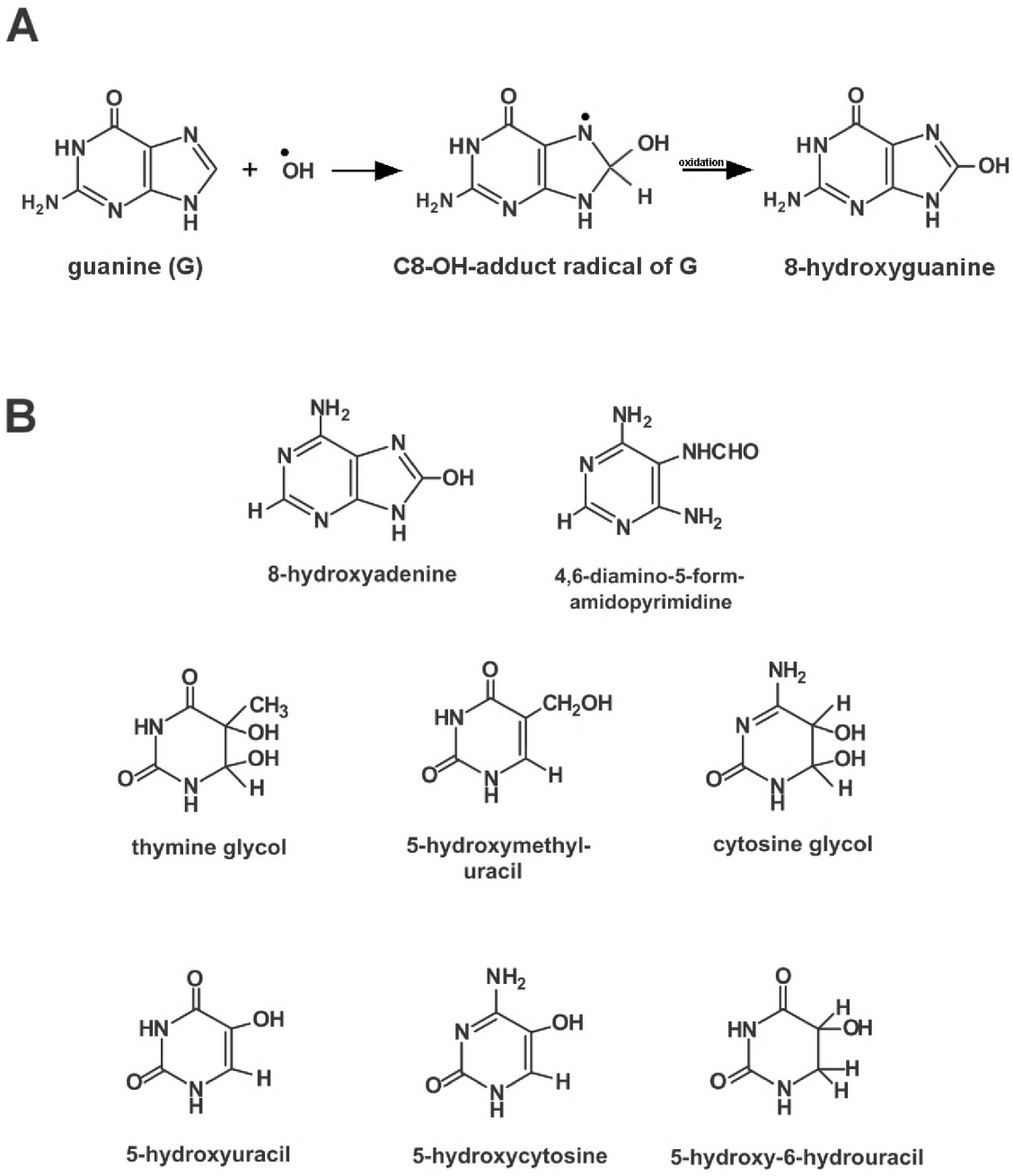


Figure 1.1: **Oxidation of DNA bases.** **A** – Formation of 8-oxoG through one electron oxidation of the C8-OH-adduct radical. **B** – The structures of some other oxidative modifications of the DNA bases.

## 1.2 Other DNA adducts

Apart from oxidative DNA modifications, multiple other DNA adducts are formed due to the action of endogenous and exogenous agents. The smallest covalent modification of DNA is *methylation*. Each ring nitrogen and exocyclic oxygen of the DNA bases are potential nucleophiles, but their reactivity is different depending on their position and whether DNA is single or double-stranded. **7-methylguanine (N7-MeG)** is the most frequent among the products of DNA methylation, which is caused by the fact the N7 position of guanine possesses the highest negative electrostatic potential |18|. This modification is relatively harmless, yet the destabilization of the glycosyl bond caused by the substitution on guanine may lead to **apurinic/apyrimidinic (AP) sites** and the ring opened methyl-formamidopyrimidine adduct of N7-MeG can block DNA polymerases in vitro |19, 20|. Other common products of DNA methylation: 3-methyladenine (N3-MeA) and O6-methylguanine (O6-MeG) |21| can block replication and transcription |22| or lead to mutations |23|. Numerous exogenous agents, such as MMS, DMS and MNU are capable of methylating DNA, while the most important intracellular donor of the methyl group is S-adenosylomethionine (SAM) |24|.

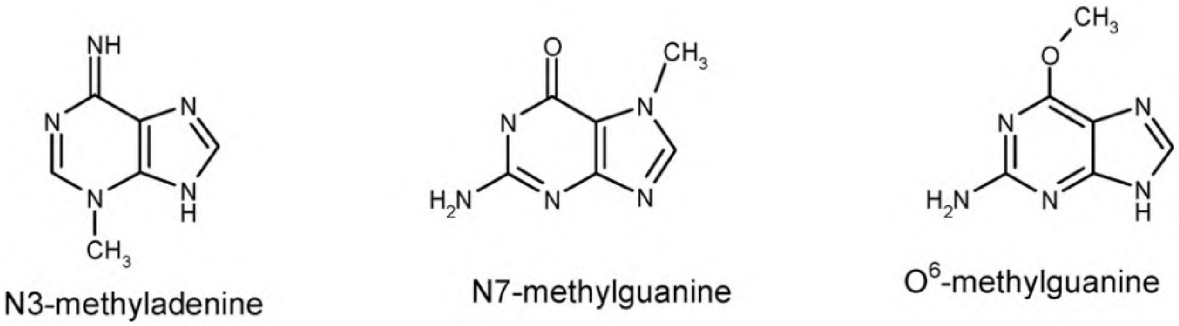


Figure 1.2: **Most common products of guanine and adenine methylation.**

Exocyclic DNA adducts constitute another group of mutagenic DNA lesions. These modifications are formed by compounds that attack at one side of the base moiety followed by ring closure at the other site. Many endogenous compounds, mostly aldehydes which are the products of lipid peroxidation (crotonaldehyde, acrolein, 4-hydroxynonetal (HNE), malondialdehyde) |25| as well as a broad range of chemicals may give rise to **exocyclic DNA adducts**. The reaction of DNA with acrolein, crotonaldehyde and HNE yields propano adducts, but the most studied are etheno adducts, formed by epoxyaldehydes |26|. Etheno adducts were shown to be highly mutagenic as well as capable of halting replication and generating deletions |27, 28|. Importantly, these adducts are now widely recognized as oxidative stress markers |29|.

## 1.3 Apurinic/apyrimidinic sites

The most frequent spontaneous modifications of DNA are *deamination* and *depurination*. AP sites occur by a non-enzymatic hydrolysis of base-sugar bonds, but can also be generated during **Base Excision Repair (BER)** pathway. The total number of AP sites created per cell per day is estimated at 10000 |30|. Guanine and adenine

are released from DNA at similar rates, much higher than the rate of release of pyrimidines [30]. On the other hand, it is the *transition of cytosine to uracil*, which occurs 100-500 times per day per human cell, that is the most frequent among hydrolytic deaminations of DNA bases [31]. The rate of transition from cytosine to uracil is greatly increased in single-stranded regions of DNA, thus it takes place usually during DNA replication or transcription [30]. If unrepaired, the appearance of uracil in DNA leads to CG $\rightarrow$ TA transition during replication [32]. Apart from cytosine, also purines are subject to hydrolytic deamination, although at a much lower rate. It is estimated that the transition of adenine to hypoxanthine occurs at 2–3% of the rate of cytosine to uracil transition [33], while the rate of guanine to xanthine transition is similar or even lower [30]. Still, since hypoxanthine forms a more stable base pair with C than with T, it is a mutagenic lesion.

## 1.4 Photoproducts

Photoproducts are the type of DNA lesions that cannot be formed spontaneously, but require an exogenous agent – **ultraviolet (UV)** radiation. Irradiation of DNA with UV results in a plethora of lesions, but those that are formed directly and most frequently are **cyclobutane pyrimidine dimers (CPDs)**, **pyrimidine(6-4)pyrimidone photoproducts (6-4PPs)** and their Dewar isomers [34]. CPDs and 6-4PPs arise as a result of absorption of UV by a double bond in pyrimidine bases and a subsequent opening of this bond, which makes it prone to react with neighbouring molecules. The estimates are that 50-100 reactions of this type occur in every cell in the skin during every second of sunlight exposure [35]. Both photoproducts require for their formation an extensive rotation of neighbouring pyrimidines from their normal positions which results in the distortion of the DNA double helix [34]. CPDs are usually formed in those sequences which are easily bent and unwound [34] – away from the surfaces of histones [36] and usually not in the minor groove [34]. This preference results in the observed 2.3 base average periodicity of CPDs formation [34, 36]. These lesions are also formed in a sequence specific manner, most commonly at 5'-TT sites and within runs of adjacent pyrimidines [34]. No periodicity is observed for 6-4PPs, yet they are 6 times more abundant in linker than in nucleosomal DNA [34]. 5'-TC and 5'-CC are the sequences in which 6-4PPs are usually found. The ratio of CPDs to 6-4PPs is estimated at 3:1 but is strongly dependent on the DNA sequence and on the chromatin environment [34, 36].

The presence of UV-induced photoproducts not only leads to deformation of the double helix, but also to mutations. The most frequently encountered are C to T or CC to TT double transitions [34], which usually occur at pyrimidine runs. CPDs and 6-4PPs are considered to be almost equally mutagenic, but due to the fact that the latter are more efficiently repaired, CPDs are thought to be more harmful [34].

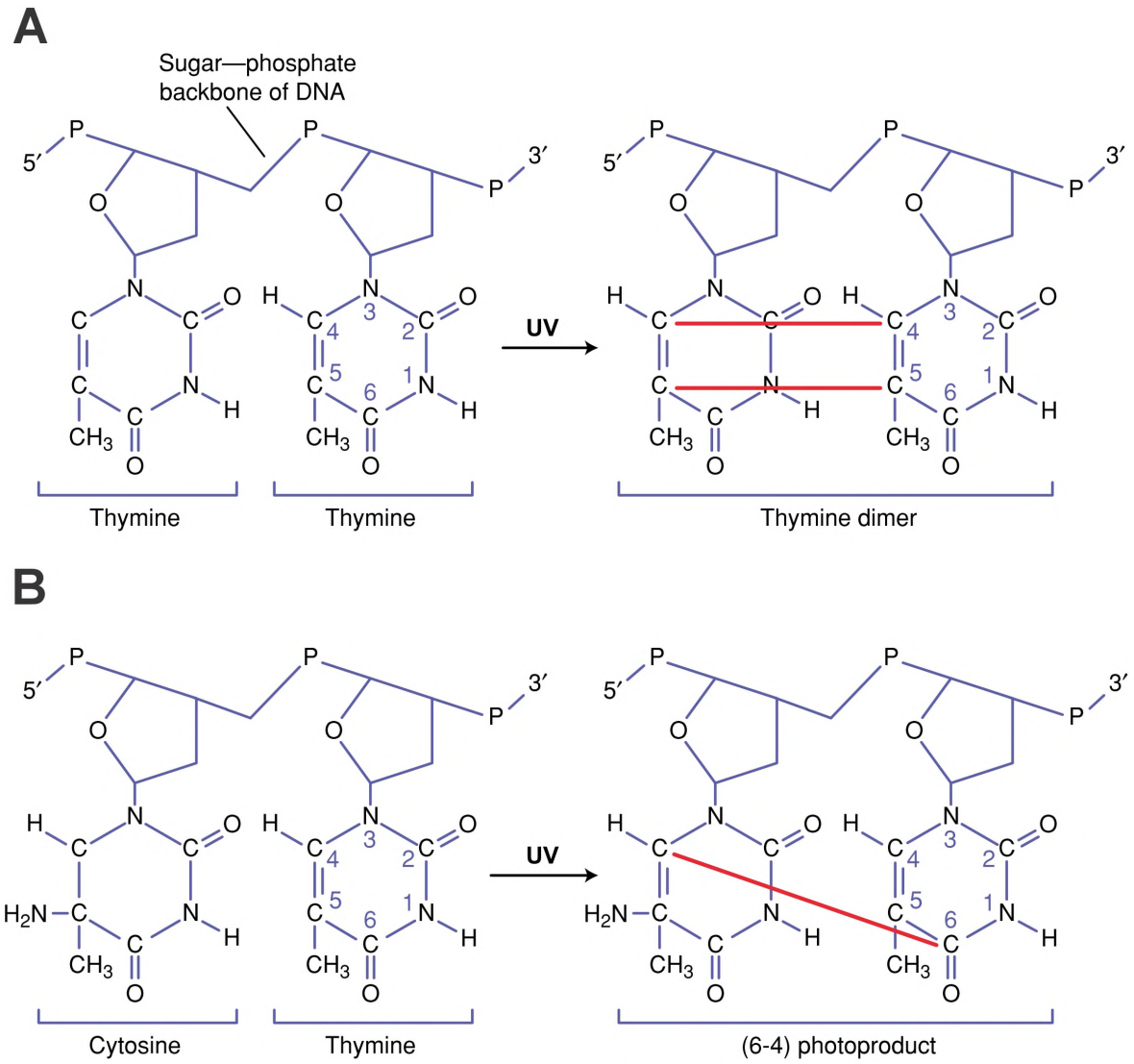


Figure 1.3: **Structure of major photoproducts generated in DNA by UV-radiation.** Upon UV radiation two neighbouring pyrimidines might be converted into two types of mutagenic photoproducts. **A** – Formation of a thymine dimer from two adjacent thymines. **B** – Formation of a 6-4 pyrimidine-pyrimidone photoproduct from adjacent cytosine and thymine. Figure from [37] (modified).

Other photoproducts that arise as a result of interaction of DNA with UV radiation are pyrimidine monoadducts and purine photoproducts. These lesions are formed with a much lower frequency than CPDs and 6-4PPs - the ratio of pyrimidine monoadducts to CPDs is estimated at 1:100. Nevertheless, the mutagenic effect of these lesions cannot be ruled out [34].

## 1.5 Strand breaks

Among all types of DNA lesions, DNA strand breaks are considered the most deleterious. If unrepaired, breakage in the phosphate backbone of the DNA strand, especially when occurs in both strands simultaneously, may directly lead to chromosomal

rearrangements and eventually, to cancer. Both **single- (SSBs)** and **double-strand breaks (DSBs)** can be produced endogenously or by exogenous agents. The number of spontaneously formed single-strand breaks is estimated at 10-50 breaks per cell per minute [38], which corresponds to at least 3000 SSBs produced during S-phase of the cell cycle [39]. A single-strand break can occur as a result of the interaction of DNA with reactive oxygen species, due to thermal fluctuations and hydrolysis or by the action of topoisomerases. Some SSBs are also formed indirectly from AP sites or oxidized bases (mostly 8-oxoG). It is thought that most of the spontaneously formed DSBs are produced during DNA replication because of a collapse or stalling of replication forks on SSBs or base damage (together called single-strand lesions, SSLs). Only 1% of all SSLs are estimated to give rise to DSBs, but this suffices to produce 10-50 endogenous double-strand breaks per S-phase in a mammalian cell.

The most common exogenous sources of DNA strand breaks are **ionizing radiation (IR)** and certain chemicals. IR can produce DNA strand breaks directly, when a photon or a high-energy particle collides with a DNA strand breaking the phosphodiester bond, or indirectly - through the action of hydroxyl radicals formed as a result of radiolysis of water. When two such breaks are present in complementary DNA strands within one helical turn, as it often happens for high doses of irradiation, a double-strand break is formed [40]. The ratio of SSB/DSB produced by IR is estimated at 10:1 [41].

The production of DNA strand breaks by chemicals can again go via a direct or an indirect route. Compounds like **bleomycin** or bicyclic enediynes, which act directly, are often referred to as „*radiomimetic*", as they possess the ability to induce single and double-strand DNA breaks with a SSB/DSB ratio comparable to IR [42, 43]. The presence of other chemicals, e.g. MMS, cisplatin or mitomycin C, usually leads to products which interfere with cellular processes, most often replication, and thus lead to DNA breaks [44].

## 1.6 DNA-protein crosslinks

The close, stable or transient association of DNA with proteins, although necessary for normal functioning of a living cell, sometimes leads to the formation of toxic **DNA-protein crosslinks (DPC)**. These modifications can be induced under physiological conditions and by a plethora of chemical and physical agents: ionizing and ultraviolet radiation, aldehydes, some chemotheraupetic drugs and certain metals [45–49]. DNA can be linked with proteins either directly through an oxidative free radical mechanism or indirectly, via a chemical linker or coordination with a metal atom.

DPCs are usually classified into four groups depending on the type of association with flanking DNA nicks [50]. The most common products of cellular metabolism and various physical and chemical agents, i.e. the crosslinks of proteins with intact DNA, constitute Type 1 DPCs. Type 2 and 3 DPCs concern **topoisomerases** (topo I and II, respectively) trapped at the DNA through a tyrosinyl-phosphodiester bond. TopoI is usually attached to the 3' end of an SSB, while TopoII binds two 5' ends of a DSB. Short-lived covalent intermediates between these proteins and DNA are produced to permit topological changes in the DNA helix. However, these intermediates may be *frozen* due to the action of topoisomerase inhibitors [51] or when the enzymes act on

a DNA lesion [52, 53]. The last type of DPCs are formed by the binding of proteins engaged in to the 5' end of a SSB. This kind of covalent modification usually concerns Pol$\beta$ or PARP-1 and is possible due to the action of APE1, which cleaves an oxidized AP site generating a 5' terminal oxidized sugar [54–56].

The biological consequences of DPCs are hard to elucidate because of the lack of agents that would exclusively induce these kinds of modifications. However, due to their size and structure, DPCs are expected to interrupt most DNA-associated processes. The best documented is the detrimental impact of DPCs generating compounds on replication [57, 58]. Moreover, several compounds able to produce DPCs, such as chromium and formaldehyde, were shown to produce mutations [59, 60].

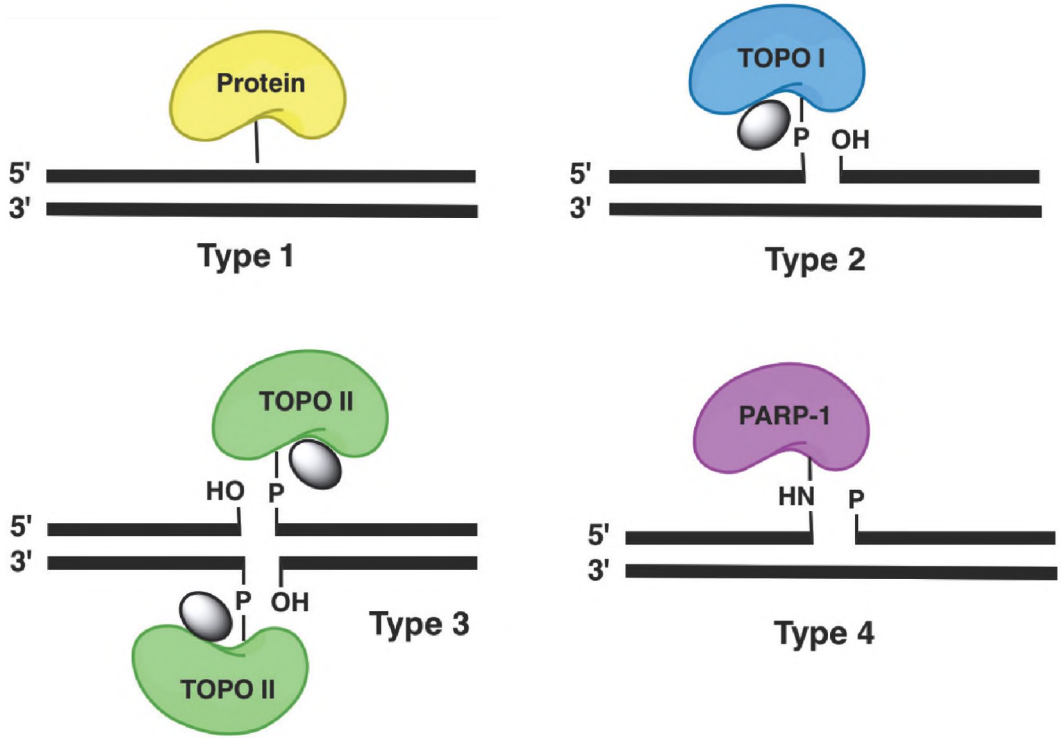


Figure 1.4: **Different types of DNA-protein crosslinks.** Type 1 DPCs are proteins attached to intact DNA, types 2 and 3 concern topoisomerases and type 4 are covalently bound BER proteins. The ovals shown next to TopoI or TopoII molecules depict Topo inhibitors. Figure from [61] (modified).

# Chapter 2

# INDUCTION OF DNA DAMAGE

## 2.1 Chemical agents

A plethora of different chemicals possess the ability to modify or damage DNA. While only some of these compounds are in widespread laboratory use, either for studies of DNA repair or for cancer treatment, a great number is classified as carcinogens. The DNA-damaging chemicals are naturally occurring or related to human action. They differ in their structure, mechanism of action and most importantly for studies of DNA repair, in the type of lesion they create.

### 2.1.1 Intercalators and groove binders

The two major modes of non-covalent binding of small molecules to DNA are **intercalation** and **groove binding**. It should be stressed out that not all compounds that posses the ability to bind to DNA are cytotoxic [62], yet a great number of intercalators and groove binders can impact cell-cycle progression and cell viability.

Intercalation of a flat chromophore between the base pairs usually leads to structural changes in DNA, which impedes the action of polymerases, transcription factors, DNA repair proteins and topoisomerases. This results in inhibition of replication and transcription. The second major effect of intercalators is induction of DNA damage, manifested by the occurence of sister chromatid exchange and micronuclei [63, 64]. It was also shown that intercalators are capable of *inhibiting topoisomerases*, leading to DNA cleavage [65, 66]. Poisoning of topo I and II produces single and double-strand DNA breaks, respectively, with their ratio dependent on the drug used. Importantly, the breaks induced by intercalators are blocked by tightly bound protein (topo I or II) and are usually rapidly reversible. The most extensively studied and frequently used as chemotherapeutics are actinomycin D, elsamicin A, epirubicin, ethidium, m-AMSA and anthracyclines such as doxorubicin, daunomycin or mitoxantrone [67]. It is worth noting that despite years of clinical and laboratory use, the mechanism of action of these compounds is still far from being completely understood. For example, it was recently shown that binding of daunomycin causes dissociation of histone H1.1 from the DNA and a subsequent aggregation of chromatin [68].

In contrast to intercalators, crescent shaped **minor groove binders (MGBs)** do not cause significant structural alterations in the DNA double helix. These compounds

usually prefer AT rich regions in the minor groove of DNA, where they are stabilized by hydrophobic and van der Waals interactions |69|. Some of the most known MGBs are distamycin A, netropsin or DAPI (and their synthetic derivatives), but the one that is the most studied and often considered as a model minor groove binding compound is **Hoechst** |69|. Hoechst compounds belong to the bis-benzimidies family and among its four known commercial forms, Hoechst 33258 and Hoechst 33342 are used most frequently. Hoechst 33342 is *more lipophilic*, generates significant amounts of DNA-protein crosslinks and DNA strand breaks |70|. Studies have also shown that Hoechst dyes interfere with multiple DNA processing proteins, poison topoisomerases and significantly enhance UV- and radiation-induced cytotoxicity |69|. Interenstingly, some of the MGBs (DAPI, Hoechst 33258) are also able to intercalate into GC-rich sequences, which probably contributes to the inhibition of topoisomerases |67|.

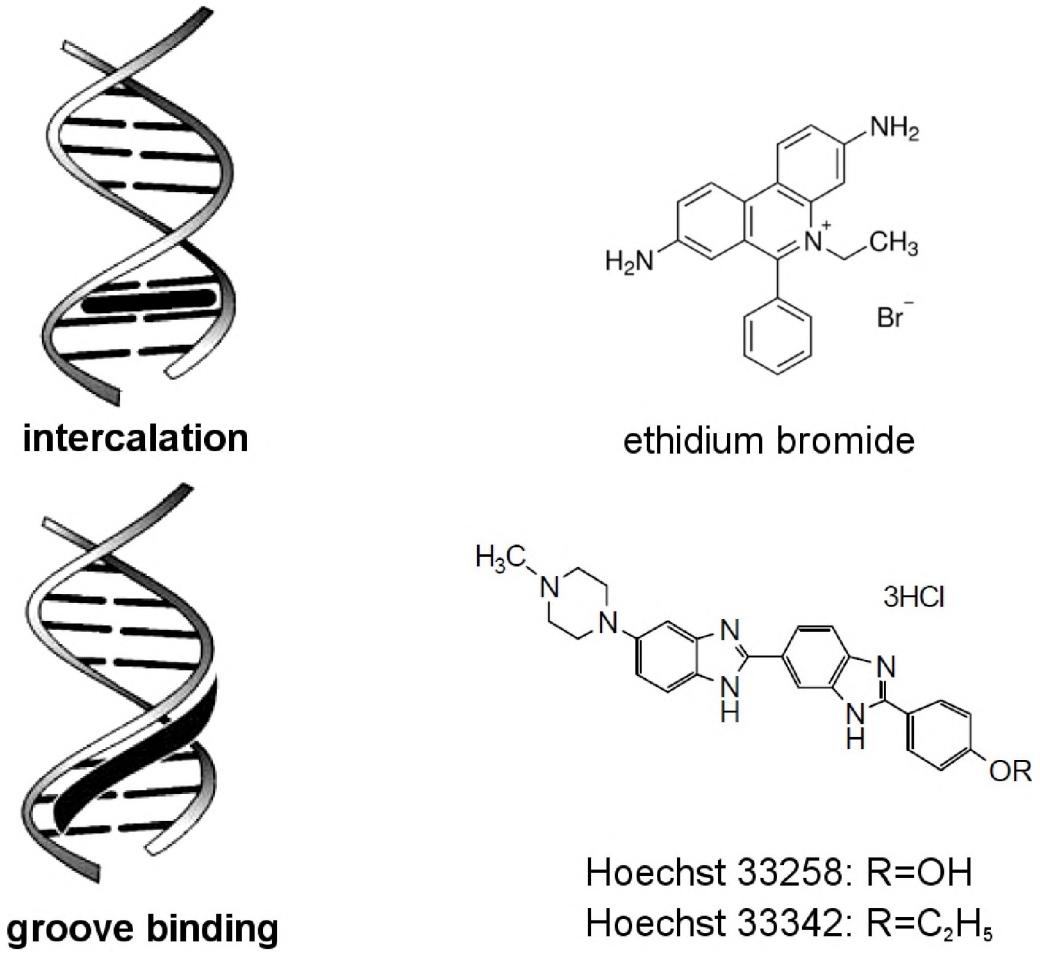


Figure 2.1: **Intercalation and groove binding as the two main modes of DNA-binding for small molecules.** A simplified view of intercalation and groove binding and the structures of two compounds (ethidium bromide and Hoechst) utilizing these binding modes are shown. These molecules are also used as photosensitisers enabling efficient DNA damage induction in cells irradiated with UV or visible light. Figure from |71| (modified).

### 2.1.2 Alkylating agents

Chemicals which posses the ability to form covalent bonds with DNA were among the first discovered carcinogens. **Benzoapyrene (BaP)**, the main chemical carcinogen in soot and coal tar, is rather unreactive, yet when activated, it becomes capable of forming covalent DNA adducts. Metabolic activation to reactive intermediates is required also for other **polycyclic aromatic hydrocarbons (PAHs)** and for aromatic or heterocyclic amines. The list of carcinogens related to human action, usually alkylating agents, is long and ever growing, yet it was found that also naturally occurring substances are able to form DNA adducts. The most toxic of these are aflatoxins, specifically the B1 type, which is metabolized to exo-8,9-epoxide that binds covalently to DNA. Another example is aristolochic acid, which also requires metabolic activation.

Due to their capability to indirectly kill proliferating cells, alkylating agents were the first used anti-cancer drugs. The best characterised and widely used in treatment of testicular and ovarian tumours are platinum compounds, **cisplatin** and carboplatin [72, 73]. Cisplatin usually binds to the N7 atom of guanine residues and, less frequently, to the N7 atom of adenine residues. The formation of intra-strand diadducts (cross-links), which unwind the double helix and prevent transcription is thought to be the direct cause of cisplatin-mediated cell death [74]. Another frequently used alkylating chemotherapeutic agent is mitomycin C (MMC). Its metabolites prefer to form DNA adducts with the N2 atom of guanine and in contrast to platinum compounds, interstrand cross-links of MMC are considered the most harmful [72]. A number of cancers are also treated with nitrogen mustard derivatives (mechloroetamine, melphalan, cyclophosphamide, chloroambucil) or with chloroethylnitrosoureas (CENUs; carmustine, lomustine, fotemustine). These compounds usually form monoadducts, most frequently at N7G, but again intra- or interstrand diadducts are thought to be the major cytotoxic lesions [72, 75].

Of special interest for DNA repair studies are **methyl methane sulfonate (MMS)**, dimethyl sulfonate (DMS), N-methyl-N-nitrosourea (MNU) and N-methyl-N'-nitro - N-nitrosoguanidine (MNNG). These chemicals, considered prototypical methylating agents, have been extensively studied and used in a variety of experiments. When taking into account relative concentrations, MNU and MMNG are considered more toxic and mutagenic than MMS. Nevertheless, for all these compounds N7-MeG is the prevalent adduct. Other adducts formed in appreciable amounts are N3-MeA and O6-MeG [77]. Although both N7-MeG and N3-MeA lead to destabilization of the N-glycosidic bond and, in consequence, to the formation of an abasic site, it was found that only N3-MeA blocks replication [22]. No evidence was found for N7-MeG to miscode or to impede replication so its toxic properties are thought to stem solely from depurination. On the other hand, A:T to T:A and G:C to A:T mutations can occur as a result of the formation of N3-MeA and O6-MeG, respectively. It is worth noting that MMS also produces single and double-strand breaks, but while SSBs observed after MMS treatment are probably BER intermediates, DSBs likely occur when these intermediates or methyl bases are encountered by replication forks.

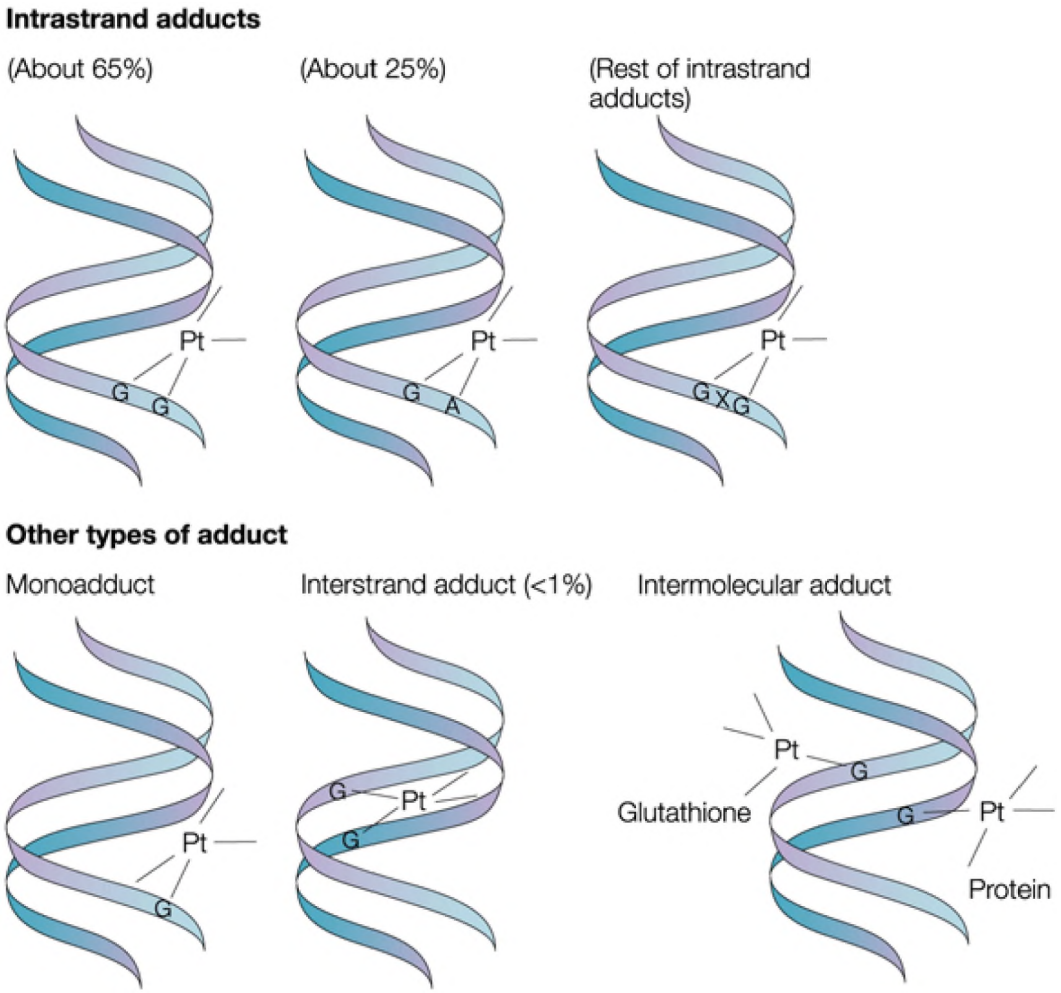


Figure 2.2: **Types of cisplatin-DNA adducts.** Interaction of cisplatin with DNA usually results in intrastrand adducts. The links are most often formed between adjacent guanines or neighbouring guanine and adenine. Other intrastrand adduct, monoadducts and interstrand adducts arise less frequently. Figure from [76] (modified).

### 2.1.3 Radiomimetic drugs

Another group of chemicals, widely used in cancer therapy and also in the studies of DNA repair processes, are radiomimetic drugs. As mentioned in Chapter 1, the term „*radiomimetic*" originates from the observation that the effect of these compounds on cells is similar to that exerted by ionizing radiation, despite the fact that the scope of lesions induced by IR is much wider (discussed below). **Bleomycin** is the most studied of these chemicals, but all of them share the same mechanism, which is based on oxidation of deoxyribose in DNA [42]. The process is initiated by hydrogen abstraction usually at the C-1', C-4' (bleomycin) and C-5' (enedyines) positions. Subsequent reactions result in strand breaks with different termini or in the formation of abasic sites, which often spontaneously break down into strand breaks [78]. A fraction of lesions induced by radiomimetic agents are bistranded and consist of two breaks or an abasic site and a strand break in opposing strands. The ratio of single to bistranded

lesions can vary significantly with the drug used. In the case of bleomycin bistranded lesions constitute only 10% of all the lesions while for calicheamicin most of the lesions (98%) are bistranded. Interestingly, it was shown that bleomycin does not directly interfere with DNA replication and it induces more lesions in G1 or G2/M than in S phase cells [43], usually in actively transcribed chromatin. The binding of the activated form of this drug to DNA is based on intercalation or interactions with the minor groove [79, 80].

## 2.2 Ionizing radiation

Ionizing radiation (IR) is a known carcinogen – the evidence for its harmful properties has been accumulating since the discovery of X-rays by Roentgen in the late 1800's. However, years of studies have allowed it to be safely used in medical diagnostics, cancer therapy or as a popular tool for inducing DNA damage in research.

Exposure of cells to high energy radiation ($\alpha$ and $\beta$ particles, $\gamma$ and X-rays, protons, heavy ions) leads to loss of genetic information, mutations, genetic instability and apoptosis [81]. These effects are a consequence of interaction of IR with DNA or its surroundings. IR can thus damage DNA directly, when atoms are *ionized* along the radiation tracks or indirectly, through the action of *water radiolysis* products. The relative contribution of these two routes for the total DNA damage produced by IR is still a matter of debate [82,83]. However, it is assumed that the direct effect is dominant for radiations with high **linear energy transfer** (**LET**; $\alpha$ particles and neutrons), while the indirect effect plays a major role for sparsely ionizing radiation [84].

IR induces multiple types of DNA damage: base damage, AP sites, crosslinks and most importantly, single and double-strand DNA breaks. While all of these lesions initiate a repair process, it was found that those responsible for lethal effects of IR are DSBs [85, 86]. There are two ways for a DSB to arise - a single radical can lead to lesions on both strands or, most often, two separate single-strand breaks are formed in close proximity [87]. Several attempts have been made to measure the dose-response for DSBs after IR. While most of the studies found a linear relationship between the applied dose and DSB yields, the numbers vary significantly, from 13 to 70 DSBs per cell per Gy [86]. For SSBs, it was estimated that approximately 1000 lesions per cell per Gy are produced at biologically significant doses of radiation (1-10 Gy) [88].

Although the fact that DSBs have deleterious consequences was well established, it was found that DSBs yields observed after low LET radiation are not sufficient to account for the cell lethality caused by IR [89]. This led to the introduction of the idea of *„clustered" DNA damage*, originally termed as **locally multiple damaged sites (LMDS)** [90, 91]. A clustered damage is defined as two or more lesions within one or two helical turns of DNA, produced by a single track of ionizing radiation [92]. The complexity of clustered DNA damage increases with increasing LET [93] and simulations show that for densely ionizing radiation more than 90% of DSBs contain other lesions in close proximity [94, 95]. Even low doses of IR (1 Gy) are capable of inducing clustered damage. Processing of closely spaced lesions located on opposite strands may lead to the induction of additional DSBs, which explains the phenomenon of post-irradiation increase in DSBs yields, reported in several studies. Clustered damage, even when not embracing a DSB, possesses a greater challenge for the repair machin-

ery than individual lesions, leading to reduced repair efficiency, repair retardation and non-canonical DNA conformations [92, 96].

## 2.3 Ultraviolet and visible light, photosensitised damage

Solar radiation is a well established genotoxic agent, which induces DNA modifications either directly by DNA excitation or indirectly, by *excitation of endogenous chromophores* acting as *photosensitisers* [97]. The most potent in inducing DNA damage and thus having most grievous consequences for human health is the UV range of the solar spectrum ($10 - 400\ nm$). A part of the UV spectrum is *directly absorbed* by DNA, with two maxima in the UVB ($280 - 315\ nm$) and UVC ($< 280\ nm$) regions. The lesions that are most frequently formed after exposing cells to UV radiation are CPDs and 6-4PPs. The most efficient in producing CPDs is UVC radiation, with a rate of 2-10 lesions / $10^6$ bases per $J/m^2$, while for UVB this rate is estimated at one lesion / $10^7$ bases per $J/m^2$ [98]. Another lesion detected after treating cells with UVB is 8-oxoG, but the frequency of this lesion is much lower than that observed for pyrimidine dimers. Induction of CPDs and 8-oxoG is also possible after irradiation with UVA – the ratio of these lesions is estimated at 5:1 [99]. Other lesions induced by UVA are abasic sites and strand breaks [100]. The ability of UVA to induce DSBs was discussed for a long time, but the formation of replication-dependent DSBs is now widely accepted [101]. Interestingly, recent data suggest a possibility of replication-independent formation of DSBs after UVA through clustered single-strand breaks [102]. Initially, it was thought that generation of DNA lesions by UVA requires an endogenous photosensitiser, but recent studies have shown that the weak absorption of UVA by DNA is significantly *enhanced by base pairing* [103] and that UVA is capable of inducing CPDs in cellular as well as isolated DNA [99]. On the other hand, since UVA photons lack sufficient energy to enable one-electron oxidation of bases, a photosensitiser-based mechanism might be involved in the formation of oxidized bases, mainly 8-oxoG, by UVA [99].

In contrast to UV-radiation, the mechanisms of mutagenic action of **visible light** are *less studied and not that well understood.* It is essential to realize that the majority of experiments concerning the influence of visible light on DNA were performed by *irradiating the whole cells.* Thus, the derived lesion types and their yields do not solely stem from the interaction of visible light with the nucleus and DNA within, but with *all components of the cell* (see Fig. 2.3 for comparison of global and local DNA damage). Cytoplasm contains various compounds that absorb visible light, including flavin derivatives that are known to be capable of acting as photosensitisers.

The first hints that also radiation above $400\ nm$ might be involved, directly or indirectly, in the production of DNA damage came from studies which have shown the deleterious effect of fluorescent light on cultured cells. These early experiments provided evidence that exposure of mouse cells to light emitted from commonly used lamps for $20\ h$ at $4{,}6\ W/m^2$ results in chromatid breaks and exchanges together with DNA crosslinking [104–106]. Subsequent studies aimed at the *characterisation* and *quantitation* of DNA damage by means of the **alkaline elution assay**. Different cell lines were irradiated with halogen or mercury lamps with doses ranging from several

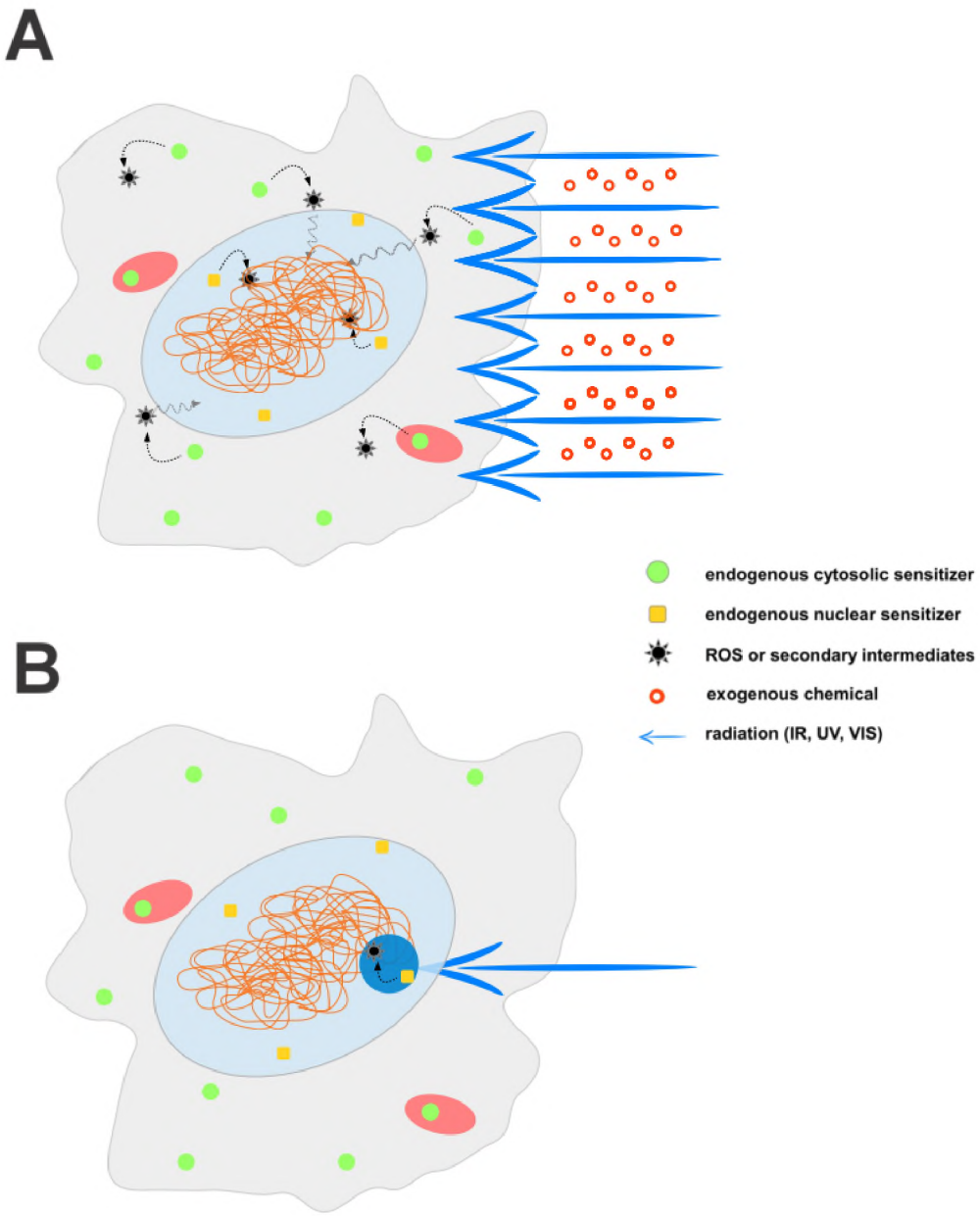


Figure 2.3: **Schematic representation of global and local DNA damage. A** – Global DNA damage can be induced by various exogenous chemicals or by IR, UV or visible light irradiation. IR, UVB and UVC radiation can damage DNA directly, but UVA and visible light require endogenous, cytosolic photosensitisers. There is a possibility that the damage is also partly mediated by an unknown nuclear photosensitiser. When whole cells are irradiated with UVA or visible light, ROS and secondary intermediates formed in the cytosol or in cytosolic organelles can migrate to the nucleus, leading to DNA damage. **B** – Local DNA damage is usually induced by IR microbeams, lasers or endonucleases (not shown). In the case of laser irradiation, the beam is focused into a diffraction limited spot. Generated DNA lesions are confined to a small region in the nucleus (a 3-D volume) and the excitation of sensitisers located in the cytoplasm is minimized.

**kJ/m²** to **MJ/m²** or were exposed to **natural sunlight** [107]. These studies agree that the most abundant lesions induced by visible light are those sensitive to Fpg protein (probably mostly 8-oxoG), but single-strand breaks, AP sites and DNA-protein crosslinks are also produced [108–110]. The yield of Fpg sensitive lesions have been shown to be several times greater than that of SSBs with no significant variations between different cell lines [107]. The number of these lesions decreases with longer wavelengths but their ratio remains unaltered [109].

While there is agreement that most lesions are induced by wavelengths between 400 and 500 *nm*, there are discrepancies in the obtained **action spectra**. For instance, in one of the studies a significant peak around 450 *nm* is observed in the action spectrum for DNA strand breakage [111]. However, this peak is either not visible in spectra obtained by other researchers [112] or is shifted towards shorter wavelengths [110]. In the latter study the action spectrum suggests that no strand-breaks are induced by wavelengths greater than 450 *nm*. One of the possible explanations of these inconsistencies might lie in the method, which was used for assessing DNA damage. All of these studies have utilized the alkaline elution assay. This method, although sensitive in the detection of DNA damage, was also shown to be extremely inconsistent [113]. Moreover, it only enables to measure single-strand DNA breaks, so the possibility of induction of DSBs by visible light was not assessed so far.

### 2.3.1 Photosensitised damage

It is reasonable to expect that induction of DNA lesions by visible light, *when the whole cells are illuminated*, is mediated by an **endogenous photosensitiser** [107,110]. Thus, one should consider the possible mechanisms of photosensitised damage to DNA and the types of lesions typically formed in these reactions. An excited photosensitiser can react with DNA directly or the damage can be mediated by **ROS** or other **secondary intermediates**. The direct reactions can be further subdivided into covalent binding, triplet-triplet energy transfer and one-electron transfer or hydrogen abstraction. An example of the covalent binding photosensitisers are psoralens, which intercalate and then bind to the DNA [114]. Triplet-triplet energy transfer gives rise to cyclobutane thymine dimers due to the fact that thymine possesses the lowest triplet-energy of all DNA bases. Some UVA absorbing photosensitisers such as acetophenone, pyridopsoralens and fluoroquinolones have been shown to damage DNA using this mechanism [115–117]. The last type of the direct photosensitiser-DNA reactions is an electron or a hydrogen abstraction by the triplet-excited state (so-called type-I reaction). Because guanine has the lowest one-electron oxidation potential of the DNA bases, the most frequent DNA modification formed through this mechanism is 8-oxoG [118]. However, some type-I photosensitisers (e.g. harmine) are able to attack the sugar moiety of DNA, leading to SSBs [119].

ROS-mediated DNA damage requires the interaction of a photosensitiser with molecular oxygen (type II reaction), which generates the superoxide anion (electron transfer) or singlet oxygen (energy transfer) [120]. In contrast to singlet oxygen, the superoxide anion does not react with DNA directly, but can lead to the formation of a highly-reactive hydroxyl radical. Since hydroxyl radical is also responsible for the indirect effect of ionizing radiation the damage spectrum induced by some type II

photosensitisers (N-hydroxypyridinethiones, furocumarin hydroperoxides) closely resembles that produced by IR [121, 122]. On the other hand, singlet oxygen generated by photosensitisers leads mostly to 8-oxoG and other, not yet indentified purine modifications [123].

Importantly, the studies of photosensitised damage to DNA have shown that the ratio of modifications caused by the interaction of radiation with a photosensitiser allows to *determine the mechanism of damage induction*. The type and ratio of DNA modifications induced by visible light interacting with all components of the cell suggest that the damage is caused by a direct DNA-photosensitiser interaction (type I) or by singlet oxygen (type II). However, for the former mechanism to occur the potential photosensitiser would have to be *enclosed in the nucleus* and so far no data has been published regarding this possibility. On the other hand, numerous cytosolic endogenous compounds, such as **flavins**, **porphyrins**, **melanin** and **bilirubin** have been proposed to mediate the formation of DNA modifications in cells treated with visible light [108, 124]. Both flavins and poprhyrins have been shown to transduce blue light into ROS [125] and to induce high yields of 8-oxoG in cells [107]. One of the possible candidates responsible for the induction of SSBs is bilirubin, due to its efficient absorption in the $420 - 500$ $nm$ range [126]. Some studies have also shown that continuous irradiation of whole cells with visible light results in the saturation of DNA damage, which might be explained by the *decomposition* of the photosensitiser [109].

### 2.3.2 Selective irradiation with visible light

Localised DNA damage induced by irradiation of the cell's nucleus with visible light, accompanied by very limited excitation of endogenous, cytosolic photosensitisers, was so far demonstrated in a few studies. This was achieved by using focused laser beams emitting at 405, 435, 514 or 532 $nm$ [127–131]. In some cases DNA damage was induced in cells containing DNA-binding **exogenous photosensitisers** (405 nm with BrdU or Hoechst, 514 nm with ethidium bromide). In other cases, when no exogenous photosensitiser was used, the power of the incident radiation was usually *very high, reaching hundreds of* $TW/m^2$ [132]. Also, very often too little information about the irradiation setup was provided by the authors (see Chapter 4 for detailed information regarding these issues) [128, 131]. In one of these studies, although the nucleus was irradiated with a visible light emitting laser (532 $nm$) and no photosensitisers were introduced into cells, the observed DNA breaks were probably caused by *photomechanical pressure* resulting from optical breakdown of the medium [127]. Thus, the possibility of DNA damage induction and the scope of potential lesions resulting from the selective irradiation of the cell nucleus with visible light, in the absence of exogenous photosensitisers, remains to be established.

## 2.4 Methods of inducing global or local DNA damage for experimental purposes

Some of the fundamental steps in the **DNA Damage Response (DDR)** have been uncovered by *in vitro* reconstitution of the repair pathways. However, the re-

sponses to DNA damage are now often studied in intact living cells. Since the repair of DNA lesions caused by endogenous factors is rather difficult to track, it became necessary to develop tools for the induction of well defined DNA damage, possible to implement in laboratory conditions. The methods of inducing DNA damage for experimental purposes can be classified based on several features, but the most general division is between methods that allow to induce the damage *globally* (in the whole nucleus, in many cells) or *locally* (in a chosen region of the nucleus in one cell).

### 2.4.1 Global DNA damage

Induction of a global DNA damage has been utilized since the early days of the DNA repair field and is still the method of choice in many current studies. The major advantage of this approach is the possibility to almost simultaneously *generate lesions in many cells.* This allows to measure cell survival after treatment with a certain agent or to obtain averaged data regarding, for example, the number of lesions induced or the time required for the repair processes to be completed. The shortcoming of these methods is related to the fact that it is not only the DNA but the *entire cell* that is exposed to the damaging agent.

Virtually all of the aforementioned and many other DNA damaging agents could be used in the laboratory for placing lesions throughout the nuclear DNA. However, among the broad range of agents, only several are routinely used for the studies of DNA repair. The choice of a particular agent is usually dictated by the type of expected DNA lesion, which makes it possible to monitor a specific DNA repair pathway. Oxidative DNA lesions are most often induced by various concentrations of $\mathbf{H_2O_2}$. For alkylation damage, **MMS**, **DMS**, **MMNG** and **MNU** are commonly used. On the other hand, the repair of strand breaks is usually studied after treating cells with physical agents, such as ionizing or ultraviolet radiation. Alternatively, bleomycin or other radiomimetic drugs are used for inducing DSBs. Somehow uniquely, the studies of repair of pyridimine dimers and other photoproducts can only be conducted by using UV radiation. Nonetheless, it is important to note that despite using these agents in the context of certain DNA lesions or repair pathways, *neither of them is capable of inducing only one type of DNA modification.* Also, the experimental procedure contributes to the final outcome of the treatment with different DNA damaging agents. While for chemicals the concentration and exposure time play a major role, DNA damage induced by physical agents is influenced by multiple factors, such as the type of radiation (low or high LET for IR; wavelength for UV and visible light), the total energy delivered to the sample or by the rate of radiation delivery.

### 2.4.2 Local DNA damage

There are several assets of inducing damage confined to sub-nuclear regions. First of all, this approach gives the experimenter a free choice of the part of the nucleus subjected to the damaging agent, which allows to study the DDR in structurally and functionally different regions. Furthermore, coupling with modern live cell imaging techniques enables to obtain wide range of data regarding the proteins involved in the repair processes as well as the structure of chromatin in DDR. Most of the valuable

information gained from the studies involving local DNA damage induction, such as the kinetics of protein recruitment and their retention times, cannot be obtained with methods resulting in global DNA damage. The two techniques of sub-nuclear damage induction which are now frequently used in the studies of DNA repair are **ionizing radiation microbeams** and **laser microirradiation**.

#### 2.4.2.1 Microbeams

Ionizing radiation microbeams enable to deliver exactly specified doses of radiation with *high spatial accuracy*. Despite a great interest in the interaction of ionizing radiation with cellular components, it was not until the 1990s that the technology for microirradiation devices was developed. Originally developed to study the bystander effect, i.e. the induction of stress and increased lethality in non-irradiated cells (neighbours of the irradiated ones), today ion microbeams provide new insights into the DDR.

The most popular are ion microbeams, but X-ray and electron microbeams are also used. Charged particle microbeams, although can embrace a large range of ions and energies (up to 15000 $keV/\mu m$) [133], often suffer from significant scattering, which influences the size of the beam. One of the requirements for using these devices in research is the ability to precisely *control the dose delivered* to the sample, which is possible with high efficiency detection systems. The advantages of X-ray and electron microbeams are a very small beam size (X-ray microbeams) and the ability to easily vary the delivered dose. The major drawback of using microbeams for inducing localised DNA damage is their *limited availability*, as there are only a few facilities worldwide which fulfil the requirements essential for the use of microbeams in research.

Irradiation of cells with ionizing radiation microbeams is expected to *generate a mixture of DNA damage types*. In agreement with that, repair factors and modifications involved in many different repair pathways have been detected after high-LET radiation [134]. It was shown that although the number of DNA breaks per unit dose is constant, the complexity of these lesions is significantly enhanced with *increasing LET* [95]. Recent studies conducted with the use of ion microbeams have focused on the repair of clustered DNA damage induced by particle irradiation. These experiments have shown that the complexity of induced damage can influence the kinetics of protein recruitment to the damage site [135] and that the difficulties with the repair of clustered lesions might eventually lead to chromosome breakage [136]. Ion microirradiation was also used to study the DDR in the context of chromatin compaction. This was possible by placing lesions with high precision in densely packed chromocenters, which allowed to study the recruitment of repair proteins to these regions [137].

#### 2.4.2.2 Laser light

The first use of a laser beam for inducing alterations in DNA dates back to 1960s. In these early experiments, Berns and colleagues have shown that a pulsed argon laser microbeam can be utilized to place localised lesions on mitotic chromosomes [138]. The induction of lesions was manifested by so-called *chromosome paling*, i.e. irradiated regions were brighter than other parts of the chromosomes when visualized by phase contrast microscopy. Initially, induction of damage required that the chromosomes

were photosensitised with acridine orange, but it was soon found that using higher laser powers enabled to induce lesions without photosensitisation [139]. The laser was coupled to a microscope, which allowed to visualize the specimen before and after irradiation. Interestingly, comparison of lesions induced in the presence and without a photosensitiser led to the suggestion that the damage is markedly different in these two settings.

It is worth noting that even before the advent of lasers, localised lesions on chromosomes were induced taking advantage of a UV microbeam (Uretz microbeam), constructed by focusing heterochromatic ultraviolet radiation emitted from a lamp to a spot several micrometers in size [140]. Irradiation of chromosomes with this apparatus also resulted in the appearance of phase-paled regions.

The induction of localised DNA damage in interphase chromatin with subsequent antibody staining or detection of **unscheduled DNA synthesis (UDS)** was shown for the first time by Cremer and collaborators. In these experiments cells were damaged by a UV laser emitting radiation at 257 or 365 $nm$ wavelengths [141–143]. Nevertheless, the use of lasers for the induction of local DNA damage was substantially boosted after two findings published in the 1990s. First, Limoli and Ward have shown that single and double-strand DNA breaks are induced after UVA irradiation of cells *sensitised with BrdU and Hoechst* [144] and later Rogakou and colleagues have substituted the initial UVA source with a UVA laser (390 $nm$), creating a tool for localised induction of DNA strand breaks in living cells [145]. Since then, multiple similar setups, combining UVA ($337, 390$ $nm$) or even visible light emitting lasers ($405, 514$ $nm$) with different photosensitisers (BrdU, Hoechst, ethidium bromide), have been used [129, 146].

Experiments in which a UV laser was utilized as a means for local DNA damage induction have confirmed that the major lesions induced by irradiation at 266 $nm$ are CPDs and 6-4PPs [147]. However, base damage [132] (8-oxoG) along with single and double-strand breaks can also be detected when using longer UV wavelengths (337, 365) [132, 148]. Interestingly, some studies suggest that irradiation of cells with a low dose of a UVA laser *selectively* induces SSBs, without the formation UV photoproducts, oxidative base modifications or DSBs [148].

In recent years, due to its wide accessibility, a 405 $nm$ emitting laser has became the choice of many researchers to localise DNA lesions in living cells. Usually used in the presence of photosensitisers (BrdU or Hoechst), this wavelength was shown to induce a mixture of lesions: both single and double-strand breaks, 8-oxoG and even CPDs (but no 6-4PPs) [147, 149]. Similar damage spectrum, with the exception of UV photoproducts, was also observed after irradiation with green laser light ($514$ $nm$) in the presence of ethidium bromide [129]. Without a photosensitiser, the 405 $nm$ laser was shown to induce *only SSBs* (at certain doses) and no DSBs or oxidative damage [131, 150]. A selective induction of SSBs without DSBs was also proposed to occur after irradiation with a 435 $nm$ emitting laser [130].

The desire to confine the damage into a very small 3-D volume of the nucleus has also led to the popularization of pulsed lasers, which deliver high-intensity ultrashort pulses (ps to fs) that can lead to *multiphoton excitation* [149]. The most popular of these is a Titanium:sapphire laser emitting femtosecond pulses at 800 $nm$. Simultaneous absorption of three photons of this radiation corresponds energetically to irradiation with a UV laser at around 260 $nm$, which leads to direct DNA excitation.

In agreement with that, UV photoproducts have been detected after damage induced with this setup. Nonetheless, other types of damage were shown to be formed as well (strand breaks and base modifications) [149], hinting at an additional mechanism, probably low-density plasma formation, which needs to be considered [149]. Similar lesions were also observed after two-photon excitation with a 532 *nm* emitting femtosecond laser [132]. The ratio of strand breaks to UV photoproducts was shown to be substantially increased when using a higher (1050 *nm*) wavelength with femtosecond pulses [151].

The major rationales for inducing local DNA damage with lasers are their wide accessibility and the simplicity in coupling them with modern imaging devices. The last decade have seen a substantial boost in the DNA repair field, which was mainly driven by the developement of several laser microirradiation techniques. These techniques have allowed to visualize the recruitment of proteins known to be involved in the DDR, but also led to the discovery of new repair factors and repair-related functions in proteins so far not recognized as members of the DDR. Moreover, much has been learned about the changes in chromatin structure, which are necessary for the successful repair of induced lesions. Nevertheless, the existing laser-based methods for local DNA damage induction *suffer from important drawbacks*, e.g. the activation of multiple DNA repair pathways caused by the generation of a mixture of lesions or the induction of heavy, sometimes lethal damage. Very often researchers using these methods share *little information* regarding the laser power or the total dose of light delivered to the irradiated region. Also, the use of photosensitisers raises doubts about the *structure of chromatin* and the ability of cells to proceed with normal DNA repair processes with the photosensitiser present in the nucleus. These issues (discussed in detail in Chapter 4) imply that new methods, free of the mentioned shortcomings of the existing approaches, are highly desirable.

#### 2.4.2.3 Other techniques

Induction of spatially confined DNA damage is also possible with other techniques. These methods, although technically more challenging, have been successfully used for studying the DDR.

The first approach enables to induce single DSBs into defined regions of the genome and is based on the **yeast endonuclease I-SceI**. The requirement for this is the generation of cell lines whose genomes contain the 18-nt recognition site for the I-SceI restriction enzyme. I-SceI is then introduced into these cells with exogenous expression and cuts the DNA. Additionally, the I-SceI recognition site can be flanked by LacO/TetO operator array sequences. This allows to *visualize the site of the damage* by binding of fluorescently tagged LacR and TetR repressor proteins. The I-SceI based approach has been so far utilized in a few DNA damage related studies, e.g. it served to track the positions of broken DNA ends [152] and to reveal the spatial dynamics of chromosome translocations [153]. One of the drawbacks of this method is the lack of information regarding the timing of DSB induction, which limits the studies of kinetics of DNA repair factors.

Another method involves the use of a highly phototoxic fluorescent protein termed **KillerRed (KR)**. This protein generates ROS in a light-dependent manner but at the same time retains its function as a genetically encoded fluorescent tag [154, 155].

It was shown that green light irradiation of cells in which tandem KillerRed (tKR) was fused to histone H2B results in formation of DNA damage and blockage of cell division [156]. A more spatially confined induction of DNA lesions by the KR protein might be achieved by irradiation of a small region in the nucleus. In another study, KR protein was fused to tetracycline repressor (tetR) and the transcription activator (TA). Binding of TetR-KR or TA-KR to a TRE cassette integrated at a defined genetic locus enabled to induce ROS mediated damage in hetero- or euchromatin [157]. Limitations of using KR in the studies of DNA repair are its dimerization and a necessity to tightly control its expression.

Finally, one has to mention the potential usefulness of **CRISPR** [158] **(Clustered Regularly Interspaced Short Palindromic Repeats)** for the induction of strand-breaks in defined genetic loci. This technique, which has rapidly become one of the most popular approaches for genome editing [159, 160], is based on targeting of a Cas9 endonuclease to specified genetic sequences by so-called guide RNA (gRNA). The Cas9-gRNA recognizes the target sequence and if a sufficient homology exists, the endonuclease generates a DSB in the target DNA [161]. This technique has not been exploited in the field of DNA repair so far, but its simplicity makes it a promising tool for the induction of DNA strand-breaks for the purpose of this kind of research.

# Chapter 3

# DNA REPAIR PATHWAYS

In the late 1950s the first DNA repair pathway, termed enzymatic photoreactivation (EPR), was discovered in bacteria. It was shown that this pathway *repairs UV lesions in a light-dependent manner* and is catalyzed by a photoreactivating enzyme – the photolyase. Later studies suggested that in mammalian cells, where photoreactivation is not conserved, UV generated photoproducts can be repaired in the absence of light, which led eventually to the discovery of **Nucleotide Excision Repair (NER)**. The realization that the DNA is not a stable molecule, but frequently *undergoes chemical modifications*, sparked the research on the repair of small base lesions. Subsequent steps in the **Base Excision Repair (BER)** were gradually deciphered and finally the entire pathway could be reconstituted with purified enzymes. Similarly, a series of papers enabled to reconstitute another pathway, termed **Mismatch Repair (MMR)**, which was shown to eliminate nucleotides erroneously incorporated during DNA replication. The value of the findings regarding NER, BER and MMR was recognized by the Nobel Committee in 2015 as **Tomas Lindahl, Paul Modrich and Aziz Sancar** were awarded the **Nobel Prize in Chemistry** „for mechanistic studies of DNA repair".

## 3.1 Nucleotide Excision Repair

Nucleotide Excision Repair (NER) is responsible for the repair of bulky, often structurally unrelated DNA lesions that usually result in the *distortion of the DNA double helix*. The most popular of these are CPDs and 6-4PPs produced by UV radiation, but also some less frequent lesions produced by various chemicals are repaired through this pathway [162–164]. Two repair sub-pathways exist – the choice between them is dictated by the *location of the damage* [165, 166]. While **global genome NER (GG-NER)** is able to conduct the repair anywhere in the genome, **transcription-coupled NER (TC-NER)** can only remove lesions in the transcribed strand of active genes. The major difference between GG and TC-NER is in the detection step. In GG-NER, the lesions are usually recognized by the XPC-hHR23B-CEN2 complex, sometimes with the help of UV-DDB [167]. In TC-NER, on the other hand, the repair is initiated by a **RNA polymerase II (RNAPII)** blocked in front of a bulky lesion [168]. A stalled RNAPII is bound by CBS [169], which then recruits the CSA complex [170], NER factors and histone acetyltransferase p300 [171]. Other proteins required in the recognition step of TC-NER are HMGN1 [172], XAB2 [173] and TFIIS [174]. GG

and TC-NER sub-pathways *converge* after the recruitment of **transcription factor II H(TFIIH)**, responsible for the unwinding of the DNA around a lesion and stabilization of single-stranded DNA [175] (ref 4). The stabilization of the opened state of the DNA is assisted by XPA, RPA and XPG [176,177]. Next, the 3' and 5' side of the nucleotide fragment which contains the lesion is cleaved by (ERCC1)-XPF. The final step of repair, i.e. filling of the single-stranded gap is accomplished by polymerase $\delta$ or $\epsilon$, accompanied by PCNA and RFC [178]. Finally, ligation is carried out by DNA Ligase I or XRCC1/DNA Ligase III [179].

## 3.2 Mismatch repair

The role of DNA Mismatch Repair (MMR) is to correct the *mispaired bases* omitted by the proofreading function of the replicative DNA polymerase. This mechanism allows to increase the accuracy of DNA replication by about 1000-fold [180]. Additionally, MMR was shown to repair lesions caused by some alkylating agents and certain environmental carcinogens [181, 182]. The repair process is *evolutionarily conserved* and best understood in *Escherichia coli* (E. coli). In this organism, detection of the mispaired bases is carried out by the MutS homodimer, which then recruits the MutL homodimer [183]. This leads to the activation of the MutH endonuclease that is able to *discriminate* between daughter and parent DNA strands on the basis of the state of adenine methylation at d(GATC) sites [184]. Nicks introduced by MutH on the unmethylated newly replicated strand are used as a starting point for the helicase UvrD, which unwinds the DNA [185,186]. The unwound strand, which contains the mismatch, is then *eliminated* by exonucleases and DNA is *re-synthesized* using the parental strand as a template [187, 188].

In eukaryotes, detection of mispaired bases is *similar* to that observed in E. coli and is carried out by MutS and MutL homologs (heterodimers MutSalpha and MutSbetha for MutS and Mutlalpha for MutL) [189, 190]. In contrast to *E.Coli*, MutL homologs in most other organisms posses the ability to introduce nicks into the daughter strand [191]. Another difference is that discrimination between the two DNA strands is not based on methylation, but rather on the nicks at the 3' and 5' ends of Okazaki fragments [192] or nicks formed as a result of excision of ribonucleotides incorporated during DNA replication [193]. There is also evidence that detection of the daughter strand is facilitated by the *asymmetric* nature of the loaded PCNA [194, 195].

## 3.3 Homologous Recombination and Non-Homologous End Joining

Apart from the basic repair pathways, another one that has gained much attention concerns the repair of the most deleterious DNA lesions - double-strand breaks. The repair of these lesions usually proceeds through one of the two pathways – **Non Homologous End Joining (NHEJ)** or **Homologous Recombination (HR)** (Fig. 3.1). These pathways differ in regard to their occurrence in the cell cycle phases [196] and to the proteins engaged, yet the most important difference lies in their *ability to restore the original DNA sequence* in which the strands were broken.

NHEJ is a very efficient but also *error-prone* repair pathway, operating throughout the cell cycle. The broken DNA ends are recognized and bound by the **Ku70/Ku80** heterodimer, which stabilizes and protects the DNA ends, serving as a *scaffold* for other proteins involved in the pathway [197, 198]. The first protein recruited by Ku is the DNA-PK (DNA-dependent protein kinase catalytic subunit). Interaction with Ku leads to the activation of the kinase function of DNA-PK, which then phosphorylates itself and other proteins involved in NHEJ [199]. One of the substrates of DNA-PK is the nuclease Artemis. The Artemis/DNA-PK complex is responsible for the *processing* of DNA ends, which is necessary before *ligation* can occur [200]. The final step of NHEJ is carried out by DNA Ligase IV/XRCC4 complex, recruited by Ku [201].

The above-described pathway is termed the canonical NHEJ, to distinguish it from the **Alternative NHEJ (A-NHEJ)**, responsible for the repair of DSBs when the classic route is disabled [202]. A-NHEJ is initiated by PARP1 instead of Ku [203], while the end resection requires MRN, CtIP and BRCA1 [204–206]. The repair is completed by ligation of DNA ends by LigIII/XRCC1 complex or by DNA Ligase I [207, 208].

Due to the fact that the rejoining of broken DNA ends occurs *regardless of the sequence homology*, the accuracy of both NHEJ pathways is low. In contrast, the repair of DSBs by the second major pathway, Homologous Recombination, *requires the presence of a homologous sequence* and leads to error-free restoration of the original sequence. The recognition of a DSB in HR is carried out by the **MRN (Mre11-Rad50-Nbs1)** complex [209] which, through homodimerization of Rad50, can connect and stabilize the DNA ends [210]. The interaction of Nbs1 with ATM leads then to recruitment and activation of the latter protein [211]. Activated ATM phosphorylates multiple substrates, including histone H2AX [212, 213]. **Phosphorylated histone H2AX** (**$\gamma$H2AX**) is considered an early marker of DSB repair and serves as an anchorage for other HR factors [214]. The DNA damage signal is then further *amplified* by MDC1 through its interaction with $\gamma$H2AX and Nbs1 [215]. The next step in HR is the resection of DNA ends which involves proteins such as MRN, CtIP, EXO1, BLM and DNA2 [216–218]. The resulting 3'-single-stranded DNA overhangs are bound and *stabilized* by **RPA (replication protein A)** [219]. This protein is later replaced by **Rad51**, loaded by BRCA2 [220]. Rad51 is an essential factor for the completion of DSB repair by HR, as it is able to form *a nucleoprotein filament* that searches and invades a homologous duplex DNA template, forming a displacement loop (D-loop) [219]. From this point, HR can proceed through one of two sub-pathways. Usually, after limited elongation the invading strand is released and annealed to the other DNA end. The repair is then completed by gap-filling and ligation. This sub-pathway is known as Synthesis-Dependent Strand Annealing (SDSA) [219]. Another sub-pathway involves the formation of a double Holliday junction, which can be resolved in several ways, giving crossover and non-crossover products. There are multiple enzymes engaged in the resolution of HJs of which the best studied is the complex of BLM with topoisomerase III$\alpha$, responsible for the formation of non-crossover products [221].

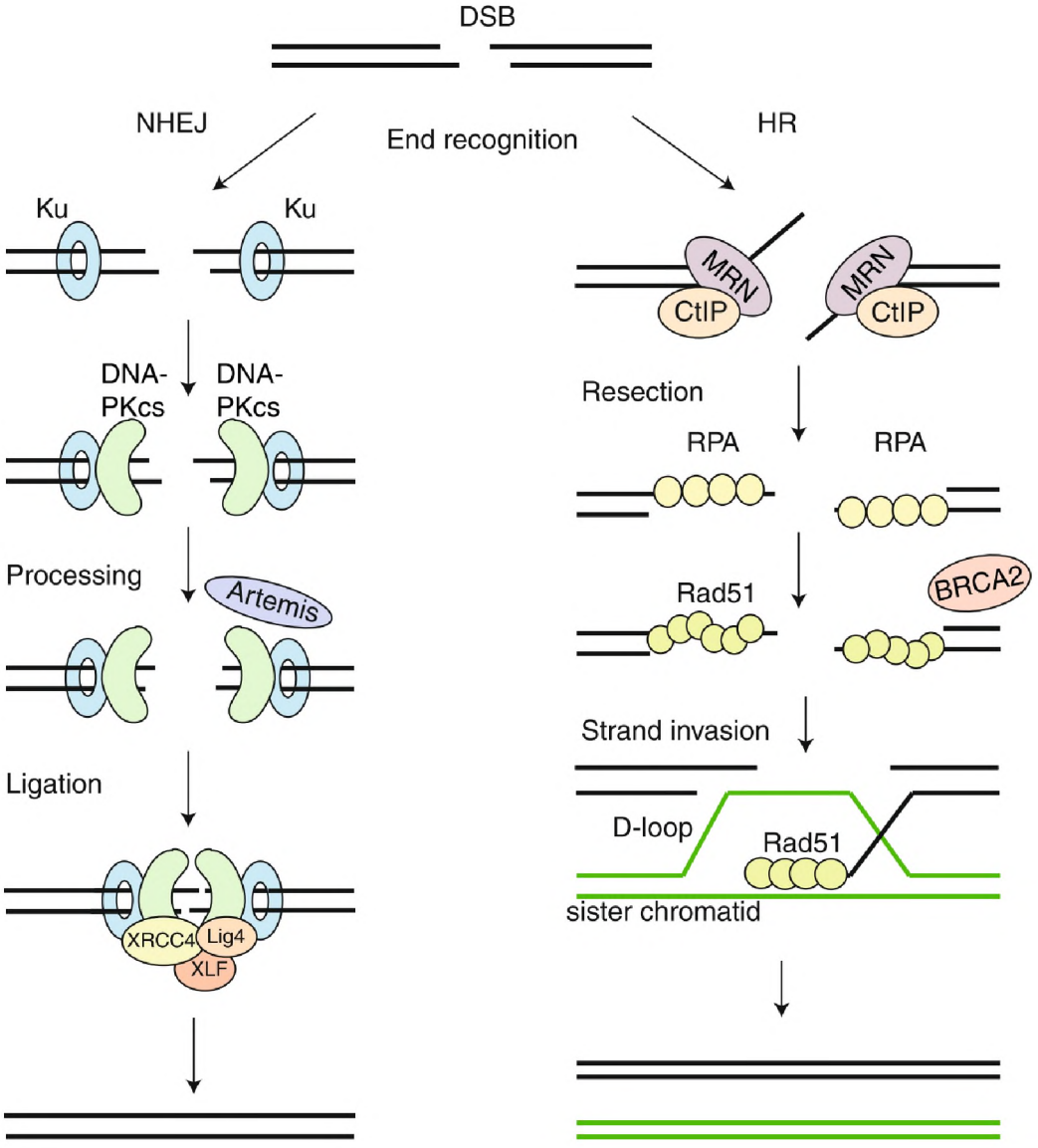


Figure 3.1: **Homologous Recombination and Non-Homologous End Joining.** See text for details. For simplicity only the crucial steps in HR are depicted. Figure adapted from: |222|.

## 3.4 Base Excision Repair and Single-Strand Break Repair

Base Excision Repair (BER) is a highly conserved DNA repair pathway mainly responsible for the correction of endogenous DNA damage (oxidations, alkylations, deaminations, depurinations). BER is usually initiated by a *lesion-specific* DNA glycosylase and completed by one of two sub-pathways - short or long-patch BER (Fig. 3.2) |223|. After lesion recognition, DNA glycosylase removes the modified base and leaves an abasic site. Next, APE1 (apurinic (AP) endonuclease) cleaves the AP site which results in a 3'OH and a 5'deoxyribose-phosphate moiety (5'dRP) at the ends |224|. DNA polymerase then removes the sugar and fills the nucleotide gap. Finally, the strand is ligated by a DNA ligase. The short and long-patch BER sub-pathways *differ in the*

*number of nucleotides incorporated* during the repair: one in the case of SP-BER |225| and two or more nucleotides in LP-BER |226, 227|. The gap filling step in SP-BER is carried out by DNA Polymerase $\beta$ (Pol$\beta$). The same polymerase is also thought to incorporate the first nucleotide in LP-BER |228|, but the elongation step requires the presence of replicative DNA polymerases ($\delta$, $\epsilon$). Additional proteins required in LP-repair are **PCNA (proliferating cell nuclear antigen)** and FEN1, the former serves as a sliding clamp for Pol$\beta$ while the latter removes the ensuing DNA flap. Another protein, **PARP1 (poly (ADP-ribose) polymerase-1)**, was shown to form a complex with APE1, Pol$\beta$ and FEN1 and to stimulate their action. The final step - ligation, is carried out by the XRCC1/LigIII complex in SP-BER |229| and by Ligase I in LP-BER |230|.

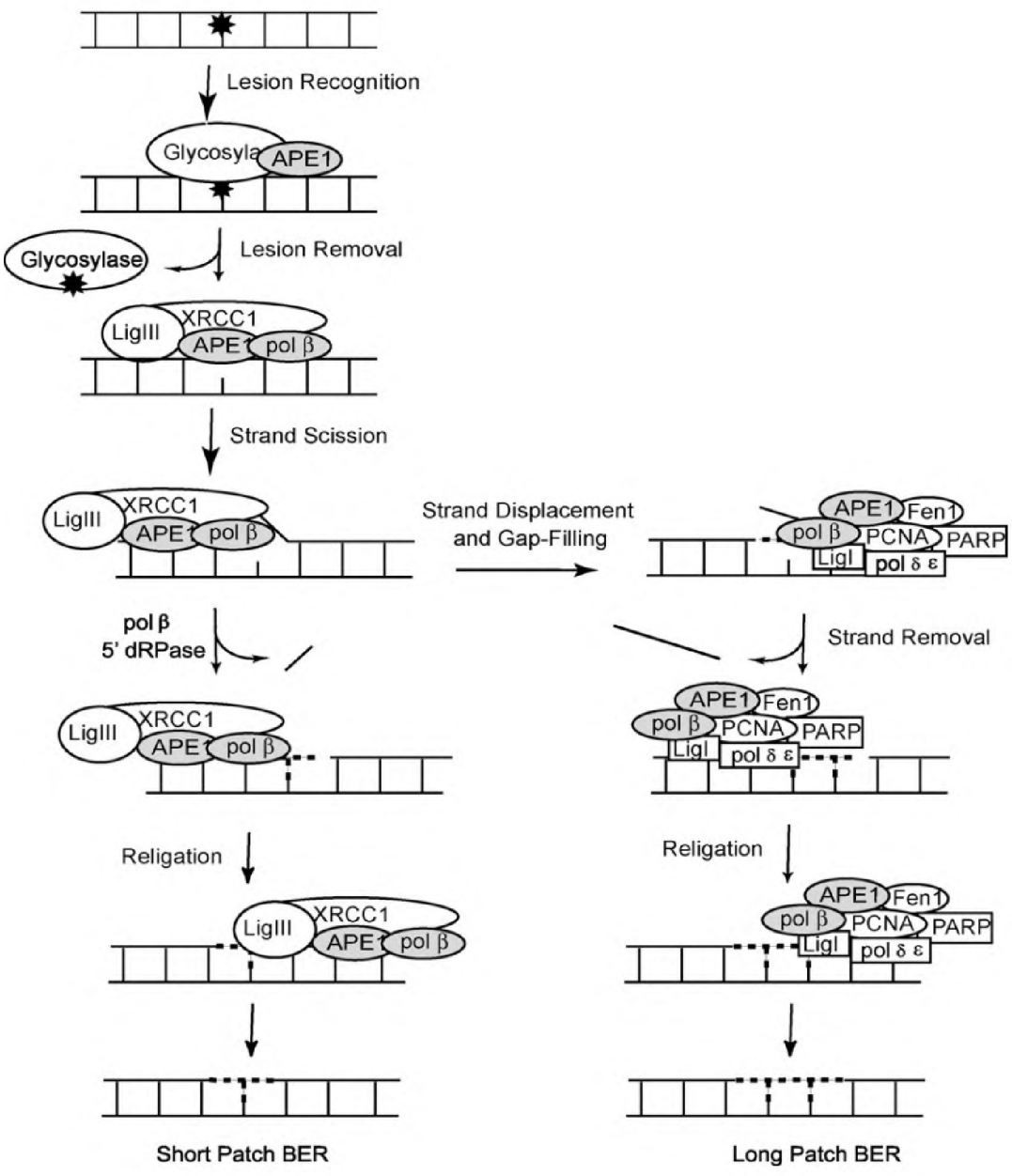


Figure 3.2: **Classic BER pathway.** Figure adapted from |231|.

BER and Single-Strand Break Repair (SSBR) are *closely related* pathways. SSBR is responsible for the repair of both *direct SSBs*, as well as those arising as *BER intermediates* [232,233]. Different sub-pathways exist for the repair of lesions with different origins, yet they share many proteins and biochemical steps (Fig. 3.3). Detection of direct SSBs is thought to be carried out by PARP1 [234]. When activated by binding to DNA breaks, PARP1 modifies itself and a multitude of other proteins by adding chains of **poly(ADP-ribose) (PAR)**. This modification is, however, transient as poly (ADP-ribose) glycohydrolase degrades PAR in minutes after detection of the break by PARP1 [235]. PAR moieties on PARP1 and other proteins are recognized by **XRCC1 (X-ray repair cross complementing protein 1)**, which is then promptly recruited to the damage site [236–238,274]. XRCC1, although without enzymatic activity, acts as a *scaffold* for the binding of other members of the pathway and is thus often regarded as a *central SSBR protein* [239,240]. XRCC1 is especially important during DNA end processing, due to the fact that it interacts with most of the proteins involved in this step: PNKP, APTX, Pol$\beta$ and TDP1. Restoration of modified 3' and 5' termini to conventional ends is often necessary for directly induced SSBs but also some SSBs arising during BER require processing. Subsequent steps of SSBR, i.e. DNA gap filling and ligation are very similar to those observed during BER. The repair can thus be completed by short or long-patch pathways, with Pol$\beta$, Pol $\delta/\epsilon$, LigI and LigIII responsible for these reactions.

The basic steps in BER and SSBR are well established. However, recent years have brought interesting new insights regarding these pathways and revealed their complexity. Many of these studies have taken advantage of introducing a local DNA damage in the nuclei of living cells and then studying the response to this damage. Mortusewicz et al. [238] have shown that both XRCC1 and PCNA are rapidly recruited to DNA damage generated by a 405 *nm* emitting laser in cells presensitised with BrdU (the power of the laser was not specified), but the former protein displays a higher turnover at the irradiated region. The initial transient binding of XRCC1 with subsequent decrease in mobility at the damage site was confirmed in a study by Tomas et al. [242], which utilized multiphoton absorption at 1050 *nm* to generate DNA lesions. Interesting insights regarding SSBR were also brought by Hanssen-Bauer et al. [150]. Irradiation of cells at 405 *nm* revealed that the recruitment of LP-BER proteins (PCNA, FEN1) requires a more extensive damage (higher total dose) than the recruitment of SP-BER factors. Interestingly, PARP1 was recruited to sites of local damage later than XRCC1 and inhibition of PARylation did not cause a significant reduction in the accumulation of XRCC1, questioning the role of PARP1 in early steps of SSBR. On the other hand, in a paper by Campalans et al. [243], the authors have shown that PARP1 is necessary for the recruitment of XRCC1 to damage induced by a 405 *nm* emitting laser in the absence of an exogenous photosensitiser, but is dispensable when the cells are presensitised before irradiation. Since oxidative damage was only detected in the latter scenario, it was concluded that the different requirement of PARP1 for the recruitment of XRCC1 reflects its role in BER and SSBR. Also, the experiments revealed that the BRCT1 domain of XRCC1 is only required for its accumulation in SSBR but not in BER. Important insights concerning XRCC1 in SSBR were also presented in a paper by Wei et al. [244]. The authors have taken advantage of a similar setup for local damage induction (405 *nm*, no photosensitiser) and have been able to show that while BRCT1 domain of XRCC1 is indeed essential for its initial recruitment to the damage

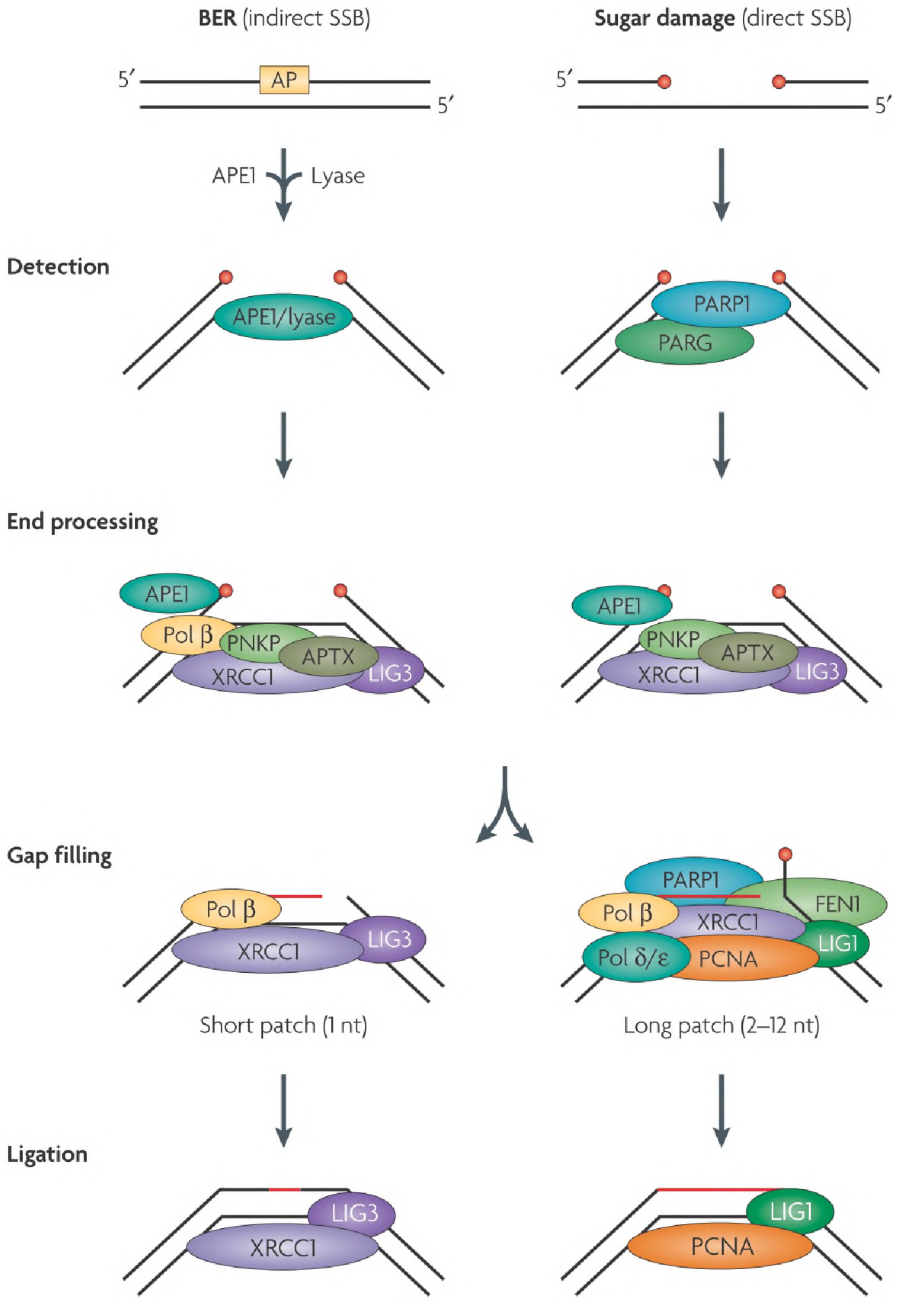


Figure 3.3: **Single-strand break repair.** Figure adapted from [241].

site, its retention is dependent on the BRCT2 domain. The process of accumulation of XRCC1 is supposed to occur in two phases – first, XRCC1 is recruited to sites of PAR synthesized by PARP1, but since PAR is degraded in minutes after the formation of a SSB, XRCC1 dissociates and binds again, this time using its BRCT2 domain.

The above referred papers are extremely valuable for the understanding of the early steps in SSBR and BER. Nevertheless, direct comparison between these studies is difficult. Although seemingly similar damaging setups were used in these experiments (usually laser irradiation at 405 $nm$), no information regarding the power of the laser was revealed (Mortusewicz et al., Campalans et al.) or the specified laser powers and total doses of light delivered to the irradiated region were markedly different (Hanssen-

Bauer et al., Wei et al.). One should note that despite the fact that the difference in laser power between these studies is almost one order of magnitude, both research groups claim that the their conditions induce only SSBs and little or no DSBs. Finally, interpretation of some of these experiments is further complicated by the presence of photosensitisers in damaged cells (Mortusewicz et al., Campalans et al.). In the latter study, the photosensitiser was intentionally used for the induction of oxidative damage, but one cannot ignore the possibility that its presence in the nucleus after damage induction influences the ongoing repair processes. Finally, it is important to note that it is possible that apart from SSBs and DSBs, the 405 $nm$ emitting laser induces also UV photoproducts. This issue was not addressed in either of the cited studies.

# PAPER 1:

## *Inducing local DNA damage by visible light to study chromatin repair*

DNA Repair 11 (2012) 996–1002

Contents lists available at SciVerse ScienceDirect

DNA Repair

journal homepage: www.elsevier.com/locate/dnarepair

Brief communication

# Inducing local DNA damage by visible light to study chromatin repair

Kamil J. Solarczyk, Mirosław Zarębski, Jurek W. Dobrucki*

*Division of Cell Biophysics, Faculty of Biochemistry, Biophysics and Biotechnology, Jagiellonian University, 7, Gronostajowa St., 30-387 Kraków, Poland*

ARTICLE INFO

*Article history:*
Received 15 March 2012
Received in revised form 8 September 2012
Accepted 10 September 2012
Available online 22 October 2012

*Keywords:*
Local DNA damage
Visible light
DNA breaks
H2AX phosphorylation
ATM
RPA
XRCC1
Lig III
PCNA
8-oxodG
TFIIH

ABSTRACT

Dynamics of DNA repair and recruitment of repair factors to damaged DNA can be studied by live cell microscopy. DNA damage is usually inflicted by a laser beam illuminating a DNA-interacting photosensitizer in a small area of the nucleus. We demonstrate that a focused beam of visible low intensity light alone can inflict local DNA damage and permit studies of DNA repair, thus avoiding potential artifacts caused by exogenous photosensitizers.



## 1. Introduction

Dynamics of DNA repair processes, including recruitment of repair proteins to locally damaged DNA, can be studied in live cells using optical microscopy techniques. When DNA damage is inflicted in a small region of a nucleus, recruitment and dissociation of repair factors (tagged with fluorescent proteins) can be visualized and analyzed quantitatively. Most existing methods of inflicting local chromatin damage involve the use of a DNA-bound photosensitizer [1–9]. The presence of a sensitizing agent is undesirable, however, since it may alter higher order chromatin structures, interfere with the process of DNA repair and cause additional damage as well as photodamage during imaging of the repair processes [8,10–12]. Although photosensitizer-free methods of inflicting local damage exist, they employ UV laser microbeam [13], pulsed visible or NIR lasers that often cause collateral damage, i.e. a broad spectrum and large numbers of DNA lesions in and around the illuminated area [8,14–16]. Some high power and pulsed lasers have been shown to cause such an extensive nuclear damage that morphological changes were readily detectable even by phase contrast microscopy [14,15,17]. These observations suggest that such a damage may be so extensive as to raise concern about the relevance of the experiment to studies of cellular response to sublethal genome lesions [7].

We report that local DNA damage can be inflicted by low intensity visible light, in the absence of any exogenous photosensitizers. This method of inducing DNA damage permits studies of recruitment of repair factors while any potential artifacts arising from interaction between photosensitizers and DNA or the repair machinery can be avoided.

## 2. Materials and methods

### 2.1. Cell culture and transfection

HeLa 21-4 cells were maintained in DMEM (Sigma–Aldrich) supplemented with 10% fetal bovine serum (FBS) (Gibco, UK) at 37 °C and 5% $CO_2$. 1 or 2 days before experiment cells were seeded on 20 mm-diameter coverslips (Menzel; Braunschweig, Germany) and imaged in DMEM/F12 (Sigma–Aldrich, Poznań, Poland) supplemented with 2% FBS. 24–48 h after seeding, cells in logarithmic growth phase were transfected with pmRFP-XRCC1 or LigIII-GFP plasmid [18,19] using FuGene 6 transfection reagent (Roche; Basel, Switzerland), according to the manufacturer's instructions, cultured for 48 h and imaged.

* Corresponding author. Tel.: +48 12 6646382; fax: +48 12 6645503.
*E-mail address:* jerzy.dobrucki@uj.edu.pl (J.W. Dobrucki).

1568-7864/$ – see front matter © 2012 Elsevier B.V. All rights reserved.
http://dx.doi.org/10.1016/j.dnarep.2012.09.008

### 2.2. Immunofluorescence

After damage induction cells were incubated under standard conditions in order to allow the repair factors to accumulate (γH2AX: 15–45 min, pATM: 10 min, RPA: 2 h, XRCC1 and PCNA: 5 min, TFIIH: 30 min), fixed (15 min) in 4% formaldehyde (EMS, Hatfield, PA), permeabilized (5 min) with 0.1% Triton X-100 (Sigma, Poznań, Poland), blocked (30–60 min) in 3% BSA (Sigma, Poznań, Poland) and incubated with primary (1 h) and secondary antibodies (2 h). Antibody dilutions were prepared in 1% BSA in PBS, washes were done with PBS. For 8-oxodG detection cells were fixed (15 min, 4 °C) in methanol:acetone (1:1), permeabilized (5 min) with 0.5% Triton X-100 and treated with 2 M HCl (30 min) for antigen retrieval (DNA denaturation). Blocking step, washes and antibody dilutions were prepared in PBT (PBS, 0.05% Tween-20 (Sigma, Poznan, Poland) and 1% BSA, pH 7.8). For PCNA staining cells were treated with 0.25% Triton X-100 (15 min, 4 °C) and then fixed (15 min) in methanol (−20 °C). All procedures were carried out at room temperature, unless otherwise stated. Primary antibodies were: mouse anti-phospho-H2A.X, Ser 139 (clone JBW301; Upstate/Millipore, Billerica, MA), mouse anti-pATM, Ser 1981 (clone 10H11.E12; Millipore, Billerica, MA), mouse anti-RPA, p32 (ab16850; Abcam, Cambridge, UK), rabbit anti-XRCC1 (ab9147; Abcam, Cambridge, UK), mouse anti-PCNA (PC10, sc-56, Santa Cruz Biotechnology, Santa Cruz, CA), mouse anti-TFIIH (p62, sc25329, Santa Cruz Biotechnology, Santa Cruz, CA), mouse anti-8-oxo-dG (clone N45.1; Japan Institute for the Control of Aging, Shizuoka, Japan). Secondary antibodies were: goat anti-mouse Alexa Fluor 488 and goat anti-rabbit Alexa Fluor 488 (A11001 & A11034, Invitrogen, Carlsbad, CA).

### 2.3. Local DNA damage induction

Local DNA damage was introduced on Leica TCS SP5 II confocal microscope equipped with a 63× NA 1.4 oil immersion lens using the FRAP Wizard implemented in LAS AF (Leica Microsystems, Wetzlar, Germany). The laser beam was scanning only the defined region and the time between subsequent scans was minimized. A region of approximately 2.7 μm × 2.4 μm was scanned with 488 nm light at a resolution set to 512 × 512 pixels (the actual pixel number was 512 × 414 since the chosen region was a rectangle) and a scanning speed of 200 lines/s was used (the pixel dwell time was 2.88 μs). The total dose delivered during one exposure (understood as scanning one full frame, i.e. 414 lines at this pixel number) of the 488 nm light was approximately 3.4 mJ. A minimum of 5 exposures (17 mJ) were necessary to induce detectable γH2AX signal. For the induction of spatially confined damage a spot in the nucleus was chosen and the laser beam was parked there from 2 to 20 s. A line-shaped area of damage was induced using the FRAP XT Wizard. A line of approximately 7 μm (110 pixels) was repeatedly scanned with a frequency of 10 lines/s (57.6 μs pixel dwell time). A minimum of 200 scans were necessary to induce detectable γH2AX signal.

### 2.4. Confocal imaging

Cells were imaged using Leica TCS SP5 II confocal microscope equipped with a 63× NA 1.4 oil immersion lens. For live cell experiments (including local damage induction) the cultures were maintained at 37 °C in DMEM/F12 without Phenol Red buffered for air (pH 7.0) and supplemented with 2% FBS. Fixed cells were imaged in PBS. Images (8 bit) were acquired at 512 × 512 or 1024 × 1024 pixel resolution, at a speed of 200 lines/s (2.88 or 1.44 μs pixel dwell time, respectively), with 1–3 frames averaged. The voxel size was 32 nm × 32 nm × 420 nm for immunofluorescence and pmRFF-XRCC1 images and 64 nm × 64 nm × 420 nm for LigIII-GFP image. For GFP and Alexa Fluor 488 excitation the 488 nm line (argon gas laser) was used and fluorescence emission was collected in the range of 510–610 nm. Laser power was measured with a parked beam, at the focal plane of the objective with a Thorlabs PM100 power meter equipped with S130A sensor head. For the 488 nm laser line and the maximum intensity transmitted the measured power was 5.7 mW. Approximately 1–6% of the maximum power was used for image acquisition and approximately 30% for the damage induction.

### 2.5. Image processing

Fluorescence images of γH2AX are maximum projections of 3D stacks, other fluorescence images are single confocal planes. All images were processed using ImageJ (http://imagej.nih.gov/ij/). The background noise was reduced in all fluorescence images by histogram stretching (the lowest 6% of a histogram). The contrast was improved using gamma correction, as described in figure legends. In transmitted light images the contrast was also improved by histogram stretching. All these operations were applied to whole images. Insets were additionally processed with an averaging filter (3 × 3) and rescaled.

## 3. Results

Visible light is not absorbed by DNA thus it is generally thought to cause no direct DNA damage. We report here that we detected sublethal DNA damage in cells exposed to a focused laser beam of low intensity (1.7 mW). Such a beam of focused light is readily available on a typical confocal microscope; it can be used for confocal imaging, FRAP or FLIP experiments. To assess the type and level of damage introduced with focused beam of low-power visible laser light we conducted a series of immunofluorescence and live cell experiments. Subnuclear region of approximately 2.7 μm × 2.4 μm was scanned with a focused beam of blue (488 nm, 1.7 mW) light. 30 min after the light exposure cells were fixed and immunolabeled for a phosphorylated histone H2AX, a marker of DNA double strand breaks (DSBs) [3,5]. Formation of phosphorylated histone H2AX foci indeed occurred in the illuminated region, suggesting that DSBs have been generated. Five exposures using the 488 nm laser beam were sufficient to induce a detectable γH2AX (phosphorylation) signal (Fig. 1a). 66 foci in the illuminated region were found, while the average number of endogenous damage foci in similar unilluminated regions was 18. 20 exposures resulted in numerous DNA breaks (at least 148 foci; note that this number is underestimated since some foci overlap) and a correspondingly bright fluorescence in the illuminated region (Fig. 1b). The latter procedure was chosen as the standard for further experiments. Phosphorylation of histone H2AX was also detected following irradiation with 405 nm (170 μW) and 514 nm (1.7 mW) laser beams (data not shown). Formation of DNA double strand breaks by visible light was confirmed by immunodetection of recruitment of known DDR (DNA damage response) signaling and repair factors, phosphorylated ATM and RPA, into the previously illuminated region (Fig. 2a and b).

In order to further define the type of lesions created by exposure to a focused beam of visible laser light, we investigated recruitment of XRCC1 and Lig III, i.e. single strand break repair factors, to the illuminated area. Local accumulation of XRCC1 was revealed by immunofluorescence (Supplementary Fig. 1) as well as live cell imaging using a fluorescent tag with negligible absorption in the blue region (Fig. 2c), i.e. it could not have played a role of a photosensitizer. A rapid recruitment of LigIII-GFP protein was also demonstrated by live cell experiments (Fig. 2d). Moreover, immunofluorescence revealed a higher local concentration of PCNA in the illuminated spot (Fig. 2e). Since these repair factors are also

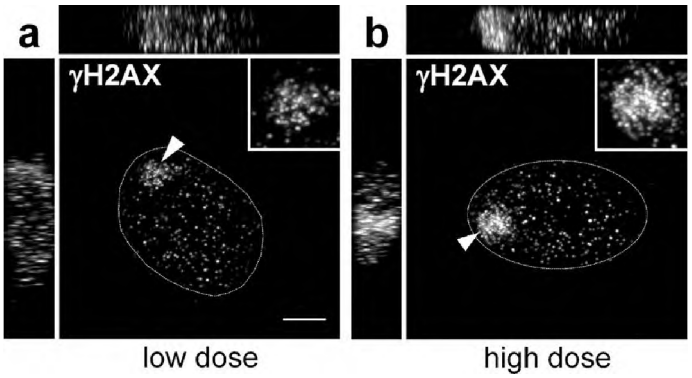


**Fig. 1.** Detection of local DNA damage caused by blue light in the absence of exogenous photosensitzers. Phosphorylation of histone H2AX, which marks DNA breaks (arrowhead), in response to 5 (a) and 20 (b) exposures elicited by the 488 nm laser beam. Inset – enlargement of the damaged area. A horizontal and vertical cross-section of the 3D image in the damaged area is shown. Scale bar – 2 μm.

involved in BER, a pathway which responds to oxidative damage, we investigated generation of oxidized guanine residues following local illumination. No significant 8-oxodG immunostaining was found in the region subjected to a focused beam of blue light, hinting at the absence of any detectable oxidative damage (Fig. 2g). Such lesions were readily created in a positive control experiment, i.e. in the presence of an intracellular photosensitizer, ethidium, as shown in Fig. 3. Finally, to check if any UV-specific damage was created, we performed immunofluorescence against TFIIH, a factor known to be involved in NER pathway. No TFIIH recruitment to the damaged region was detected (Fig. 2h). In these experiments no nuclear damage was detected by standard transmitted light microscopy (Fig. 2f and Supplementary Fig. 1) thus artifacts resulting from an excessive light dose, which were discussed previously [7,14,15] did not occur. Taken together, these data suggest that the only type of detectable DNA damage induced by a focused beam of low-power visible laser light were DNA strand breaks.

To examine the severity of the induced damage and cellular ability to complete the repair process, local DNA lesions were induced in 5 interphase cells, which were subsequently filmed for 11 h (Supplementary Movie 1). Upon irradiation we did not detect any morphological changes in the illuminated region or other parts of the nucleus. Three of the damaged cells entered mitosis (one after approximately 6 and two after 10 h). Two of these cells completed the division during recording; this suggests that the damage has been repaired. The fact that the repair process proceeded successfully was further confirmed by a decrease in the number of γH2AX foci in the illuminated region that were detected at different time points after inducing local damage (Fig. 4a and b).

## 4. Discussion

The method of inducing local DNA damage with a beam of focused low power visible laser light that is described above may facilitate studies of DNA damage and repair in several ways. Potential artifacts arising from interactions between a photosensitizer with DNA and photodamage effects inflicted during imaging of the repair processes are eliminated. The lesions are well defined, thus DNA strand break repair mechanisms can be studied, while other repair pathways are not activated. Finally, the possibility to induce local DNA damage with a low-power laser typically used in confocal microscopes makes this method immediately accessible for every confocal user. Laser beam power adjustment permits control over the severity of the damage, while different scanning modes make it possible to vary the size and shape of the damaged subnuclear region (Fig. 5 and Supplementary Fig. 2).

Unfortunately, the data reported here constitute a warning that DNA breaks can be induced in live cell imaging experiments when the intensity of exciting visible light reaches the level of 1–2 mW. This is especially important for FRAP and FLIP experiments, where a high laser power is employed during the bleaching phase of the experiment. DNA damage induction is probably unavoidable in FRAP experiments when the beam is parked in a selected spot of the nucleus ('single-point' bleach). We report phosphorylation of histone H2AX after parking the beam for 2 s (Fig. 5), but even 500 ms were sufficient to induce pmRFP-XRCC1 recruitment to the bleached point (data not shown). Thus, our data indicate that special care is needed in executing and interpreting FRAP experiments.

Inducing DNA damage by visible light under different experimental conditions was reported previously, but there is no agreement on the mechanism or nature of the lesions. For instance when CHO cells were irradiated with 434 nm light at 560 W/m$^2$ (a total dose of 1 MJ/m$^2$) at 0.5 °C, induction of DNA single strand breaks was detected [20]. A 20 min illumination of L1210 mouse leukemia cell suspension with light in the range of 400 and 800 nm (450 kJ/m$^2$) emitted by a 1000 W halogen lamp, in a shallow dish on ice, resulted in DNA oxidative modifications, and much less numerous single strand DNA breaks [21]. Also, in human melanoma cells exposed to a broad range of visible light wavelengths, induction of oxidative damage but also a low number of single strand breaks were detected [22]. However, 24, 48 and 74 h exposures of cells in multiwell dishes to visible light emitted by an 8 W strip-light led to induction of strand breaks detected by TUNNEL assay [23]. Conspicuously, when isolated plasmids were exposed to visible light, double strand breaks were also induced [23]. These reports can be interpreted as evidence in favor of a notion that when cell cultures are exposed to visible light in the blue region (400–500 nm) that illuminates a large volume of the sample and all components of the cell, the oxidized flavin derivatives in cytoplasm act as photosensitizers and initiate a chain of reactions that lead to oxidative damage inflicted on various cell components, including DNA. Although the authors of the report [21] suggest that an unknown endogenous nuclear photosensitizer may exist, we are not aware of any reports confirming this suspicion. In contrast to the experiments cited above, when a focused laser beam is used to induce local damage, as in our experiments, the probability of oxidizing flavins in mitochondria adjacent to the nucleus is low. This can explain the absence of oxidative damage to nitrogen bases in our experiments. However, why are DNA breaks induced under such conditions? DNA damage

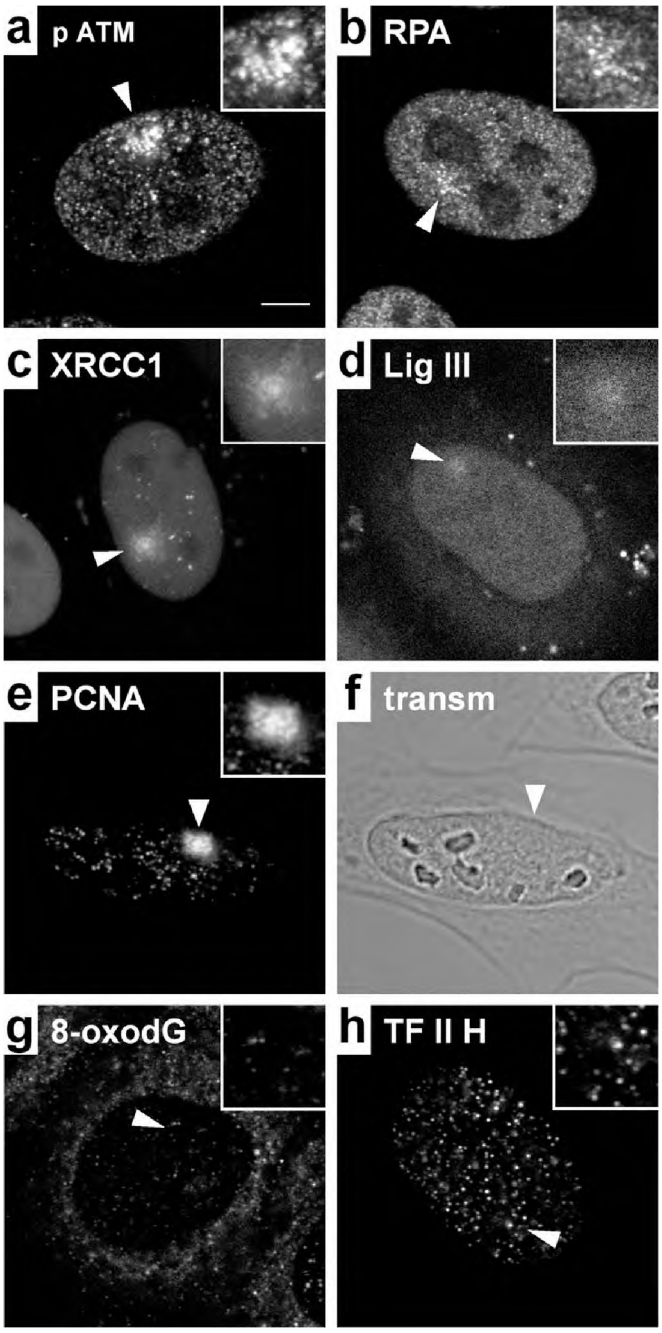


**Fig. 2.** DNA damage response in the region of the nucleus which was damaged by blue light. Hela cells were locally illuminated with 488 nm laser light (arrowhead), fixed and processed for immunofluorescence (a, b, e, g and h) or studied for the recruitment of RFP and GFP-tagged repair factors (c and d). Recruitment of phoshorylated ATM (a) and DSB repair factor RPA (b), SSB repair factors XRCC1 (c), Lig III (d; recruitment occurs within 3 min after exposure to blue light) and PCNA (e) is detected. No guanine oxidation is detected after exposure to blue light, in the absence of a photosensitizer (g; see also Fig. 3 for a positive control); no recruitment of NER associated protein TFIIH is detected, either (h). Scale bar – 2 μm. Gamma function: (c, e – 0.7; a – 0.8, d – 0.85; b, g h – 1.5). Histogram stretching was used in panel (d).

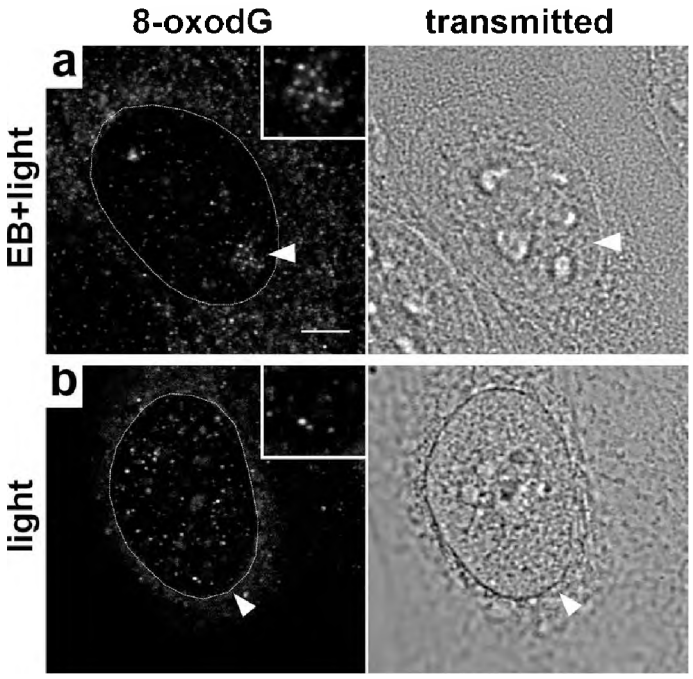


**Fig. 3.** Visible light causes oxidative DNA damage only in the presence of an exogenous photosensitizer. HeLa cells were incubated with ethidium bromide (400 nM, 20 min; a), or without ethidium (b), washed and locally illuminated with 514 nm light, which excites ethidium (20 exposures) (a) or 488 nm light (20 exposures) (b). After exposure to light cells were fixed and immunostained for 8-oxodG. No oxidation of guanine residues is detected in cells illuminated without a photosensitizer. Scale bar – 2 μm. Gamma function: 0.7.

resulting from a direct interaction of 488 nm photons with DNA seems unlikely since DNA does not absorb light of this wavelength. Two-photon excitation and free radical mechanism resulting from absorption of photons by water, and subsequent damage inflicted on DNA should be considered as possible mechanisms.

Two-photon excitation by blue light emitted by a pulsed laser induced UV damage in isolated DNA [24]. The incident laser powers used in these experiments were greater than 100 mW, and the peak irradiance which was used to induce two-photon photodamage was approximately 0.704 TW/cm$^2$. The authors note that in a typical cell imaging system that employs 1.2 numerical aperture lens the expected peak irradiance is not significantly different, since the power reaches 4–5 mW. In our experiments the mean irradiance in a focal spot was in the order of 1 MW/cm$^2$. We have not observed recruitment of a NER factor TFIIH. Based on these considerations two-photon excitation of DNA leading to the DNA strand breaks observed in our experimental system seems unlikely.

Flash photolysis of water using UV light is well documented. Absorption coefficient of water at 488 nm is approximately $1.5 \times 10^{-4}$/cm, therefore a possibility of creating a low number of free radicals via this mechanism cannot be ruled out considering the intensity of the focused blue light involved. Such a mechanism

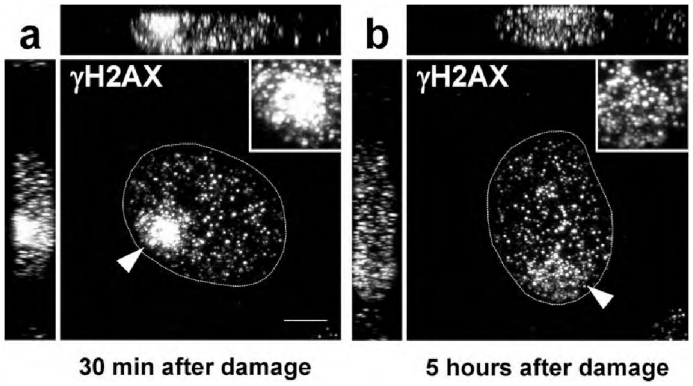


**Fig. 4.** Repair of light-induced damage, demonstrated by a decrease in the number of γH2AX foci at the damaged area in cells fixed at different times (30 min and 5 h) following the induction of damage (20 exposures, 488 nm). Insets – enlargements of the damaged areas. Horizontal and vertical cross-sections of the 3D images in the damaged area are shown. Scale bar – 2 μm.

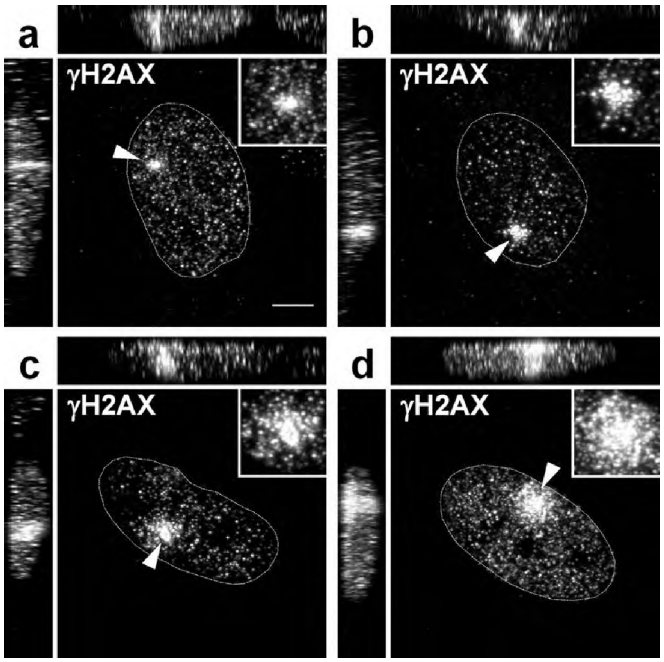


**Fig. 5.** Induction of spatially confined DNA damage as a function of the light dose. Phosphorylation of histone H2AX is detected after parking the laser beam (488 nm) in the selected spot in the nucleus of a HeLa cell for 2 s (a), 5 s (b), 10 s (c) and 20 s (d). Insets – enlargements of the damaged areas. Horizontal and vertical cross-sections of the 3D images in the damaged area are shown. Scale bar – 2 μm.

might also explain the observation of the damage inflicted on isolated plasmids by visible light [23]. However, because of a lack of sufficient experimental evidence, the mechanism of inflicting DNA breaks by focused blue light remains unknown and requires further studies. Finally, it is important to note that our considerations outlined above refer to DNA damage caused by 488 nm light. The mechanism of damage caused by 405 nm or 514 nm light that we also observed may include other components, since water absorption at 405 nm is 3 times lower, while at 514 nm is almost 3 times higher than at 488 nm. Moreover, induction of a low level damage typical for UV cannot be excluded when the 405 nm focused light interacts with DNA.

## 5. Conclusion

We report here that local DNA damage can be inflicted using a low-power laser beam (approximately 1.7 mW) typically used in confocal microscopes, in the absence of any exogenous photosensitizers. This approach permits studies of DNA repair in the absence of potential artifacts that would arise from interactions of a photosensitizer with DNA and the repair machinery during imaging of the repair processes. Immunofluorescence and live cell experiments suggest that the only type of DNA lesion induced by this method is DNA breaks. This method of creating local damage can be used to induce a controllable, low number of well defined sublethal lesions.

## Conflict of interest statement

The authors declare that there are no conflicts of interest.

## Acknowledgments

This research was supported by Jagiellonian University and National Committee for Science (UMO-2011/01/B/NZ3/00609). The confocal instrumentation was purchased through an EU structural funds grant BMZ no. POIG.02.01.00-12-064/08.

## Appendix A. Supplementary data

Supplementary data associated with this article can be found, in the online version, at http://dx.doi.org/10.1016/j.dnarep.2012.09.008.

## References

[1] T. Cremer, S. Peterson, C. Cremer, M. Berns, Laser microirradiation of Chinese Hamster cells at wavelength 365 nm: effects of psoralen and caffeine, Radiat. Res. 85 (1981) 529–543.
[2] C.L. Limoli, J.F. Ward, A new method for introducing double-strand breaks into cellular DNA, Radiat. Res. 134 (1993) 160–169.
[3] E.P. Rogakou, C. Boon, C. Redon, W.M. Bonner, Megabase chromatin domains involved in DNA double-strand breaks in vivo, J. Cell Biol. 146 (1999) 905–916.
[4] S. Tashiro, J. Walter, A. Shinohara, N. Kamada, T. Cremer, Rad51 accumulation at sites of DNA damage and in postreplicative chromatin, J. Cell Biol. 150 (2000) 283–292.
[5] A. Celeste, O. Fernandez-Capetillo, M.J. Kruhlak, D.P. Pilch, D.W. Staudt, A. Lee, R.F. Bonner, W.M. Bonner, A. Nussenzweig, Histone H2AX phosphorylation is dispensable for the initial recognition of DNA breaks, Nat. Cell Biol. 5 (2003) 675–679.
[6] P.S. Bradshaw, D.J. Stavropoulos, M.S. Meyn, Human telomeric protein TRF2 associates with genomic double-strand breaks as an early response to DNA damage, Nat. Genet. 37 (2005) 193–197.
[7] S. Bekker-Jensen, C. Lukas, R. Kitagawa, F. Melander, M.B. Kastan, J. Bartek, J. Lukas, Spatial organization of the mammalian genome surveillance machinery in response to DNA strand breaks, J. Cell Biol. 173 (2006) 195–206.

[8] C. Dinant, M. de Jager, J. Essers, W.A. van Capellen, R. Kanaar, A.B. Houtsmuller, W. Vermeulen, Activation of multiple DNA repair pathways by sub-nuclear damage induction methods, J. Cell Sci. 120 (2007) 2731–2740.
[9] M. Zarebski, E. Wiernasz, J.W. Dobrucki, Recruitment of heterochromatin protein 1 to DNA repair sites, Cytometry A 75 (2009) 619–625.
[10] P.R. Turner, W.A. Denny, The mutagenic properties of DNA minor-groove binding ligands, Mutat. Res. 355 (1996) 141–169.
[11] C.M. White, O. Heidenreich, A. Nordheim, T.A. Beerman, Evaluation of the effectiveness of DNA-binding drugs to inhibit transcription using the c-fos serum response element as a target, Biochemistry 39 (2000) 12262–12273.
[12] K. Wojcik, J.W. Dobrucki, Interaction of a DNA intercalator DRAQ5, and a minor groove binder SYTO17, with chromatin in live cells – influence on chromatin organization and histone–DNA interactions, Cytometry A 73 (2008) 555–562.
[13] C. Cremer, T. Cremer, M. Fukuda, K. Nakanishi, Detection of laser-UV microirradiation-induced DNA photolesions by immunofluorescence staining, Hum. Genet. 54 (1980) 107–110.
[14] J.S. Kim, T.B. Krasieva, V. LaMorte, A.M. Taylor, K. Yokomori, Specific recruitment of human cohesin to laser-induced DNA damage, J. Biol. Chem. 277 (2002) 45149–45153.
[15] X. Kong, S.K. Mohanty, J. Stephens, J.T. Heale, V. Gomez-Godinez, L.Z. Shi, J. Kim, K. Yokomori, M.W. Berns, Comparative analysis of different laser systems to study cellular responses to DNA damage in mammalian cells, Nucleic Acids Res. 37 (2009) e68.
[16] D. Träutlein, M. Deibler, A. Leitenstorfer, E. Ferrando-May, Specific local induction of DNA strand breaks by infrared multi-photon absorption, Nucleic Acids Res. 38 (2010) e14.
[17] M.W. Berns, W.K. Cheng, A.D. Floyd, Y. Onuki, Chromosome lesions produced with an argon laser microbeam without dye sensitization, Science 171 (1971) 903–905.
[18] O. Mortusewicz, U. Rothbauer, M.C. Cardoso, H. Leonhardt, Differential recruitment of DNA Ligase I and III to DNA repair sites, Nucleic Acids Res. 34 (2006) 3523–3532.
[19] O. Mortusewicz, L. Schermelleh, J. Walter, M.C. Cardoso, H. Leonhardt, Recruitment of DNA methyltransferase I to DNA repair sites, Proc. Natl. Acad. Sci. U.S.A. 102 (2005) 8905–8909.
[20] M. Churchill, J. Peak, M. Peak, Repair of near-visible and blue-light induced DNA single-strand breaks by the CHO cell lines AA8 & EM9, Photochem. Photobiol. 54 (1991) 639–644.
[21] M. Pflaum, S. Boiteux, B. Epe, Visible light generates oxidative DNA base modifications in high excess of strand breaks in mammalian cells, Carcinogenesis 15 (1994) 297–300.
[22] S. Hoffmann-Dorr, R. Greinert, B. Volkmer, B. Epe, Visible light (>395 nm) causes micronuclei formation in mammalian cells without generation of cyclobutane pyrimidine dimmers, Mutat. Res. 572 (2005) 142–149.
[23] G.Y. Li, B. Fan, T.H. Ma, Visible light may directly induce nuclear DNA damage triggering the death pathway in RGC-5 cells, Mol. Vis. 17 (2011) 3279–3289.
[24] M.A. Tycon, A. Chakraborty, C.J. Fecko, Generation of DNA photolesions by two-photon absorption of a frequency-doubled Ti:sapphire laser, J. Photochem. Photobiol. B: Biol. 102 (2) (2011) 161–168.

# PAPER 2:

***Two stages of XRCC1 recruitment and two classes of XRCC1 foci formed in response to low level DNA damage induced by visible light, or stress trigerred by heat shock***

DNA Repair 37 (2016) 12–21

Contents lists available at ScienceDirect

DNA Repair

journal homepage: www.elsevier.com/locate/dnarepair

# Two stages of XRCC1 recruitment and two classes of XRCC1 foci formed in response to low level DNA damage induced by visible light, or stress triggered by heat shock

Kamil J. Solarczyk, Magdalena Kordon, Krzysztof Berniak, Jurek W. Dobrucki *

*Division of Cell Biophysics Faculty of Biochemistry, Biophysics and Biotechnology, Jagiellonian University ul. Gronostajowa 7, 30-387 Kraków, Poland*

ARTICLE INFO

*Article history:*
Received 13 August 2015
Received in revised form 13 October 2015
Accepted 13 October 2015
Available online 2 November 2015

*Keywords:*
DNA damage
DNA repair
Light-induced DNA damage
XRCC1
Sp-100
RIF
Repair foci
PML
Poly (ADP-ribose)

ABSTRACT

Induction of local photosensitised DNA damage has been used to study recruitment of repair factors, spatial organisation and subsequent stages of the repair processes. However, the damage induced by a focused laser beam interacting with a photosensitiser may not fully reflect the types of damage and repair encountered in cells of an animal under typical conditions in vivo. We report on two characteristic stages of recruitment of XRCC1 (a protein engaged in BER and SSB repair pathways), in response to low level DNA damage induced by visible light. We demonstrate that, when just a few DNA breaks are induced in a small region of the nucleus, the recruited XRCC1 is initially distributed uniformly throughout this region, and rearranges into several small stationary foci within minutes. In contrast, when heavy damage of various types (including oxidative damage) is induced in cells pre-sensitized with a DNA-binding drug ethidium bromide, XRCC1 is also recruited but fails to rearrange from the stage of the uniform distribution to the stage of several small foci, indicating that this heavy damage interferes with the progress and completion of the repair processes. We hypothesize that that first stage may reflect recruitment of XRCC1 to poly(ADP-ribose) moieties in the region surrounding the single-strand break, while the second-binding directly to the DNA lesions. We also show that moderate damage or stress induces formation of two types of XRCC1-containing foci differing in their mobility. A large subset of DNA damage-induced XRCC1 foci is associated with a major component of PML nuclear bodies - the Sp100 protein.



## 1. Introduction

In recent years, introduction of several techniques of inducing DNA damage, which is confined to a small region of the cell nucleus, has boosted the field of DNA repair [1–4]. A number of proteins have been shown to be recruited to locally inflicted DNA damage, and their kinetics and interactions have been studied extensively. However, some concern has been voiced regarding the relevance of the local lesions, which are usually induced by a combination of focused laser light and exogenous photosensitisers, with respect to naturally occurring DNA damage. The main reservations stem from the fact that laser-based techniques often lead to massive DNA damage and activation of multiple DNA repair pathways [5,6].

A variety of techniques or agents, capable of inducing DNA damage distributed randomly throughout the whole nucleus, have also been used [7]. DNA lesions induced in many locations within the whole nuclear volume are usually manifested by formation of so-called Radiation Induced Foci (RIF) [7–9]. These foci, representing local accumulation of repair proteins, are thought to be formed at the sites of double- as well as single-strand DNA breaks [10].

Interestingly, the small foci rich in repair factors, of the type that are formed in response to ionizing radiation affecting the whole cell, are usually not observed after laser-induced local damage. In the majority of published microscopic images, repair proteins recruited to the damaged region (as well as phosphorylated histone H2AX [5,11–15]) are evenly distributed and remain there in a form of a diffused, cloud-like region [1,11,12]. The cause of this difference between spatial patterns of DNA repair proteins and markers in IR-like and laser-induced damage is unclear, but it is plausible that the density of the induced lesions is the major factor involved. Immediate induction of hundreds of double-strand breaks, and possibly

*Abbreviations:* BER, base excision repair; DSB, double-strand DNA break; IF, immunofluorescence; mJ, milliJoul; MMS, methyl methane sulfonate; NB, nuclear (subnuclear) body; PAR, poly(ADP-ribose); PML, promyelocytic leukemia; RIF, radiation-induced foci; SSB, single-strand DNA breaks; RFP, red fluorescent protein; XRCC1, X-ray repair cross-complementing protein 1.

* Corresponding author. Fax: +48 12 664 55 03.
*E-mail address:* jerzy.dobrucki@uj.edu.pl (J.W. Dobrucki).

http://dx.doi.org/10.1016/j.dnarep.2015.10.006
1568-7864/

even more lesions of other types (including photo-oxidised bases and single-strand breaks) by a focused laser beam, all within a small nuclear volume, is practical as it facilitates microscopy detection of the damage site. However, induction of such an extensive damage leading to accumulation of multiple copies of fluorescently tagged DNA repair proteins raises doubts regarding the ability of cells to repair this damage, and exposes the experimenter to a risk of missing important clues concerning spatial organization of the DNA damage response.

One of the best examples of the influence of damaging conditions on spatial organisation of DNA repair processes is provided by recruitment of XRCC1, a protein engaged in BER and SSB repair pathways [16–24]. Rapid recruitment of XRCC1 to locally induced DNA damage has been demonstrated in many studies [19,25–27]. XRCC1 begins to accumulate at the damage site within seconds, and reaches its maximum concentration within minutes after induction of local damage [19]. Similarly to other DNA repair factors, XRCC1 tagged with a fluorescent protein usually forms a cloud-like pattern at the site of local laser-induced damage [19,26,28]. There is evidence, however, that this protein can also form a pattern of foci in response to local DNA damage. XRCC1 foci have been observed after treatment with various agents - MMS[26], $H_2O_2$ [29], $KBrO_3$[27], ionizing radiation [10] or even after siDNA introduced to cells to mimic single-strand breaks [30]. Recently, it has been shown that XRCC1 can form foci after illumination with a low intensity 405 nm light [31] (in the absence of exogenous photosensitisers), as well as in the vicinity of regions illuminated with a UV-laser [32]. All these observations, combined with the fact that some XRCC1 foci can also be found in nuclei of cells grown under physiological conditions, indicate that accumulation of multiple copies of XRCC1 in a small focus in the nucleus is functionally important, but the architecture and role of these structures, and the influence of damaging conditions on their formation, remain unclear. The goal of this work was to image recruitment of XRCC1 to localized, low level DNA damage induced by visible light in order to provide new insights into the spatial patterns formed by the accumulated protein within the damage site. We demonstrate that initially the concentration of XRCC1 is uniform throughout the previously illuminated region, within minutes, however, XRCC1 is drawn into several small stationary foci. In contrast, when heavy damage of various types (including oxidative damage) is induced in cells presensitized with ethidium bromide, XRCC1 is also recruited but fails to rearrange from the stage of the uniform distribution to the stage of several small foci, indicating that this heavy damage interferes with the progress and completion of the repair processes. Highly mobile as well as almost immobile foci are formed in response to DNA damage induced by visible light or stress triggered by heat shock. A subset of XRCC1 foci is associated with a major component of PML nuclear bodies - the Sp100 protein.

## 2. Materials and methods

### 2.1. Cell culture and transfection

HeLa 21-4 cells were maintained in DMEM (Sigma–Aldrich, D5523) supplemented with 10% fetal bovine serum (FBS) (Gibco, UK, 10,106–169) at 37 °C and 5% $CO_2$. Cells were seeded on 18 mm–diameter coverslips (Menzel–Glaser; Braunschweig, Germany) and after 24 h either imaged in DMEM/F12 (Sigma–Aldrich, Poznań, Poland) supplemented with 2% FBS, or transfected with RFP-XRCC1 and/or GFP-Sp100A plasmid [33] using FuGene 6 transfection reagent (Roche; Basel, Switzerland), according to the manufacturer's instructions, cultured for another 24 h and then imaged.

### 2.1. Immunofluorescence

For the visualisation of PAR and XRCC1, cells were locally damaged using blue light and then incubated under standard conditions (1 and 5 min, respectively) in order to allow the formation of PAR polymers and the recruitment of XRCC1 protein. Then the cells were fixed with 4% formaldehyde (15 min; EMS, Hatfield, PA), permeabilised (10 min) with 0.1% Triton X-100 (Sigma, Poznań, Poland), blocked (30–60 min) in 3% BSA (Sigma, Poznań, Poland) and incubated with primary (1 h) and secondary antibodies (2 h). Antibody dilutions were prepared in 3% BSA in PBS, washes were done with PBS. All procedures were carried out at room temperature. Primary antibodies were: mouse anti-XRCC1 (ab1838; Abcam, Cambridge, UK) and mouse anti-PAR (clone 10H, Enzo Life Sciences). The secondary antibody used was goat anti-mouse Alexa Fluor 488 (A11001, Invitrogen, Carlsbad, CA).

### 2.2. DNA damage induction

Local DNA damage was induced in cells maintained under optimal growth conditions on the stage of Leica TCS SP5 II confocal microscope as described before [34]. Briefly, a region of a nucleus of 2.5 × 2.5 μm was scanned several times (using the FRAP Wizard implemented in LAS AF; Leica Microsystems, Wetzlar, Germany) with 488 nm laser beam (in the absence of exogenous photosensitisers) at a resolution of 512 × 512 pixels and at a scanning speed of 200 lines per second. The total dose of energy delivered by the laser beam to the illuminated region (2.5 × 2.5 μm in the confocal plane when local damage was induced) was 3, 5 or 12 mJ (0.48, 0.8 or 1.92 mJ/μm$^2$). Note that, as in the case of ionising radiation, only a small fraction of this energy is absorbed by cellular components. For induction of local DNA damage in the presence of a photosensitiser, cells were incubated with ethidium bromide (400 nM) for 20 min, then rinsed, and a selected nucleus was illuminated with green laser light (514 nm). The total dose delivered to the illuminated region was 30 mJ (4.8 mJ/μm$^2$).

In order to induce stress throughout the nucleus, cells were subjected to visible (blue or green) light, or treated with heat shock. A 31 × 31 μm region was repeatedly scanned with blue (488 nm) or green (543 nm) light at a resolution of 512 × 512 pixels, at a scanning speed of 400 lines per second. The total dose delivered during this illumination was 20 mJ (0.02 mJ/μm$^2$). In order to induce heat shock a temperature of the medium was raised to 42 °C for 30 min.

### 2.3. Confocal imaging

Images and movies were acquired using Leica TCS SP5 II confocal microscope equipped with a 63x NA 1.4 oil immersion lens. For live cell experiments the cultures were maintained at 37 °C in DMEM/F12, without Phenol Red, buffered for air (pH 7.0) and supplemented with 2% FBS. Fixed cells were imaged in PBS. Images were acquired at 512 × 512 or 1024 × 1024 (8-bit) resolution with up to 3 frames averaged. For GFP and Alexa Fluor 488 excitation the 488 nm line (argon laser) was used and fluorescence emission was collected in the range 510–610 nm. RFP was excited with 561 nm laser line and the emission was collected in the range 570–750 nm. For images of cells with both GFP and RFP present, excitation was performed sequentially, using 488 and 561 nm laser lines, while the emissions were collected at 500–530 and 660–750 nm bands, respectively. The light intensities used for live cell imaging were in the range 0.24–0.35 mW (i.e. one order of magnitude weaker than the laser beam used for inducing local damage), and the doses of energy delivered to the whole field of view, while collecting data for one image, were in the range of 0.6–0.9 mJ (i.e. the doses deliv-

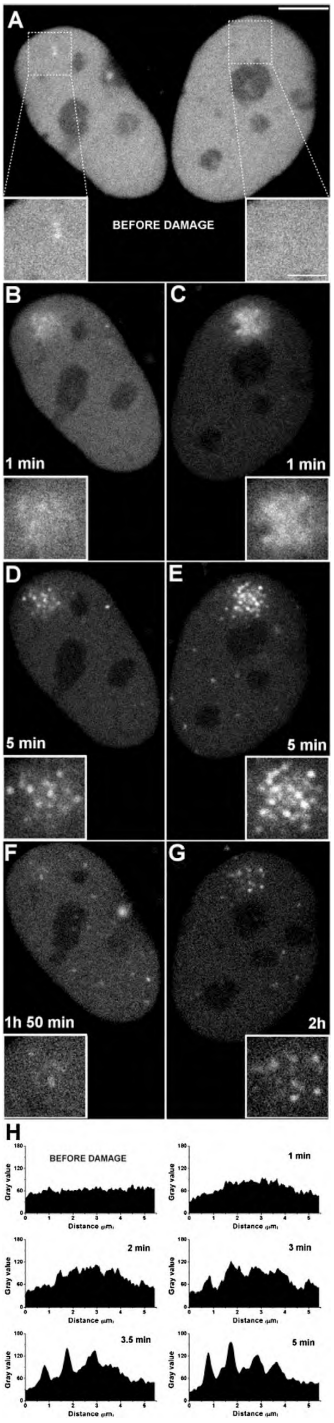


**Fig. 1.** Spatial distribution of XRCC1 at sites of local DNA damage induced by visible light.
Small regions of the nucleus (2.5 × 2.5 μm; marked with squares embracing, for clarity, larger 3.5 × 3.5 μm regions) in two neighbouring HeLa cells expressing RFP XRCC1 were exposed to different doses of focused blue light (3 mJ and 12 mJ). Subsequently the distribution of the repair factor was imaged. Before damage induction, XRCC1 was almost homogeneously distributed within each nucleus. Insets show the areas of the nuclei which were exposed to light in order to induce damage. Scale bar—5 μm (cell images) and 2 μm (insets)
A. XRCC1 before exposure to light. The protein is distributed evenly; occasionally XRCC1-rich microfoci can be observed.
B,C. XRCC1 1 min after local damage induction (B—3 mJ, C—12 mJ). XRCC1 is recruited to the previously illuminated area; the local concentration of XRCC1 is higher than prior to damage (while there is less XRCC1 in the rest of the nucleus) but no distinct pattern is formed at the damage region yet.
D,E. 5 min after the damage induction, XRCC1 is now accumulated in several distinct foci.
F,G. 2 h after the damage, XRCC1 foci are still visible in both nuclei, but their number is significantly lower than shortly after the damage induction.
H. Fluorescence profiles representing the rearrangement of XRCC1 from an almost uniform cloud-like form to individual foci within the damage site (in the cell shown in B). No substantial movement of these foci was detected (see also Suppl. Fig. 2).

ered per unit area were two orders of magnitude lower than in the case of inducing local damage).

### 2.4. Image processing

All images except for Suppl. Figs. 1 and 4 are single confocal planes. Fluorescence images presented in Suppl. Figs. 1 and 4 are maximum projections of 3D stacks (20 and 4 planes, respectively).

All images were processed using ImageJ (http://imagej.nih.gov/ij/). Brightness and contrast levels were moderately adjusted in most of the images. Contrast was enhanced individually in each image in order to avoid the disappearance of any features. All operations were applied to the whole images.

Distances between nearest neighbour foci of two classes (XRCC1 and Sp100) were measured in 3D space and analysed using our algorithm, which was described in detail previously [35].

## 3. Results

### 3.1. XRCC1 recruited to low level DNA damage rearranges into distinct foci

Induction of local DNA damage by focused visible light, in the absence of exogenous photosensitisers, is particularly well suited for studies of the behaviour of XRCC1 in damage sites, since just a few SSBs and DSBs, and no detectable oxidative or UV damage, are inflicted in the illuminated area [34,36]. Furthermore, the absence of DNA-binding molecules acting as photosensitisers assures that chromatin structure is not disturbed [37], and, most importantly, no additional photosensitised damage occurs during imaging of the repair process. Induction of low level well defined damage is particularly important in the context of XRCC1 foci formation. Based on the existing data we assumed that formation of distinct XRCC1 or γH2AX foci indicated the presence of separate SSBs and DSBs, respectively. Although we were not successful in inducing exclusively one type of damage, e.g. SSBs with no DSBs, we found that using a relatively low intensity of focused blue light facilitated induction of just a few lesions, most of them being SSBs. Thus, we optimised and used the conditions of illumination leading to induction of low numbers of SSBs, accompanied by an even lower number of DSBs.

In order to confirm that focused visible light leads to induction of single-strand breaks, we detected poly(ADP-ribose) and XRCC1 by immunofluorescence. ADP-ribose moieties, as well as XRCC1, were detected in the regions subjected to blue light (Suppl. Fig. 1), supporting our previous findings. Subsequently, we induced local DNA damage in HeLa cells transiently expressing RFP-XRCC1 protein. The insult resulted in rapid recruitment of XRCC1 to the whole illuminated area (Fig. 1).

Initially, XRCC1 remained evenly distributed within the damaged region, but soon (within less than 2 min) started to form

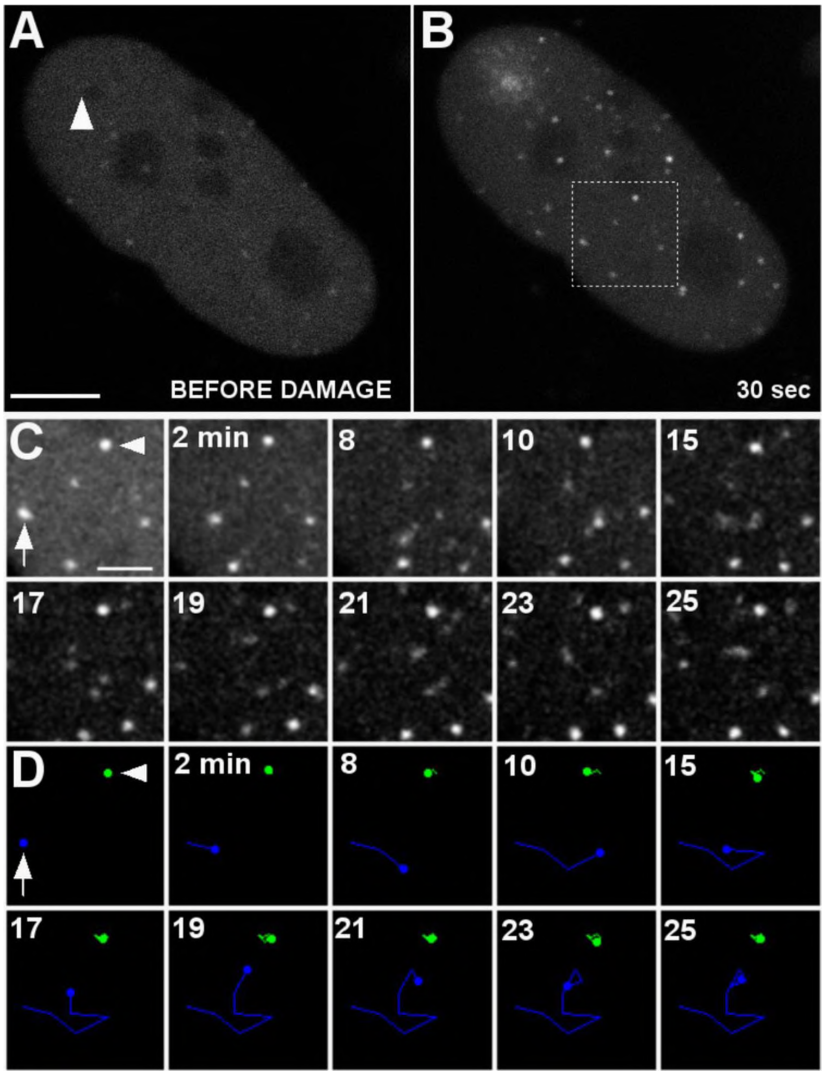


**Fig. 2.** Mobility of light induced XRCC1 foci formed outside of the directly illuminated area.
Local DNA damage was induced in a HeLa nucleus expressing RFP-XRCC1 (near the upper end of the nucleus; arrowhead). Prior to light exposure some XRCC1 foci were present in the nucleus, but scattered light caused stress which resulted in formation of many XRCC1 foci, both stationary and mobile. Scale bars-5 μm (cells) and 2 μm (insets).
A. XRCC1 before damage induction (the region to be damaged is marked with an arrowhead).
B. 30 s after damage induction (a total dose delivered to the directly illuminated region was 3 mJ), XRCC1 was already recruited to the damage site, and multiple new foci were formed outside of the directly illuminated region.
C,D. Live-cell imaging (C—subsequent images of the selected region located at a distance from the directly illuminated area (marked with a square in B) and particle tracing (D—traces of two selected foci residing within the region marked with a square) revealed that newly formed foci differed in mobility. While some did not move substantially (green focus, arrowhead, and a trace) other travelled distances of several micrometers during minutes (arrow, blue focus; the blue line is a trace recorded in subsequent images shown in C).

individual foci. The process of transition from a uniform distribution to distinct foci lasted 3–4 min and resulted in formation of several clearly separate foci with a high content of XRCC1 (Fig. 1, Suppl. Fig. 2, Suppl. Movie 1). When we used various doses of light (in preliminary experiments; data not shown), the smaller was the energy dose, the fewer foci were formed. The XRCC1 foci showed no substantial mobility (Suppl. Fig. 2). In order to verify if the repair process was proceeding normally, we followed the damaged cells for 2 h. The number of foci in the damaged region decreased significantly during that time, suggesting that many of the DNA breaks have been repaired successfully. In further experiments, XRCC1 foci induced by visible light usually disappeared completely within 1–2 h, and the cells were able to enter mitosis several hours after the induction of damage (Suppl. Fig. 3). In order to demonstrate that formation of XRCC1 foci (as well as their dismantling) was a physiological reaction which can be observed only under conditions of low level damage consisting of just a few DNA breaks, we also studied the behaviour of XRCC1 in cells exposed to heavy

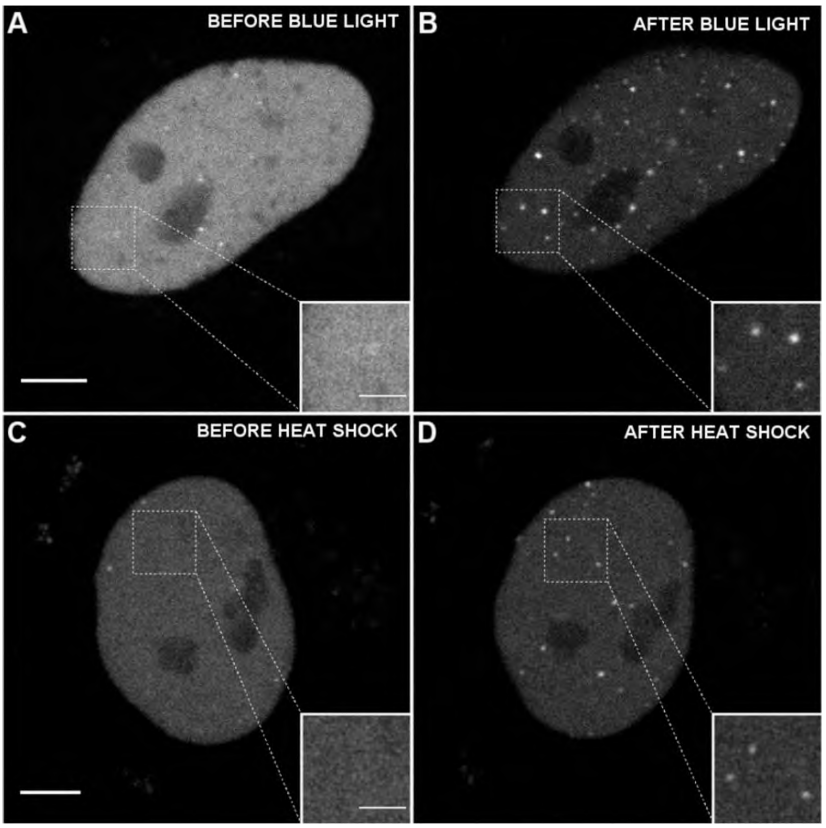


**Fig. 3.** Formation of XRCC1 foci in response to DNA damage or stress induced by visible light or heat shock.
HeLa cells expressing RFP-XRCC1 were exposed to blue light or heat shock. Before treatment with the stressing agent the nuclei contained none or just a few XRCC1 foci. A,C. XRCC1 prior to blue light (A; delivered to the whole field of view) or heat shock (C).
B,D. XRCC1 foci formed in response to blue light (total dose delivered to the field of view: 20 mJ) (B) or heat shock (D). Both DNA damage and heat shock resulted in formation of multiple foci in the whole nuclear volume. Scale bar—5 μm (cells) and 2 μm (insets).

local damage induced in the presence of a photosensitiser. We used green light and cells pre-sensitised with DNA intercalator ethidium bromide. In agreement with our hypothesis, although XRCC1 was rapidly recruited to the damaged region, it remained evenly distributed for at least 10 min and did not form any foci (Suppl. Fig. 4).

Finally, to prove that the formation of XRCC1 foci after local DNA damage is not a specific reaction occurring only in HeLa cells, we also induced DNA damage in primary human fibroblasts expressing RFP-XRCC1. The response of XRCC1 to local DNA damage in these cells (Suppl. Fig. 5) did not differ from that observed in HeLa cells. In fibroblasts distinct foci were also formed after the initial stage of uniform distribution of the recruited XRCC1 in the region which had been exposed to light.

### *3.2. Two classes of XRCC1 foci are formed in response to low level DNA damage*

One of the advantages of DNA damage induction by focused laser beam is the confinement of the damage to a small volume of the nucleus, which allows easy visualization of the recruited repair factors. However, considering that when light is focused inside the nucleus, it is also scattered efficiently [38], some additional, low-level damage may also be induced outside of the directly illuminated region, throughout the whole nuclear volume. In agreement with this hypothesis, following induction of local DNA damage by focused blue light, we observed appearance of several XRCC1 foci outside of the directly illuminated region (Figs. 1D,E and 2B).

Careful observation revealed that at least two classes of these foci can be distinguished on the basis of their mobility. Some foci showed only a constrained motion (Fig. 2C, arrowhead), as the foci formed in directly illuminated regions. Other foci, however, were able to travel distances of several micrometers within minutes (Fig. 2C, arrow, Suppl. Movie 2). These mobile foci occasionally fused (Suppl. Movie 3). In this respect their behaviour was quite different from the foci induced by direct illumination. Interestingly, longer exposure to excitation light (which was required to conduct observations for over 15 min) led to an increase in the number of both types of foci, suggesting that their formation was most likely caused by the exposure to blue light. Indeed, exposure of whole cells to moderate intensity blue or green laser light (0.02 mJ/μm$^2$) resulted in formation of some XRCC1 foci throughout the nucleus (Fig. 3A, B).

We tested a hypothesis which assumed that the increase in the number of detectable foci after exposure of the whole cell to visible light was simply a visual artefact. Emergence of previously existing small XRCC1 foci could have been a consequence of a decrease of the level of the mobile pool of RFP-XRCC1 resulting from photobleaching. Under such conditions some foci that were previously

buried under the strong signal of mobile RFP-XRCC1 would surface out and become detectable. However, as we compared fluorescence intensities prior and following the exposure to blue light in the regions where the foci were formed, we found that the fluorescence did increase significantly in the regions of foci after light exposure, suggesting that XRCC1 foci indeed formed in response to this exogenous stress. Thus, we conclude that the increase of the number of XRCC1 foci of both types (highly mobile, and those showing only constrained motion), in the whole nucleus, was a genuine result of exposing the whole cells to visible light, and a concomitant induction of some type of localised damage or stress.

### 3.3. XRCC1 and Sp100 colocalize in stress-induced foci

It was shown in a number of studies that RIF are relatively stable in space and their mobility is similar to the mobility of undamaged DNA [39–42]. Since poly(ADP-ribose) can be found in the illuminated regions within a few minutes after the insult, and XRCC1 foci, which were formed as a result of a direct exposure to focused blue light show only constrained, oscillatory motion, we postulate that these foci represent sites of repair of single-strand DNA breaks. On the other hand, a question arises regarding the role of the XRCC1-containing bodies or structures which are able to migrate large distances through the nucleus. Since the behaviour of these foci resembles characteristic features of some nuclear bodies, which were postulated to act as nuclear sensors [43], we asked if the formation of these distinct mobile XRCC1 foci might be a more general response to cellular stress (rather than a specific response to SSBs). We therefore subjected RFP-XRCC1-expressing cells to heat shock and observed the response of XRCC1. In cells with none or very few XRCC1 foci present prior to treatment, we observed formation of new foci within 30 min at 42 °C (Fig. 3C,D) (most of these foci disappeared within 2 h of return to a physiological temperature). To ensure that the exposure to light, which was unavoidable in the imaging experiment, was not a cause for formation of these XRCC1 foci, only two images of these cells were recorded—one immediately prior, and the second 30 min after elevating the sample temperature to 42 °C. This experiment confirmed that new XRCC1 foci were indeed formed as a result of heat shock. This prompted us to look further into possible links between this protein and the known nuclear bodies. Since it has been suggested before that XRCC1 might reside in PML nuclear bodies [44] and, on the other hand, it was shown that, in response to heat shock, PML NBs become disrupted and form multiple microfoci [45], we investigated the spatial positions of XRCC1 foci with respect to the structures containing Sp100, a major component of both large PML NBs and small, mobile micro-bodies formed in response to stress [46]. Prior to stress, in HeLa cells co-expressing GFP-Sp100 and RFP-XRCC1, Sp100 protein was distributed mainly between large and small nuclear bodies, but a mobile pool of this protein was also detectable. In cells with a homogenous distribution of XRCC1 in the nucleus (also prior to stress), no colocalisation of Sp100 and XRCC1 was apparent (Fig. 4A–C) (although one cannot exclude a possibility that some XRCC1 resided within Sp100-containing bodies). On the other hand, in the cells that contained several XRCC1 foci we observed colocalisation of some of these foci with small, Sp100-containing nuclear bodies (Fig. 4F,I, arrows). XRCC1 foci were also detected within or closely adjacent to larger Sp100 nuclear bodies, presumably PML (Fig. 4F, inset). In summary, careful observation of XRCC1 and Sp100 foci in cells prior to stress suggested some association between these structures.

In order to compare the spatial distribution of XRCC1 and Sp100 in response to general stress, we exposed the whole cells to blue light or heat shock. As expected, blue light illumination led to formation of XRCC1 foci throughout the nucleus. Interestingly, light exposure resulted also in formation of numerous small Sp100 nuclear bodies, which were located in close proximity to the XRCC1 foci (Fig. 4G–L). Heat shock also resulted in formation of common small XRCC1 and Sp100 foci in most cells (Fig. 4M–S). We analysed the distances between the centres of foci containing XRCC1 and structures containing Sp100, using a recently optimised image analysis method [35]. This analysis confirmed that a very large proportion of foci containing XRCC1 were located very close (within 400 nm) to the nearest Sp100 focus (Suppl. Fig. 6). These observations suggest that a heat shock and light exposure induced formation of nuclear bodies containing both proteins.

Finally, spurred by the possibility of interaction between XRCC1 and Sp100, we studied their response to local DNA damage induced by visible light in cells expressing both proteins with fluorescent tags. In agreement with our previous findings, XRCC1 was found in the illuminated region shortly after the light exposure and translocated from the diffused form into foci within minutes. Recruitment of Sp100 was also detected. Within approximately 20 min Sp100 became detectable all throughout the area, which was previously illuminated to induce damage, and within 30 min it became clearly visible in foci, which again colocalised with the previously formed foci of XRCC1 (Fig. 5).

## 4. Discussion

Although foci rich in repair proteins have been observed for the first time years ago [7–9], our knowledge about the mechanisms of their formation, structure and, most importantly, their role in the repair processes, remains limited. RIF vary in size, composition, and in the time which elapses between damage induction and their formation [47]. Moreover, it is not clear how the formation of repair foci is related to the type and density of DNA damage, or whether the cloud-like pattern formed by some repair proteins after laser microirradiation represents a physiological response to DNA damage.

The behaviour of XRCC1, which was observed in the course of our experiments, suggests that both the cloud-like form, and foci, may be natural spatial patterns formed by this protein during repair of single-strand breaks. Since the damage was not severe, this observation also suggests that the cloud-like pattern seen in numerous previous studies following laser microirradiation was not necessarily an outcome of a massive DNA damage, but could reflect the first of the two successive binding modes or spatial patterns adopted by the recruited XRCC1. On the other hand, the failure to form XRCC1 foci after heavy local damage (which consisted of numerous DNA breaks and oxidative damage), induced in cells pre-sensitised with a DNA-binding agent, confirms that the type and severity of damage influence the spatial organisation of the recruited DNA repair machinery. The excessive damage of various types created by interaction between the exciting light, a photosensitiser, and DNA may impede the successive stages of repair. The reason behind an altered behaviour of XRCC1 in the presence of a photosensitiser could be a large extent and complexity of the damage, or interactions between a photosensitiser and chromatin. Others [27] as well as ourselves [2] have shown previously that laser illumination in the presence of a photosensitiser leads to induction of oxidative damage, which might interfere with repair of SSBs [48]. Also, the influence of the photosensitiser on the structure of chromatin may play some role. It has been shown that binding of DNA intercalators leads to chromatin relaxation [49] and detachment of histone H1 [37,50] while laser illumination of pre-sensitised cells might lead to cross-linking of ethidium (and presumably other intercalators) to chromatin [51], and DNA denaturation [52], possibly blocking all repair-related chromatin rearrangements.

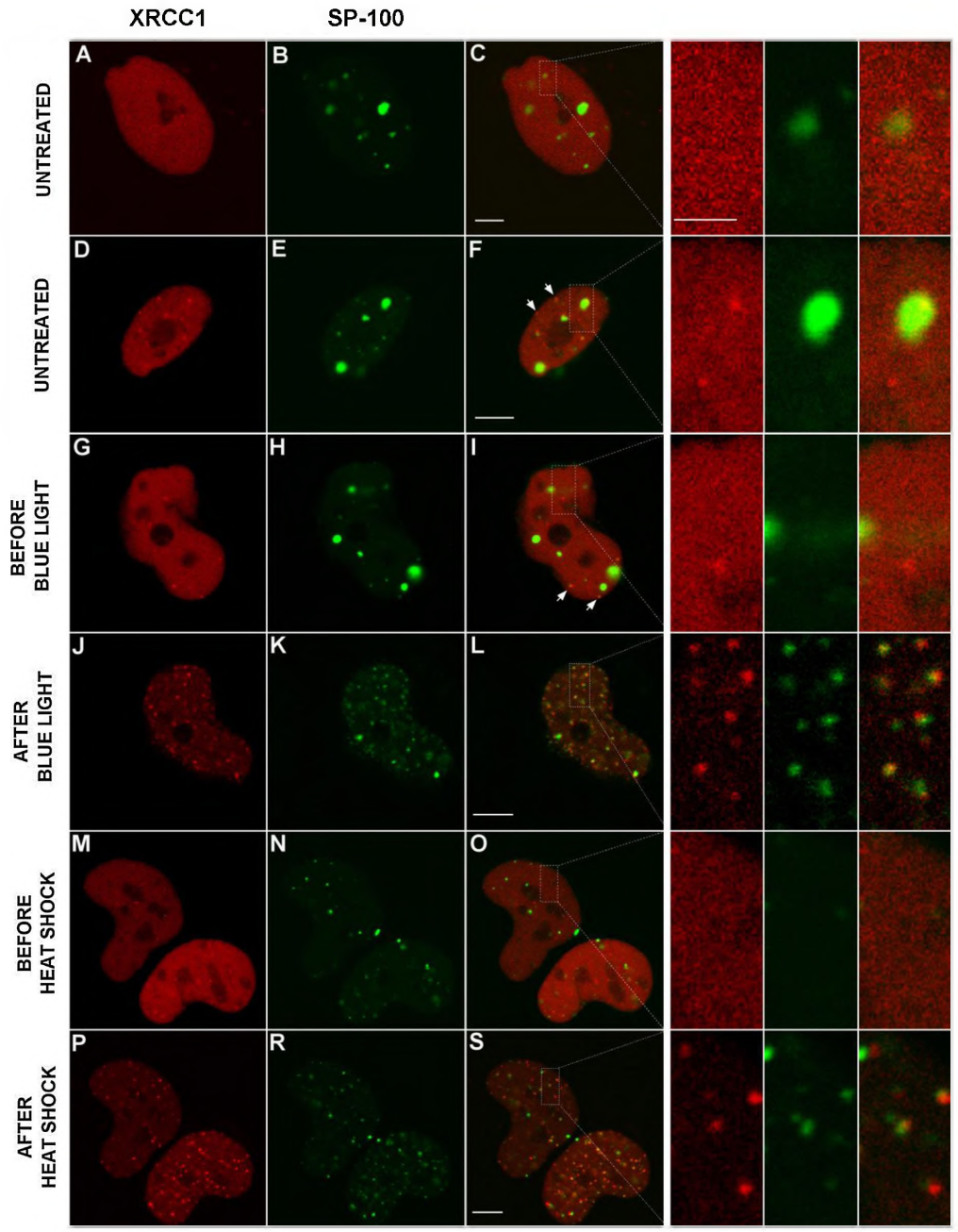


**Fig. 4.** Spatial distribution of Sp100 and XRCC1 prior and following the light- or heat-induced stress.
HeLa cells expressing GFP Sp100A and RFP XRCC1 were investigated for the possible colocalisation of these two proteins in the foci induced by stress. In a non treated cell with a uniform distribution of XRCC1 (A–C) no apparent colocalisation of Sp100 and XRCC1 was visible. In cells with some XRCC1 foci present before any treatment, colocalisation of Sp100 and XRCC1 was detected in a subset of foci (D–F, G–I, arrows and insets). After illumination of the whole nucleus with visible light, or exposure to heat shock, multiple common XRCC1 and Sp100 foci were formed (J–L, P–S). Scale bar—5 μm (cells) and 2 μm (insets).

In this study, we have shown for the first time the transition of the recruited XRCC1 from a diffused form to discrete foci at the damage site. While at this stage we cannot fully explain the mechanism of this process, several possible scenarios can be proposed. The temporal and spatial characteristics of XRCC1 recruitment indicate that it might reflect a recently unveiled mechanism of binding and retention of XRCC1 at the site of the damage [26]. When a single-strand break is formed, it is first recognized by PARP-1, which then PARylates itself and other proteins. Through its BRCT1 domain, XRCC1 recognizes PAR, and is recruited to the damaged region.

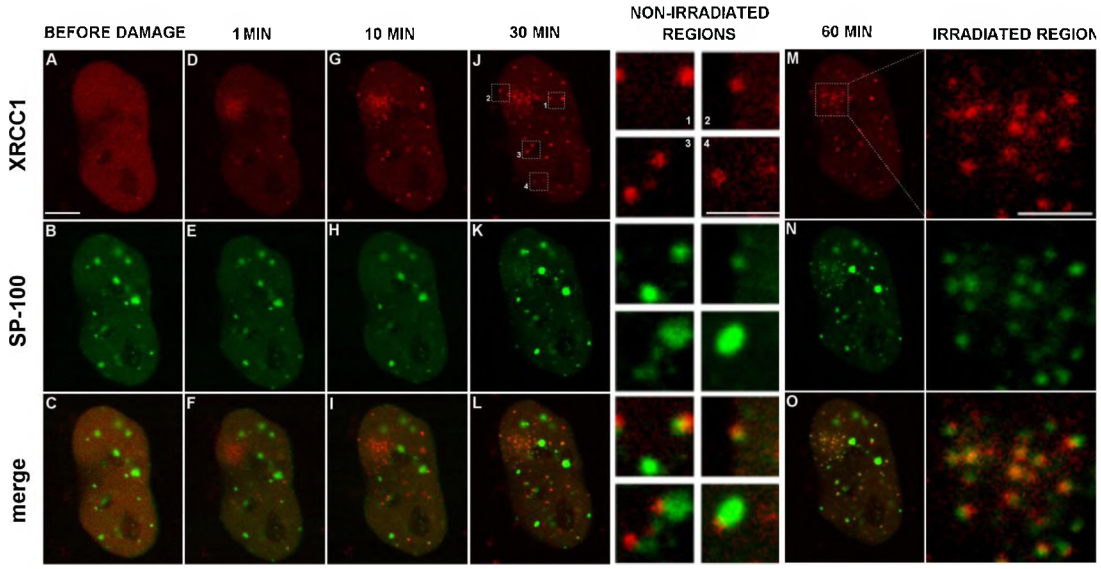


**Fig. 5.** Recruitment of XRCC1 and Sp100 to local DNA damage induced by visible light.
Local DNA damage was induced in a HeLa cell expressing RFP-XRCC1 and GFP-Sp100A. 1 min after light exposure (total dose delivered to the irradiated region was 12 mJ) XRCC1 recruited at the damage site, where it formed a cloud-like pattern. 10 min after damage induction XRCC1 was accumulated in foci. 30 min after damage Sp100 was also accumulated in the damaged region, where it colocalised with XRCC1. At this time Sp100 and XRCC1 also colocalised in a subset of foci formed outside of the directly illuminated region (insets 1–4). Scale bar—5 μm (cells) and 2 μm (insets).

However, since PAR becomes degraded by PARG minutes after the formation of the lesion, XRCC1 binds again to the damage site, this time using its BRCT2 domain. We postulate, that these two phases of XRCC1 recruitment might correspond to the two spatial patterns observed in our experiments. Since PAR moieties are added to many proteins, including histones [53–55], it is reasonable to expect that during the first stage of the recruitment, XRCC1 is present not only at the site of the lesion, but most of all in the surrounding area. On the other hand, it was shown that BRCT2 domain of XRCC1 possesses affinity to DNA nicks [26], probably resulting in the accumulation of XRCC1 exactly at the damage site during the second phase of its recruitment.

The transition from a cloud-like form to individual foci rich in XRCC1 could be related to reorganisation of chromatin in response to DNA damage. Since one cannot exclude a possibility that a single focus of XRCC1 represents the repair site embracing multiple closely spaced SSBs, the transition process could reflect recruitment of scattered lesions leading to formation of repair centres. Although the existence of repair centres embracing DSBs have been postulated before [56,57], the issue remains controversial, and formation of centres consisting of several SSBs remains to be demonstrated.

The third possible explanation of a cloud-to-foci rearrangement of the recruited XRCC1 would entail gradual recruitment of numerous XRCC1 molecules to individual single-strand breaks. Such breaks would exhibit only limited, oscillatory movements (presumably reflecting local chromatin movements) within the first minutes after damage induction. A convolution of initial small local maxima representing individual XRCC1 foci would be seen as broad elevated region on a fluorescence profile. This region would only gradually reveal the component peaks representing individual foci. Even if this simplest explanation were to be true, it is still interesting to note that the postulated process of XRCC1 recruitment to individual foci is halted at an early stage if the complexity and level of damage are high, as in the case of a photosensitised local damage.

Based on the observed mobility of XRCC1 foci, we propose that there are at least two classes of these foci. The relatively immobile foci formed at the damage site after local damage induction probably represent sites of SSBs repair. These foci are an outcome of an interaction of the incident light with DNA [38]. Similarly, the almost immobile foci present in untreated cells likely represent the repair sites of endogenous DNA lesions. The second class of foci contains those that are characterized by substantial mobility. These foci are not likely to represent the repair sites of SSBs, yet still they appear as a result of cellular stress—exposure to light or heat shock. We thus propose that these foci could act as stress-sensors, travelling through the nucleus and immediately delivering multiple copies of XRCC1 (and other repair proteins) to the encountered single-strand breaks. The association of some XRCC1 foci with a major component of PML nuclear bodies, Sp100 protein, which we describe here, further confirms the possible nuclear-bodies-like character of these XRCC1 foci.

It is interesting to note that Sp100 is also recruited (albeit at a later stage) to the XRCC1 foci formed at the damage site. This suggests that Sp100 might be involved in DNA repair. In the light of recent findings regarding the role of Sp100 in transcription promotion [58], and taking into account that DNA damage response is accompanied by inhibition and subsequent restart of transcription in the vicinity of DNA lesions [59], it is possible that Sp100 is responsible for regulation of transcription at the site of the damage. Detectable recruitment of Sp100 to the irradiated region begins 20–25 min after the damage induction, it is thus more likely that this protein is engaged in transcription restart rather than inhibition. Since little is known about the regulation of transcription during BER or SSBR, the role of Sp100 in this process calls for further studies.

## Acknowledgements

This work was supported by a National Science Center grant 2013/11/B/NZ3/00189 awarded to JD, and JU funds (DS-005341). MK is a recipient of SET doctoral studentship from JU, a doctoral research grant (Etiuda 2015/16/T/NZ3/00157) and a young researcher grant from National Science Center (Preludium 2013/09/N/NZ3/00203). Faculty of Biochemistry, Biophysics and Biotechnology is a partner of the Leading National Research Center (KNOW) supported by the Ministry of Science and Higher Education in Warsaw. Confocal instrumentation was purchased through EU structural funds program BMZ (POIG.02.01.00-12-064/08).

## Appendix A. Supplementary data

Supplementary data associated with this article can be found, in the online version, at http://dx.doi.org/10.1016/j.dnarep.2015.10.006.

## References

[1] J.S. Kim, T. Krasieva, V. LaMorte, A.M. Taylor, K. Yokomori, Specific recruitment of human cohesin to laser-induced DNA damage, J. Biol. Chem. 277 (2002) 45149–45153.
[2] M. Zarebski, E. Wiernasz, J. Dobrucki, Recruitment of heterochromatin protein 1 to DNA repair sites, Cytometry. A 75 (2009) 619–625.
[3] D. Tråutlein, M. Deibler, A. Leitenstorfer, E. Ferrando-May, Specific local induction of DNA strand breaks by infrared multi-photon absorption, Nucleic Acids Res. 38 (2010), e14.
[4] E. Ferrando-May, et al., Highlighting the DNA damage response with ultrashort laser pulses in the near infrared and kinetic modeling, Front. Genet. 4 (2013) 135.
[5] C. Dinant, et al., Activation of multiple DNA repair pathways by sub-nuclear damage induction methods, J. Cell Sci. 120 (2007) 2731–2740.
[6] X. Kong, S. Mohanty, J. Stephens, Comparative analysis of different laser systems to study cellular responses to DNA damage in mammalian cells, Nucleic Acids Res. 37 (9) (2009) e68.
[7] T. Haaf, E.I. Golub, G. Reddy, C.M. Radding, C.D. Ward, Nuclear foci of mammalian Rad51 recombination protein in somatic cells after DNA damage and its localization in synaptonemal complexes, Proc. Natl. Acad. Sci. U. S. A. 92 (1995) 2298–2302.
[8] R. Maser, K. Monsen, hMre11 and hRad50 nuclear foci are induced during the normal cellular response to DNA double-strand breaks, Mol. Cell. Biol. 17 (1997) 6087–6096.
[9] L. Schultz, N. Chehab, p53 Binding protein 1 (53BP1) is an early participant in the cellular response to DNA double-strand breaks, J. Cell Biol. 151 (2000) 1381–1390.
[10] A. Asaithamby, D.J. Chen, Mechanism of cluster DNA damage repair in response to high-atomic number and energy particles radiation, Mutat. Res. 711 (2011) 87–99.
[11] O. Mortusewicz, L. Schermelleh, J. Walter, M.C. Cardoso, H. Leonhardt, Recruitment of DNA methyltransferase I to DNA repair sites, Proc. Natl. Acad. Sci. U. S. A. 102 (2005) 8905–8909.
[12] K. Suzuki, M. Yamauchi, Y. Oka, M. Suzuki, S. Yamashita, A novel and simple micro-irradiation technique for creating localized DNA double-strand breaks, Nucleic Acids Res. 29 (2010), 38, e.
[13] A. Celeste, et al., Histone H2AX phosphorylation is dispensable for the initial recognition of DNA breaks, Nat. Cell Biol. 5 (2003) 675–679.
[14] B. Jakob, et al., DNA double-strand breaks in heterochromatin elicit fast repair protein recruitment, histone H2AX phosphorylation and relocation to euchromatin, Nucleic Acids Res. 39 (2011) 6489–6499.
[15] M. Tomas, P. Blumhardt, Imaging of the DNA damage induced dynamics of nuclear proteins via nonlinear photoperturbation, J. Biophotonics 655 (2013) 645–655.
[16] K.W. Caldecott, J.D. Tucker, L.H. Stanker, L.H. Thompson, Characterization of the XRCC1-DNA ligase III complex in vitro and its absence from mutant hamster cells, Nucleic Acids Res. 23 (1995) 4836–4843.
[17] K. Caldecott, S. Aoufouchi, XRCC1 polypeptide interacts with DNA polymerase β and possibly poly (ADP-ribose) polymerase, and DNA ligase III is a novel molecular nick-sensorin vitro, Nucleic Acids Res. 24 (22) (1996) 4387–4394.
[18] A.E. Vidal, S. Boiteux, I.D. Hickson, J.P. Radicella, XRCC1 coordinates the initial and late stages of DNA abasic site repair through protein–protein interactions, EMBO J. 20 (2001) 6530–6539.
[19] O. Mortusewicz, H. Leonhardt, XRCC1 and PCNA are loading platforms with distinct kinetic properties and different capacities to respond to multiple DNA lesions, BMC Mol. Biol. 8 (2007) 81.
[20] R.S. Tebbs, L.H. Thompson, J.E. Cleaver, Rescue of Xrcc1 knockout mouse embryo lethality by transgene-complementation, DNA Repair (Amst). 2 (2003) 1405–1417.
[21] N.T. Christie, O. Cantoni, R.M. Evans, R.E. Meyn, M. Costa, Use of mammalian DNA repair-deficient mutants to assess the effects of toxic metal compounds on DNA, Biochem. Pharmacol. 33 (1984) 166–1670.
[22] O. Cantoni, D. Murray, R.E. Meyn, Induction and repair of DNA single-strand breaks in EM9 mutant CHO cells treated with hydrogen peroxide, Chem. Biol. Interact. 63 (1987) 29–38.
[23] M.E. Churchill, J.G. Peak, M.J. Peak, Repair of near-visible- and blue-light-induced DNA single-strand breaks by the CHO cell lines AA8 and EM9, Photochem. Photobiol. 54 (1991) 639–644.
[24] L.H. Thompson, et al., A CHO-cell strain having hypersensitivity to mutagens, a defect in DNA strand-break repair, and an extraordinary baseline frequency of sister-chromatid exchange, Mutat. Res. Mol. Mech. Mutagen. 95 (1982) 427–440.
[25] L. Lan, et al., In situ analysis of repair processes for oxidative DNA damage in mammalian cells, Proc. Natl. Acad. Sci. U. S. A. 101 (2004) 13738–13743.
[26] L. Wei, et al., Damage response of XRCC1 at sites of DNA single strand breaks is regulated by phosphorylation and ubiquitylation after degradation of poly(ADP-ribose), J. Cell Sci. 126 (2013) 4414–4423.
[27] A. Campalans, et al., Distinct spatiotemporal patterns and PARP dependence of XRCC1 recruitment to single-strand break and base excision repair, Nucleic Acids Res. 41 (2013) 3115–3129.
[28] A. Hanssen-Bauer, The region of XRCC1 which harbours the three most common nonsynonymous polymorphic variants, is essential for the scaffolding function of XRCC1, DNA Repair (Amst). 11 (2012) 357–366.
[29] A. Asaithamby, B. Hu, D.J. Chen, Unrepaired clustered DNA lesions induce chromosome breakage in human cells, Proc. Natl. Acad. Sci. U. S. A. 108 (2011) 8293–8298.
[30] A. Croset, et al., Inhibition of DNA damage repair by artificial activation of PARP with siDNA, Nucleic Acids Res. 41 (2013) 7344–7355.
[31] A. Hanssen-Bauer, et al., XRCC1 coordinates disparate responses and multiprotein repair complexes depending on the nature and context of the DNA damage, Environ. Mol. Mutagen. 52 (8) (2011) 623–635.
[32] J. Della-Maria, et al., The interaction between polynucleotide kinase phosphatase and the DNA repair protein XRCC1 is critical for repair of DNA alkylation damage and stable association at DNA damage Sites, J. Biol. Chem. 287 (2012) 39233–39244.
[33] D. Negorev, M. Ishov a, G. Maul, Evidence for separate ND10-binding and homo-oligomerization domains of Sp100, J. Cell Sci. 114 (2001) 59–68.
[34] K.J. Solarczyk, M. Zarębski, J.W. Dobrucki, Inducing local DNA damage by visible light to study chromatin repair, DNA Repair (Amst). 11 (2012) 996–1002.
[35] K. Berniak, et al., Relationship between DNA damage response, initiated by camptothecin or oxidative stress, and DNA replication, analyzed by quantitative 3D image analysis, Cytometry. A 83 (2013) 913–924.
[36] C. Kielbassa, L. Roza, B. Epe, Wavelength dependence of oxidative DNA damage induced by UV and visible light, Carcinogenesis 18 (1997) 811–816.
[37] K. Wojcik, J. Dobrucki, Interaction of a DNA intercalator DRAQ5, and a minor groove binder SYTO17, with chromatin in live cells—influence on chromatin organization and histone—DNA interactions, Cytom. Part A 5 (2008) 555–562.
[38] J.W. Dobrucki, D. Feret, A. Noatynska, Scattering of exciting light by live cells in fluorescence Confocal imaging: phototoxic effects and relevance for FRAP studies, Biophys. J. 98 (2007) 1778–1786.
[39] M. Kruhlak, A. Celeste, Changes in chromatin structure and mobility in living cells at sites of DNA double-strand breaks, J. Cell Biol. 172 (2006) 823–834.
[40] E. Soutoglou, et al., Positional stability of single double-strand breaks in mammalian cells, Nat. Cell Biol. 9 (2007) 675–682.
[41] M. Falk, E. Lukasova, B. Gabrielova, V. Ondrej, S. Kozubek, Local changes of higher-order chromatin structure during DSB-repair, J. Phys. Conf. Ser. 101 (2008) 012018.
[42] B. Jakob, J. Splinter, Positional stability of damaged chromatin domains along radiation tracks in mammalian cells positional stability of damaged chromatin domains along radiation tracks in mammalian cells, Radiat. Res. 171 (2009) 405–418.
[43] M. Muratani, et al., Metabolic-energy-dependent movement of PML bodies within the mammalian cell nucleus, Nat. Cell Biol. 4 (2002) 106–110.
[44] J. Della-Maria, et al., Human Mre11/human Rad50/Nbs1 and DNA ligase IIIalpha/XRCC1 protein complexes act together in an alternative nonhomologous end joining pathway, J. Biol. Chem. 286 (2011) 33845–33853.
[45] C.H. Eskiw, G. Dellaire, J.S. Mymryk, D.P. Bazett-Jones, Size, position and dynamic behavior of PML nuclear bodies following cell stress as a paradigm for supramolecular trafficking and assembly, J. Cell Sci. 116 (2003) 4455–4466.
[46] K. Wiesmeijer, C. Molenaar, I.M.L.a Bekeer, H.J. Tanke, R.W. Dirks, Mobile foci of Sp100 do not contain PML: PML bodies are immobile but PML and Sp100 proteins are not, J. Struct. Biol. 140 (2002) 180–188.
[47] S.V. Costes, I. Chiolo, J.M. Pluth, M.H. Barcellos-Hoff, B. Jakob, Spatiotemporal characterization of ionizing radiation induced DNA damage foci and their relation to chromatin organization, Mutat. Res. 704 (2010) 78–87.
[48] M.E. Lomax, S. Cunniffe, O'N, P. eill, 8-OxoG retards the activity of the ligase III/XRCC1 complex during the repair of a single-strand break, when present within a clustered DNA damage site, DNA Repair (Amst) 3 (2004) 289–299.
[49] W. Stratling, I. Seildel, Relaxation of chromatin structure by ethidium bromide binding: determined by viscometry and histone dissociation studies, Biochemistry 15 (1976) 4803–4809.
[50] K. Wojcik, M. Zarebski, A. Cossarizza, J.W. Dobrucki, Daunomycin, an antitumor DNA intercalator, influences histone-DNA interactions, Cancer Biol. Ther. 14 (2013) 823–832.

[51] A.N. Prusov, I.I. Kireev, V.Y. Polyakov, Visible light irradiation of ethidium bromide-stained interphase nuclei causes DNA-protein linking and structural stabilization of nucleoprotein complexes, Photochem. Photobiol. 78 (2003) 592–598.
[52] T. Bernas, E.K. Asem, J.P. Robinson, P.R. Cook, J.W. Dobrucki, Confocal fluorescence imaging of photosensitized DNA denaturation in cell nuclei, Photochem. Photobiol. 81 (2005) 960–969.
[53] N. Ogata, K. Ueda, H. Kagamiyama, O. Hayaishi, ADP-ribosylation of histone H1, J. Biol. Chem. 255 (1980) 7616–7620.
[54] N. Ogata, K. Ueda, O. Hayaishi, ADP-ribosylation of histone H2B, J. Biol. Chem. 255 (1980) 7610–7615.
[55] S. Messner, et al., PARP1 ADP-ribosylates lysine residues of the core histone tails, Nucleic Acids Res. 38 (2010) 6350–6362.
[56] M. Lisby, U.H. Mortensen, R. Rothstein, Colocalization of multiple DNA double-strand breaks at a single Rad52 repair centre, Nat. Cell Biol. 5 (2003) 572–577.
[57] T. Neumaier, et al., Evidence for formation of DNA repair centers and dose-response nonlinearity in human cells, Proc. Natl. Acad. Sci. U. S. A. 109 (2012) 443–448.
[58] A. Newhart, et al., Sp100A promotes chromatin decondensation at a cytomegalovirus-promoter-regulated transcription site, Mol. Biol. Cell 24 (2013) 1454–1468.
[59] S. Adam, S.E. Polo, G. Almouzni, Transcription recovery after DNA damage requires chromatin priming by the H3.3 histone chaperone HIRA, Cell 155 (2013) 94–106.

## Supplementary Data

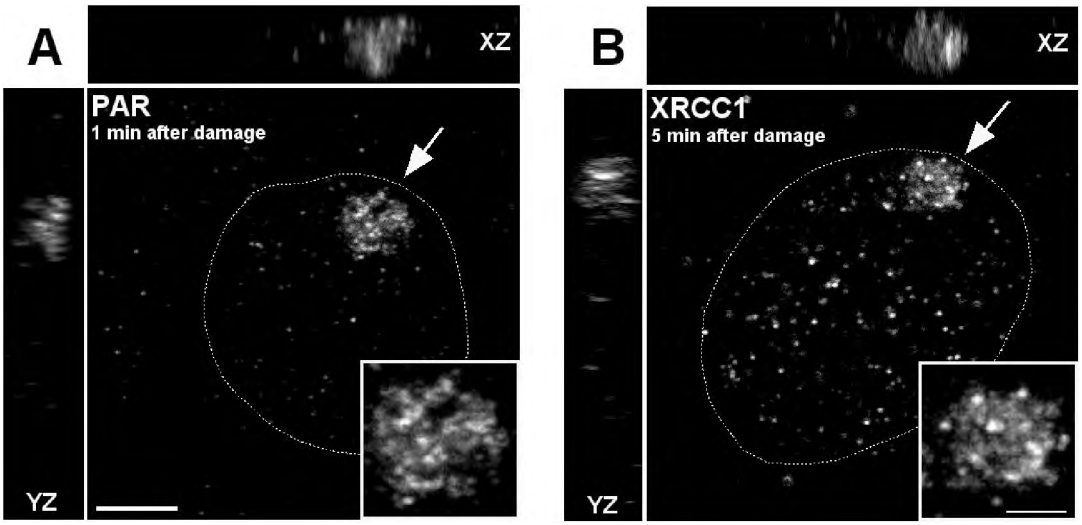


**Suppl. Fig. 1. Detection of PAR polymers and endogenous XRCC1 at sites of local DNA damage.**

Local DNA damage (total dose delivered to the illuminated region: 12 mJ) was induced in nuclei and poly(ADP-ribose) **(A)** or XRCC1 **(B)** were detected by IF. Both these factors were detected at the sites of exposure to blue light. Scale bar - 5 µm (cells) and 2 µm (insets).

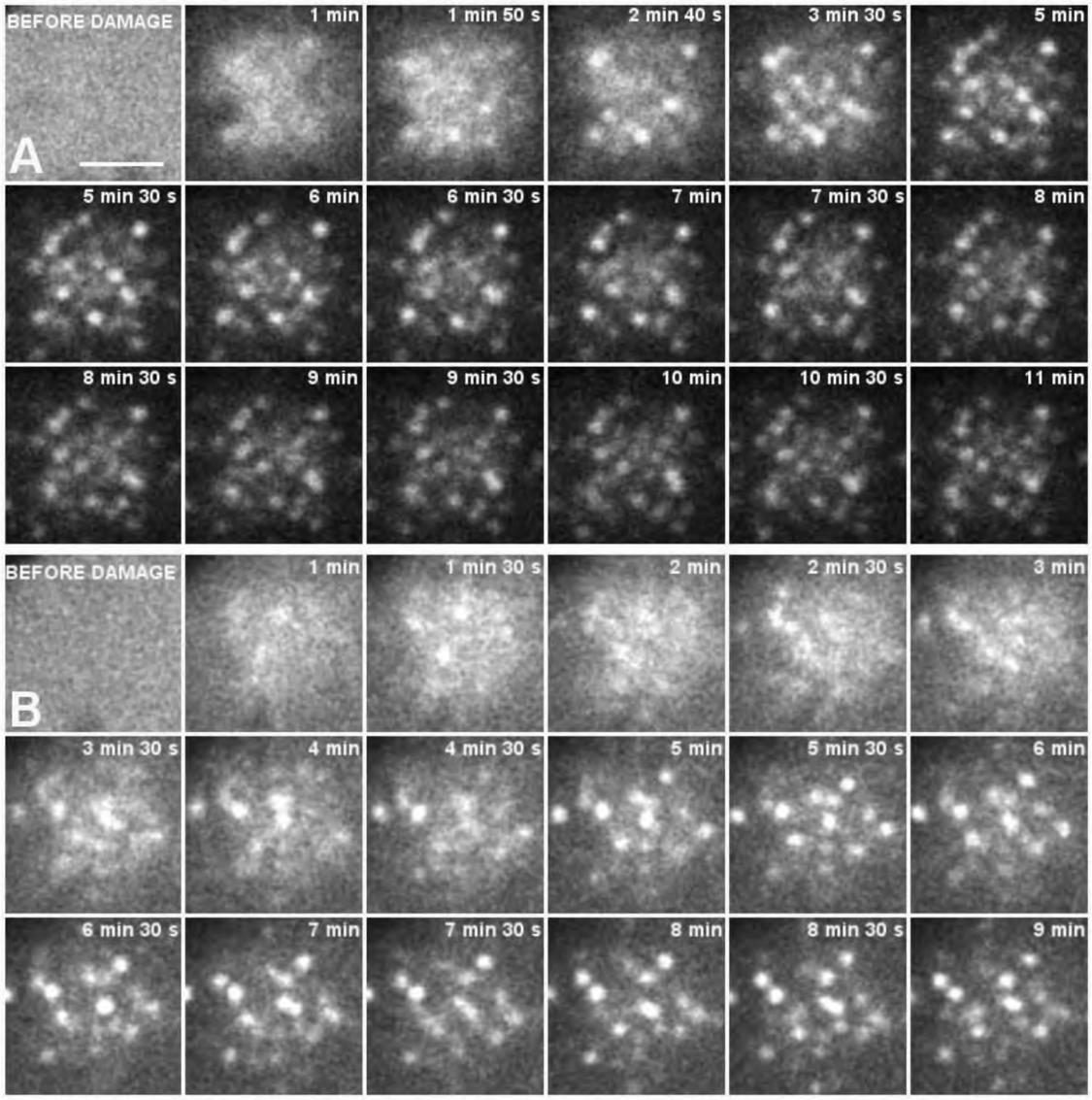


**Suppl. Fig. 2. Recruitment of XRCC1 and formation of distinct foci after local damage induction by visible.**

A full set of images, supplementing the data shown in Fig. 1, showing XRCC1 in cells in which local DNA damage was induced by blue light (A - higher dose: 12 mJ, B - lower dose: 3 mJ). The images demonstrate that the cloud-to-foci rearrangement of XRCC1 lasts several minutes regardless of the dose of energy delivered to the illuminated region, and that the resolved foci are relatively immobile. Scale bar - 2 µm.

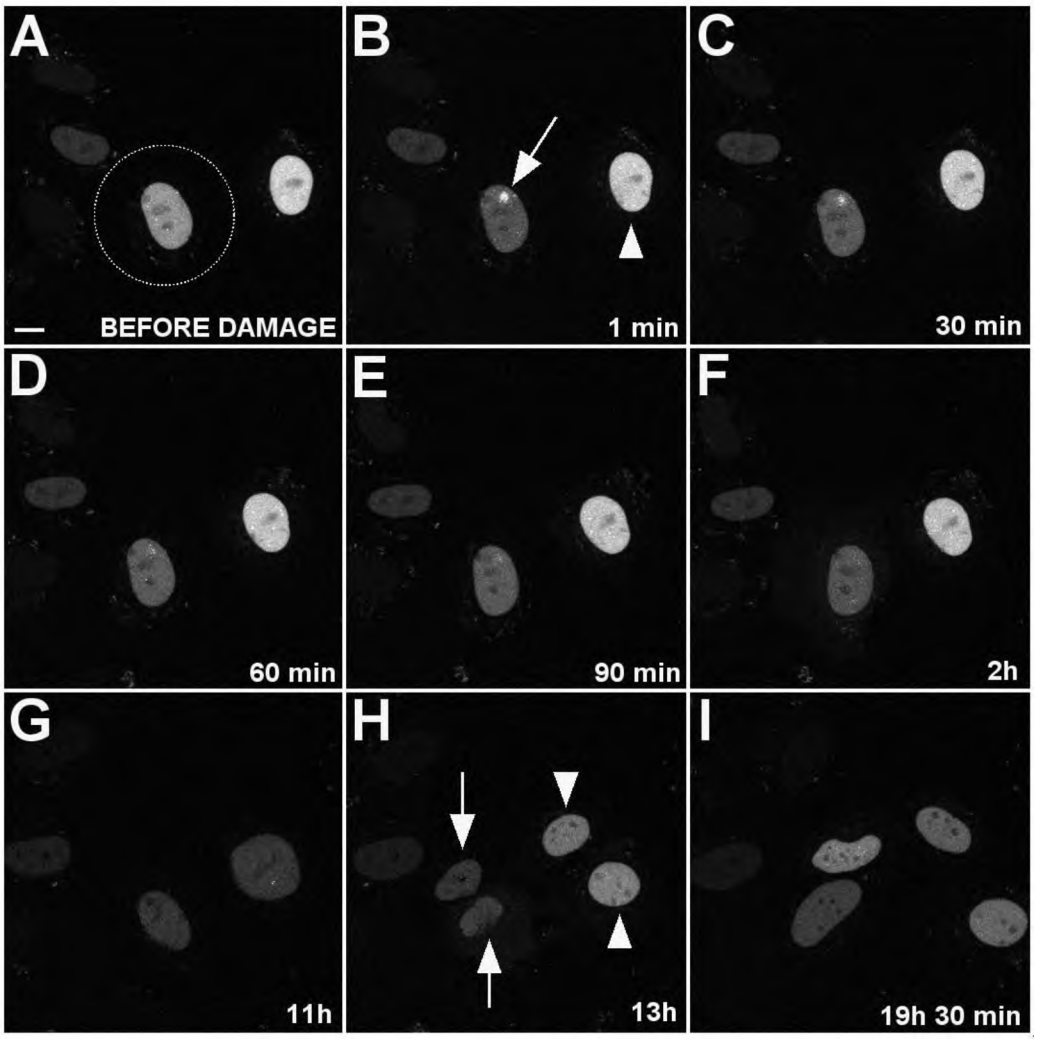


**Suppl. Fig. 3. Division of a HeLa cell which was locally damaged by visible light.**

**A.** HeLa cell (encircled) expressing RFP-XRCC1 was locally damaged by visible light (B) (total dose delivered to the illuminated region: 12 mJ) and then followed for 20 hours (B-I). Scale bar - 5 μm,

**B.** 1 minute after damage induction XRCC1 is readily visible in the illuminated region (arrow),

**C-E.** at 30, 60 and 90 minutes after damage the amount of XRCC1 in the damaged region is diminishing,

**F.** 2 hours after induction of the damage XRCC1 is no longer accumulated at the damage site, indicating that the damage was repaired,

**G-I.** at 11 hours the cell enters and successfully finishes mitosis (arrows). The cell nearby, which was not damaged, also completes division (arrowheads).

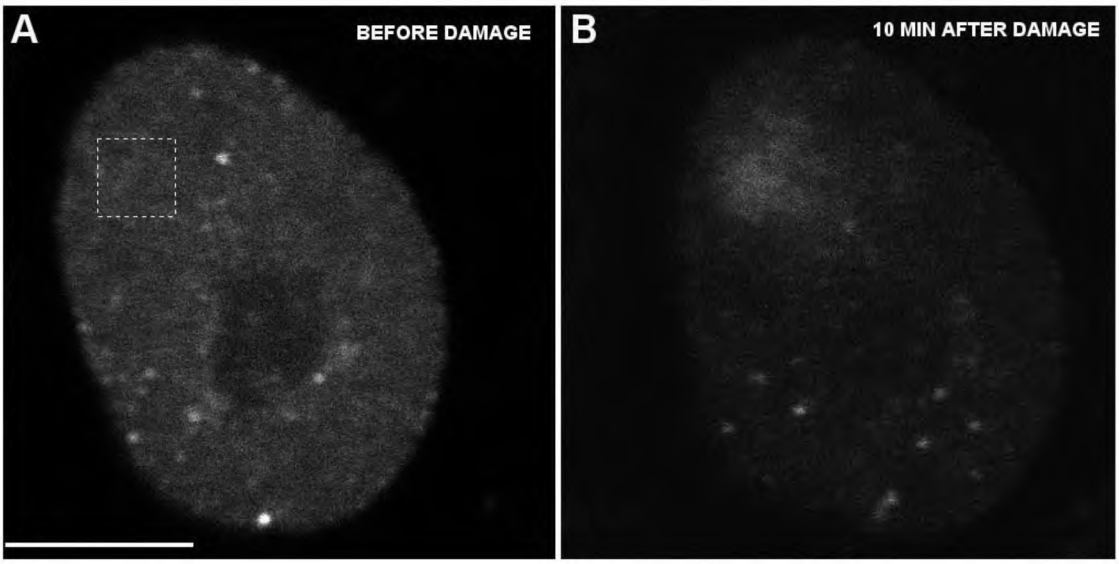


**Suppl. Fig. 4. Spatial distribution of XRCC1 after DNA damage induced by visible light in the presence of a photosensitiser.**

HeLa cells expressing GFP-XRCC1 were incubated with ethidium bromide and then locally illuminated with green laser light (total dose delivered to the illuminated region: 30 mJ)

**A**. XRCC1 prior to damage (scale bar - 5 µm),

**B**. 10 minutes after damage XRCC1 is accumulated but still remains evenly distributed throughout the illuminated area. No distinct foci are visible in this region.

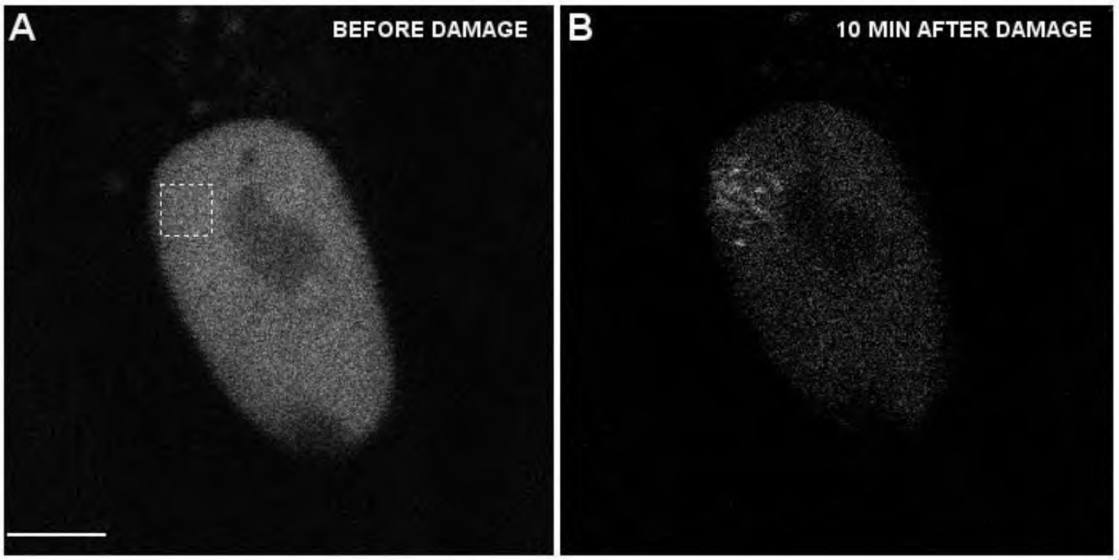


**Suppl. Fig. 5. Spatial distribution of XRCC1 in response to damage induced by visible light in primary fibroblasts transiently expressing RFP-XRCC1.**

Human fibroblasts in a primary culture were transfected using reagents and a method described in (Madeja et al. 2007). Local DNA damage was induced in a nucleus of a primary fibroblast by exposure to blue light (square, total dose delivered to the illuminated region: 5 mJ). Before damage, XRCC1 is homogenously distributed in the nucleus (**A**). 10 minutes after the insult XRCC1 foci are visible in the illuminated region (**B**). Scale bar - 5 µm.

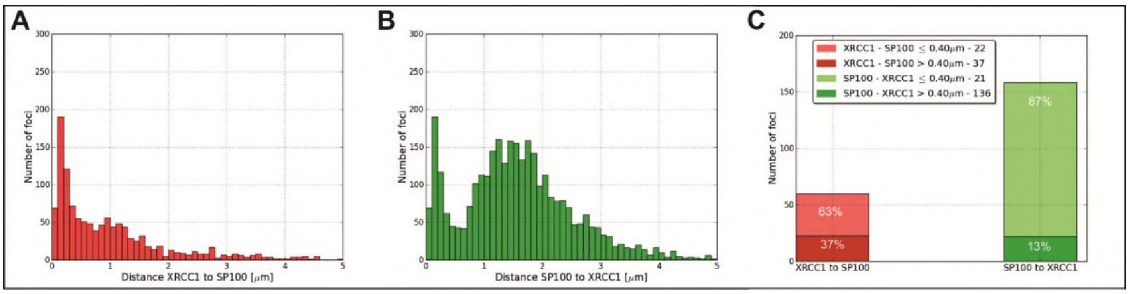


**Suppl. Fig. 6**. Many foci containing XRCC1 or Sp100 are induced by heat shock in HeLa cells expressing both FP-tagged proteins. Analysis of distances between barycenters of subnuclear structures containing XRCC1 and Sp100 in cells exposed to heat shock was performed using a method described in [Berniak et al. 2013]. Note that a simple colocalisation coefficient cannot sufficiently describe spatial relationships between XRCC1 and Sp100 foci [Berniak et al. 2013; Jain and Łos, 2013]. A – a histogram of distances measured from XRCC1 foci to the nearest Sp100 neighbour, demonstrating that a large majority of XRCC1 foci (63%, graph C) have Sp100 focus in close proximity. In turn, Sp100 foci consist of two subpopulations – members of one subpopulation (13%) have an XRCC1 focus within 400nm; members of the other, more numerous subpopulation (87%) do not have any XRCC1 foci within this distance (B). 158.35 +/- 90.88 Sp100 foci/nucleus, and 61.62 +/- 54.82 XRCC1 foci/nucleus were detected.

**Literature**

1. Madeja, Z. *et al*. New cationic polyprenyl derivative proposed as a lipofecting agent. *Acta Biochimica Polonica*, 54(4), 873–6. (2007).
2. Berniak, K. *et al*. Relationship between DNA damage response, initiated by camptothecin or oxidative stress, and DNA replication, analyzed by quantitative 3D image analysis. *Cytometry A,* 83, 913–924 (2013).
3. Jain M.V., Łos M.J. Spatiotemporal cytometry-simultaneous analysis of DNA replication and damage. *Cytometry A*, 83(11), 975-6 (2013).

# Chapter 4

# DISCUSSION AND FUTURE PERSPECTIVES

## 4.1 The types of DNA damage induced by visible light

Apart from introducing a new method of local DNA damage induction, PAPER 1 contributes to the general knowledge regarding the effects of visible light on DNA. So far, induction of DNA damage by visible light without presensitisation with exogenous compounds has been addressed in just a few studies [107–110, 126, 245]. Most of these studies have taken advantage of the alkaline elution assay with repair endonucleases, which enables to quantify the sum of strand breaks and many oxidative DNA lesions, depending on the enzyme used. As already discussed in Chapter 2, these studies have shown that the major group of lesions induced after irradiating whole cells with visible light are oxidative base modifications, but strand-breaks and DNA-protein crosslinks are also formed. Low numbers of CPDs can arise as well, but this kind of damage is not expected to be formed by radiation above 425 $nm$ [110]. In agreement with these findings, we have shown that irradiation with blue laser light leads to the recruitment of SSB and DSB-related repair factors, but not the NER-associated TFIIH. However, we were not able to detect oxidized guanine at the site of irradiation in the absence of exogenous photosensitisers. These seemingly contradictory findings regarding the ability to produce oxidative lesions by visible light have two possible explanations. First of all, as emphasized in Chapter 2, irradiation of whole cells might have different outcomes than selective irradiation of the nucleus with a laser beam. Moreover, the power and total dose of visible light delivered to the sample to induce local DNA damage is several orders of magnitude higher than that used in the referred studies. Different lamps were used to irradiate cells with a broad range of visible light and the power of the radiation that was delivered usually did not exceed 1000 $W/m^2$ (comparable to natural sunlight). For comparison, the irradiance in a focal spot of the blue laser is in the order of tens of $GW/m^2$. The differences in the applied methods allow to imply that the mechanism of damage induction and hence the types of DNA lesions formed in these two setups, might also be different. Apart from that, it cannot be excluded that some oxidation of DNA bases occurs after irradiation with blue laser light, but is beyond the detection limit of the applied method. One has to remember that the

detection of strand-breaks is significantly facilitated by the amplification of $\gamma$H2AX around a DSB or by the accumulation of multiple copies of XRCC1 at a SSB. On the other hand, an antibody directed against 8-oxoG has to detect single modified DNA bases, a task which is further hindered by the fact that these lesions are buried within chromatin.

Most of the studies regarding the induction of DNA damage by visible light have focused on the $400 - 500\ nm$ range, so little is known about the contribution of wavelengths above $500\ nm$. In PAPER 1 it was mentioned that apart from the blue laser line, also irradiation at $514\ nm$ leads to the activation of DDR. Recent experiments conducted in our laboratory indicate that both single and double-strand breaks are efficiently produced by a laser emitting at $561\ nm$. Irradiation with $594\ nm$ laser line leads to DNA damage only in a small subset of cells, while $633\ nm$ does not produce lesions at all, even at very high doses [Zarębski M., Wesołowska J., personal communication]. When the same dose of light was used for all tested laser lines, the one emitting at $458\ nm$ proved to be the most efficient in producing DNA strand breaks. The ratio of SSB/DSB induction seems to increase when using longer wavelengths – only 15% of cells irradiated with $561\ nm$ laser line showed the accumulation of a DSB-repair factor at the damage site in addition to the recruitment of SSBR factors. Strikingly, recent experiments have also shown that the induction of DNA damage by laser lines from the visible light spectrum is not abolished in the absence oxygen [Zarębski M., Górny G., personal communication].

The methods employed in previous studies for obtaining the yields of lesions caused by visible light did not allow to discriminate between single and double-strand DNA breaks. On the other hand, formation of spatially separated $\gamma$H2AX foci together with the recruitment of XRCC1 in a focal pattern allowed us to compare the relative number of these lesions formed by blue laser light. Irradiation of a selected region of the nucleus with a total dose of 12 mJ (the maximum dose utilized in PAPER 2) resulted in the formation of nearly equal number of SSBs and DSBs at the damage site (see Fig. 1.1, around 20 XRCC1 and $\gamma$H2AX foci visible in the inset). The ratio of SSB/DSB was increased for lower doses of irradiation, but since some $\gamma$H2AX foci were still visible even at the lowest dose resulting in the recruitment of XRCC1, the complete elimination of DSBs with this wavelength seems unlikely. Increasing the total dose above $70\ mJ$ (the „high dose" in PAPER 1) did not cause the formation of DNA lesions other than strand breaks.

In our experiments, the detection of DSBs induced by blue laser irradiation was performed by means of immunofluorescence, usually against $\gamma$H2AX. This approach is well suited for the detection of even small numbers of DSBs. However, the maximum phosphorylation of histone H2AX occurs several minutes after the formation of a DSB, which precludes the detection of DSBs immediately after the damage induction. Because of that, one can wonder whether DSBs formed after visible laser light arise directly or indirectly, by the coincidence of two SSBs on the opposing DNA strands. In order to asses this issue we tried to estimate the frequency of SSBs formation in our experiments. For this purpose it was assumed that $6 \times 10^9$ bp of non-replicated DNA is contained within a nucleus of a $500\ \mu m^3$ volume. The volume of the nucleus subjected to visible light irradiation was estimated at $36\ \mu m^3$ and in this volume approximately 50 foci of XRCC1 have been detected. Assuming that each XRCC1 focus represents one SSB, this results in a density of 1 SSB per 8,6 $Mbp$. Thus, the probability of two

SSBs forming in close proximity is very low, which implies that most DSBs detected in non-replicating nuclei after irradiation with visible laser light arise directly.

One has to be aware that the induction of DNA damage with focused visible laser light is probably influenced by a number of factors, e.g. the localisation of irradiation site with respect to chromatin density, cell cycle phase or the cell type. It has been shown recently, that reduction of heterochromatin levels results in an increased sensitivity to radiation-induced DNA damage [246]. In our experiments, we have observed a different pattern formed by $\gamma$H2AX when the damage was induced in eu- or heterochromatin (discussed later). Since the mechanism of the damage induction by visible laser light focused in the nucleus (in the absence of exogenous photosensitizers) is not known, the influence of the cell cycle phase is difficult to predict. However, initial experiments in which PCNA was used as a marker allowing to discriminate between G1/G2 and S phase of the cell cycle, have shown that fewer XRCC1 foci are formed in late S phase than in other subphases of the S phase or in G1/G2 [Szelest et al., unpublished data]. More studies are needed to confirm this result and to elucidate whether the ratio of SSB/DSB produced by visible light irradiation also depends on the cell cycle phase. Finally, although the vast majority of experiments was conducted in HeLa cells, we were also able to induce this kind of damage in other cell types, including mouse 3T3 fibroblasts and primary human fibroblast, and did not detect the induction of lesions other than strand-breaks or observe significant variations in the amount of energy needed to active the DDR.

## 4.2 The mechanism of induction of DNA damage by visible laser light

There are several potential mechanisms for the induction of DNA damage by laser irradiation when light is focused inside the nucleus and no photosensitisers are added to cells. These are:

- single or multi-photon absorption resulting in temperature rise or some unknown photochemical processes
- thermo-elastic stresses
- optical breakdown (plasma formation)
- absorption by endogenous photosensitisers

Since the absorption of blue light by DNA is weak and the laser power used in our experiments is not sufficient to generate two-photon excitation of some unknown chromophore, thermo-elastic stresses or optical breakdown, the photosensitiser-mediated mechanism should be considered as the most probable for the induction of DNA damage by visible laser light. Previous studies have pointed out at the possible involvement of various endogenous compounds in the formation of DNA lesions by radiation above 400 $nm$. Among these, flavins have drawn the most attention as they have been shown to be the source of ROS in cells treated with visible light [247]. Nevertheless, one has to remember that in all previous studies in which the generation of DNA damage by

visible light was examined whole cells were illuminated. Thus, the involvement of ROS from cytosolic flavins in generation of DNA damage is possible. On the other hand, in our experiments the laser beam was focused in the nucleus, so the excitation of other cellular components was minimized. The damage was always detected at the site of irradiation, no matter what part of the nucleus was subjected to light. If cytosolic flavins were indeed involved in the induction of DNA lesions by visible laser light, one would expect the damage to be scattered over a larger volume of the nucleus. This was never observed. It is worth noting that recent findings have shown that FAD is produced and also degraded in the nucleus [248]. However, since the level of flavin derivatives within the nucleus is thought to be much lower than in the cytoplasm (this is confirmed by low green flavin fluorescence in the nucleus) their involvement in the production of DNA damage by visible laser light is yet to be determined.

Other potential sources of visible-light generated ROS are water and oxygen. Although the absorption coefficient of water at the blue region of visible light is relatively low, it is possible that a low number of ROS is produced by this mechanism. Interestingly, recent findings have shown that exposure of bidistilled water (saturated with atmospheric air) to natural sunlight results in the production of hydrogen peroxide [249]. The production of $H_2O_2$ was shown to occur mainly at the maxima of absorption of molecular oxygen, i.e. at 577 and 630 $nm$ (other maxima are at 477, 760, 919, 1063 and 1264 $nm$). Also, irradiation of a DNA solution with a 632.8 $nm$ emitting He-Ne laser gave rise to oxidized bases (8-oxoG). However, since the production of $H_2O_2$ was significantly diminished in the absence of oxygen, and on the other hand, recent findings of our Laboratory indicate that oxygen is not required for the induction of DNA damage in cells by visible laser light, the significance of this last mechanism for the production of DNA damage in our setup is probably low. In summary, although several potential mechanisms exist, the route which leads to the induction of DNA damage by visible laser light remains unknown. Further studies are needed to evaluate the contribution of the proposed mechanisms to the generation of DNA strand-breaks by blue laser light.

## 4.3 Is recruitment of repair factors a proof of induction of DNA damage?

*In situ* detection of DNA lesions in cells exposed to a DNA damaging agent is usually difficult. In fact, the only lesions that can be detected directly by specific antibodies are UV photoproducts (CPDs, 6-4PPs and their Dewar isomers) [250, 251] and 8-oxoG [252], the most frequent of the oxidative base modifications. Although not directly, also strand breaks can be detected in situ with methods in which the 3' termini of DNA breaks are used as priming points for the synthesis of new nucleic acid strands. Among these methods, only TdT-mediated dUTP nick-end labeling (TUNEL) [253], which is based on the incorporation of modified nucleotides (2'-deoxyuridine 5'-triphosphate, dUTPs) by terminal deoxynucleotidyl transferase (TdT) at the 3'-OH ends of broken DNA, has been used to detect strand breaks at the site of laser microirradiation [147, 254, 255]. The low sensitivity of antibody or enzyme based methods for DNA damage detection has led to the popularization of an indirect approach. Thus, DNA damage is now usually detected by demonstrating the recruitment of proteins known to be

engaged in the DDR or by the existence of histone modifications characteristic for this response. However, one might wonder whether the detection of the response to a putative DNA lesion and not the lesion itself, is a proof of induction of DNA damage?

Formation of double-strand DNA breaks is usually demonstrated by the detection of phosphorylated histone H2AX ($\gamma$H2AX) [256]. However, the specificity of $\gamma$H2AX for DSBs has been recently called into question. It has been shown that $\gamma$H2AX can be triggered by UV radiation [257] or serum starvation [258] and $\gamma$H2AX foci have been detected in mitotic cells in the absence of DNA damage [259, 260]. Interestingly, it has been also revealed that a subset of $\gamma$H2AX foci does not recruit proteins involved in the repair of DSBs [259]. Since $\gamma$H2AX can only be detected by immunofluorescence, i.e. after cell fixation, it is the recruitment of DNA repair proteins that is thought to be an indication of formation of DNA lesions in living cells. The elucidation of the induced damage type is, however, difficult, due to the fact that many of the DNA repair factors are involved in more than one repair pathway. In addition, studies have shown that the accumulation of some DNA repair proteins at DNA in the absence of damage leads to activation of the DDR, i.e. to the recruitment of other, upstream and downstream factors as well as phosphorylation of histone H2AX [261].

In summary, taking the above into account, it seems that caution should be applied when $\gamma$H2AX is the only detected DDR marker. If direct detection of DNA damage is not possible, the evidence for the existence of the damage should be at least strengthened by the visualization of recruitment of DNA repair factors. In the case of the method of DNA damage induction described in PAPER 1, detection of DNA breaks by means other than those utilized in the experiments is difficult due to the low number of these lesions, when compared with other approaches. Nevertheless, one should note that proteins known to be engaged in the repair of DSBs, such as ATM, RPA and Rad51 were detected in the irradiated region at times which agree with the kinetics of DSB repair. This fact, together with the detection of phosphorylated histone H2AX, provide strong evidence in favour of a notion that microirradiation with blue laser light focused inside the nucleus induces DNA strand breaks.

## 4.4 Comparison of inducing DNA damage by visible laser light with other methods

The field of DNA repair was markedly affected by the development of methods allowing to localise DNA damage into subnuclear regions of living cells. These methods were already summarized in Chapter 2, but since in PAPER 1 a new method of the induction of local DNA lesions was proposed, it seems necessary to examine these methods again and compare them with the new technique. The methods were analyzed with regard to several most important features, such as selectivity of the induced damage, impact on cell viability and occurrence of undesired effects, photosensitisation and setup characterisation. This survey is also summarized in Table 4.1 (page 88).

### 4.4.1 Selectivity of induced damage

The results of experiments presented in PAPER 1 and 2 indicate that irradiation of cell nuclei with blue laser light generates single and double-strand DNA breaks, without the formation of oxidative damage to DNA bases or UV-photoproducts. On the other hand, the induction of a broad range of damage types with concomitant activation of multiple repair pathways is a serious drawback of most of the popular methods for local DNA damage induction. The types of lesions formed after laser irradiation depend on the wavelength, power and type of the laser (CW or pulsed) and are influenced by the absence or presence of exogenous photosensitisers. Only a few studies have demonstrated the possibility of selectively inducing one type of DNA damage. These include irradiation with 266 *nm*, 365 *nm*, 405 *nm* and 435 *nm* lasers. Selective induction of SSBs by a 365 *nm* or a 405 *nm* emitting lasers operated at certain powers was shown by Lan et al. [148] and Hanssenn-Bauer et al. [150], respectively. However, since these laser lines are close to the range of radiation directly absorbed by DNA, it is reasonable to expect that they will give rise to UV-photoproducts. Lan claims that there is no recruitment of NER proteins, but no data are shown. In a comparative study Kong et al. [132] have shown that a similar laser emitting at 337 *nm* generates CPDs and 6-4PPs, while the production of CPDs but not 6-4PPs was found by Dinant et al. after irradiation with 405 *nm*. In the latter study, though, the damage induction was carried out in the presence of Hoechst, so the possibility to produce CPDs by 405 *nm* alone remains to be established. Both 365 *nm* and 405 *nm* lasers were shown to induce double-strand breaks and oxidized guanine at higher laser powers [150, 262, 263]. Specific induction of SSBs was also demonstrated in a series of papers from the Bohr laboratory [130, 264, 265]. When operated at a lower dose, a laser emitting at 435 *nm* was shown to trigger accumulation of XRCC1, but not 53BP1. However, the induction of UV-photoproducts or oxidative lesions was not assessed in these studies, which does not allow to exclude the possibility that also NER and BER pathways are activated. Finally, selective induction of UV-photoproducts was shown after irradiation with a 266 *nm* emitting laser by Dinant et al [147]. Although higher laser powers give also rise to DNA strand breaks, below certain threshold only NER factors are recruited to the site of irradiation. Most other laser-based setups generate a mixture of different types of lesions. Usually, SSBs and DSBs are accompanied by oxidative modifications, but CPDs also occur, especially when the damage is caused by multiphoton absorption (pulsed green and NIR lasers). In many cases, however, the damage is too poorly characterised to define the scope of the lesions produced.

### 4.4.2 Impact on cell viability and occurrence of undesirable effects

The ability of damaged cells to proceed through the cell cycle and complete mitosis is a strong indicator that lesions generated by an insult were successfully repaired. In accordance to that, we have demonstrated that cells damaged with visible laser light do not show any morphological changes, repair factors dissociate from the damage site and the cells divide.

Information about viability and cell cycle progression of cells exposed to laser microirradiation was given in just a few papers from the plethora published during the

last 15 years. The most comprehensive set of data was delivered in a paper by Bekker-Jensen et al. [266], in which the authors have shown the percentage of cells which underwent normal mitosis or died after damage induction with a 337 $nm$ laser line (with BrdU sensitisation) in comparison to undamaged cells. Dinant et al. [147] have shown that cells damaged with a laser emitting at 266 $nm$ are able to complete mitosis (movie), while Kim et al. [127] and Meldrum et al. [267] have claimed that cells damaged with pulsed lasers at 532 $nm$ or 750 $nm$ can be observed for several hours (no data were shown to confirm this information). Division of cells damaged with another pulsed laser emitting at 800 $nm$ was shown by Mari et al. [254], but since the damaged cells were treated with caffeine to overcome the G2/M checkpoint, these observations do not prove that the induced lesions were completely repaired. On the other hand, Daddysman et al. [268] have demonstrated that the 800 $nm$ pulsed laser line operated at powers which enable to induce CPDs through multiphoton absorption leads to cell death or significant morphological changes.

An important discussion regarding the biological relevance of induced damage, somehow unintentionally, was sparked by Kim et al. and a paper which demonstrated the recruitment of cohesin to sites of local DNA damage generated by a pulsed green laser [127]. In these experiments, the damage induced by laser was readily visible in phase contrast microscopy. Apart from that, proteins such as Ku70 and cohesin, which did not accumulate at damage induced by other setups, were promptly recruited to the site of irradiation with 532 $nm$. The presence of phase dark lines at the damaged region can also be seen in studies by Kong et al. [132] and Gomez-Godinez et al. [269] involving pulsed lasers emitting at 337 $nm$ and 800 $nm$. These observations suggest that irradiation with certain setups leads to massive DNA damage and although some kind of damage response is activated, doubts exist whether the observed processes would be triggered by damage formed by cellular metabolism or any of the environmental factors. However, one should not be surprised by the extent of damage generated by the 532 $nm$ emitting or similar lasers, since as stated in the first paper by Kim and colleagues:

*„System parameters used ($2-3$ $\mu J$/pulse energy after 100 Ph3, numerical aperture 1.3 oil immersion Zeiss Neofluar objective, $4-6ns$ pulse duration, 7.5 $Hz$) are similar to those used for mitotic chromosome cutting or nuclear body ablation and correspond to irradiances $2-3$ times higher than the estimated threshold values of optical breakdown in water."*

And in a subsequent study using the same setup [270]:

*„Damage is most likely caused by ionization (optical breakdown) of the medium (water) and plasma formation rather than heat because of the extremely short duration of the pulse (5 ns; Berns et al., 1998; Venugopalan et al., 2002). The expansion of cavitation bubbles that was caused by plasma generated transient photomechanical pressure, which resulted in breakage of molecular bonding and created numerous DNA breaks in the confined area."*

### 4.4.3 Photosensitisation

Blue laser light is able to induce DNA damage in the absence of exogenous photosensitisers. However, very often the DNA is presensitised prior to laser irradiation,

usually by incubation of cells with BrdU (rarely IdU) or Hoechst. Incubation with BrdU or IdU is usually carried out for $24 - 48\ h$ and the concentrations used varied from 3 $\mu g/ml$ (papers from Lukas et al. [271, 272]) to 10 $\mu g/ml$ (other studies). While the incubation times with Hoechst are usually within 10-20 minutes, the concentration of the photosensitiser varies by a factor of 1000, from 10 $ng/ml$ [273] to 10 $\mu g/ml$. Moreover, despite the fact that Hoechst 33258 and Hoechst 33342 differ in their ability to penetrate an intact cell membrane, these compounds are used almost interchangeably.

The popularization of sensitisers for local DNA damage induction is a consequence of a paper by Limoli et al. [144], in which it was shown that treatment of cells with these compounds leads to the induction of SSBs and DSBs after UVA irradiation. The term „sensitisers" seems well suited, since a number of studies have demonstrated that the damage is enhanced in the presence of BrdU or Hoechst [147, 262, 274]. Dinant and colleagues have shown that in order to produce damage by a CW 405 $nm$ emitting laser in the absence of Hoechst, the laser power has to be increased 10 times in comparison to the threshold established for the combination of 405 $nm$ + Hoechst. In the same study it was demonstrated that the response to a sensitised damage, i.e. the kinetics of recruitment and patterns formed by repair proteins, is different from the one observed in the absence of photosensitisers [147]. Our own studies confirm these findings. In PAPER 1 it was shown that oxidized guanine is detected at the site of irradiation only when the damage is induced in cells presensitised with ethidium bromide, while in PAPER 2 the presence of this photosensitiser prevented the formation of XRCC1 foci at the damage site. Other, unpublished data, suggest that factors recruited to a photosensitised damage cannot dissociate from the site of irradiation.

### 4.4.4 Setup characterisation

In PAPER 1, in order to allow comparison with other methods, which is essential for any potential user, we have given basic information regarding the setup used and the types of created damage. We have measured the power of blue light at the focal plane and specified details on the size of the damaged region, number of pixels and the pixel dwell time. The types of lesions induced by the new approach were assessed by studying the recruitment of factors engaged in different repair pathways. However, many papers, even those in which a new method of DNA damage induction is introduced, do not provide sufficient information regarding the setup or the damage induced. In several studies, for example in those by Lukas et al. [271, 272] or Mortusewicz et al. [238, 274, 275], the energy delivered to the sample was stated as the percentage of laser maximum output (with no information regarding the value of the output) and by the duration of irradiation. However, even when the laser output is revealed, estimation of the power at the focal plane is impossible. This kind of information is thus insufficient to describe a laser setup and only measurements of the laser power after the objective provide other researchers with data enabling direct comparison of different methods.

## 4.5 Advantages and drawbacks of inducing DNA damage by visible laser light

Based on the above-presented comparison, one should notice that the method of local DNA damage induction by visible laser light described in PAPER 1 offers several advantages over the existing approaches. The first and most important one is the possibility to induce damage in the absence of exogenous photosensitisers. This is extremely important, since, as already mentioned, Hoechst dyes influence many DNA-related processes, generate DNA-protein crosslinks and DNA strand breaks. Thus, even before irradiation cells have to cope with the adverse effects of these compounds. Also, one has to remember that sensitisers remain bound to the DNA after damage induction, interfering with the repair processes and generating more photodamage. Together, these facts imply that sensitising DNA with exogenous agents for the purpose of studying the DDR should be avoided. In the case of the method introduced in PAPER 1, the damage can be generated in conditions which assure that chromatin is in its native, unperturbed state and no additional photodamage is induced during the imaging of repair processes.

Another important asset of the described method is the possibility to produce a well-defined, sublethal damage. In contrast to most other approaches, focused visible light does not lead to a massive DNA damage, but generates single and double-strand DNA breaks in numbers that are within the repair capabilities of the cell. Importantly, the specific induction of strand-breaks suggests that SSBR and DSBR but not NER or the classic BER are the major pathways expected to be activated in our setup. This might allow to discriminate the involvement of some repair factors in different repair pathways. Even more valuable for studies of DNA repair would be the possibility to induce only SSBs and no DSBs. Although some studies have shown the specific induction of SSBs with no accompanying DSBs with 405 $nm$ emitting laser, our unpublished data indicate that the complete elimination of DSBs is impossible, at least with the 488 $nm$ laser line used in our studies.

Finally, since literally all confocal microscopes are equipped with a 488 $nm$ laser line and there is no need of any hardware or software modifications and no special sample preparation, the proposed method is widely accessible. Importantly, by using relatively cheap and easy-to-use power meters it is possible to determine the intensity of light used for localising the damage, which could allow to compare data from different studies. This is currently often impossible due to the lack of sufficient information regarding the intensity and total dose of light delivered by other laser sources.

The main reservation about the proposed method stems from the fact that blue light used for damage induction also results in efficient excitation of the most popular fluorescent protein tag – the GFP. Taking into account laser intensities necessary for damage induction, the result is an undesirable bleaching of the chromophore. However, as DNA repair proteins are most often highly dynamic, tracking the recruitment of GFP-tagged factors is still possible. In fact, even the early events in the DDR can be easily visualized, as demonstrated in PAPER 1 and 2. Nevertheless, since the range of available fluorescent proteins is so vast, in order to minimize bleaching it is recommended to choose fluorescent tags other than GFP fluorescent tags (e.g. RFP, mCherry).

## 4.6 Biomedical aspects – potential importance in skin protection and phototherapy

The power of visible laser light used as an excitation source for confocal microscopy is much higher than that provided by natural sunlight or in most of the biomedical applications, thus the effects of the exposure to these radiations are not directly comparable. Nevertheless, the fact that blue laser light results in the formation of double-strand DNA breaks, which are the most harmful of all DNA lesions, underlines the necessity to treat visible light with caution in all circumstances.

For a long time, the adverse effects of solar radiation on skin have been attributed to the action of the UV part of the spectrum. However, findings which showed that visible light leads to DNA damage in cultured cells and that it contributes significantly to the production of radicals in substratum corneum [276], have shifted this view. It is accepted today that several photodermatoses, a broad group of skin disorders, have action spectrum within the visible light range and that radiation above $400nm$ can cause skin pigmentation and probably contributes to the carcinogenic effect of sunlight [245]. Despite that, most of the available sunscreens protect against the effect of UVB and sometimes against UVA radiation (total blockers), but provide poor protection against visible light. The effectiveness of sunscreens in blocking visible light can be enhanced by using larger particle size or pigmentary titanium dioxide. The latter has been utilized in a recent study, which has shown that tinted sunscreens can provide an excellent protection against visible light mediated DNA damage [124].

Visible light is also used in biomedical applications. Phototherapy is thought to enhance wound healing and treat a variety of medical conditions like chronic pain, arthritis and skin trauma. One of the most popular treatments is the phototherapy for neonatal jaundice, in which an infant is exposed to blue light ($430 - 490nm$) at powers ranging from 0,1 to 0,15 $W/m^2$ (more than 0,3 $W/m^2$ in intensive phototherapy) [277]. Absorption of visible light by bilirubin leads to several photochemical reactions. The products of these reactions can be excreted, which allows to reduce high bilirubin levels. Due to its remarkable effectiveness, this phototherapy has been used for more than 50 years. However, several studies have shown that exposure of cells in culture to visible light comparable to that used in phototherapy results in DNA damage [278] and that the levels of DNA damage are increased in newborns after PT in comparison to a control group [279–281]. One of the most recent studies have shown that this effect is transient and suggested that the PT-related DNA damage is repairable [280], but more studies are needed to assess the potential negative effects of this therapy.

## 4.7 The formation, behaviour and role of XRCC1 foci

The recruitment of XRCC1 to laser-induced local DNA damage has been demonstrated in many studies. This protein is often used as a marker of SSBs formation, but one has to remember that it is also engaged in BER. In our studies, since no oxidative damage was detected after irradiation with blue laser light, it was concluded that the cause of accumulation of XRCC1 at the site of damage was the formation of SSBs. The induction of local DNA damage by visible laser light allowed to observe a

behaviour of XRCC1 that was not described in the literature before. First accumulated in a cloud-like pattern, XRCC1 soon started forming distinct foci in the irradiated region.

The possible explanations of the transition of XRCC1 from a homogenous distribution to individual foci at the site of damage were discussed in PAPER 2.However, there are several interesting issues regarding the formation of foci (bodies) by XRCC1. First of all, one should notice that the size and registered fluorescence intensity of foci can only be explained by the presence of multiple copies of XRCC1-RFP in each focus. Thus, under the assumption that one focus represents one SSB, one realizes that there are numerous copies of XRCC1 per single-strand DNA break. While the possibility that several SSBs are present in a focus cannot be excluded, it seems unlikely, since it could only be explained by the formation of single-strand break repair centres or by a non-random induction of lesion in DNA. These two alternative explanations seem even more doubtful in the light of experiments which suggest that single and double-strand breaks are spatially separated at the site of laser irradiation (see point 4.8.1 and Fig. 4.1). The possibility that multiple copies of XRCC1 are in close proximity to a SSB raises other intriguing questions, i.e. 1) what triggers the formation of a XRCC1 focus? 2) what is the number of XRCC1 proteins in a focus? 3) are all of these proteins engaged in repair or do they constitute a type of reservoir from which proteins are delivered to the damage site?

In the course of the conducted experiments only once we observed the recruitment of a pre-formed XRCC1 focus to the site of laser irradiation (damage induced by parking the laser beam; data not shown). However, this focus reached the damage site 40 minutes after damage induction, after travelling a several micrometer distance. Moreover, XRCC1 recruited with normal kinetics was already present at the site of irradiation. When the damage was induced by irradiating a larger area ($2{,}5 \times 2{,}5\ \mu m$), we never observed the recruitment of foci present in the nucleus prior to irradiation to the damage site. This suggests that these foci are formed *de novo* at the damage site. The mechanism of formation of foci is unclear but one can imagine that it is triggered by the high concentration of XRCC1 during the first stage of its recruitment to the damage.

To estimate the number of proteins in an XRCC1 focus is not straightforward since fluorescence intensity is influenced by factors such as laser intensity or detector gain and also by the physicochemical environment of the chromophore. Moreover, because of the presence of endogenous XRCC1 as well as the fluorescent-tagged XRCC1 proteins, the obtained value would probably be an underestimate. Regarding the third question, it has been suggested before that high local concentration of proteins in DSB-associated foci increases the efficiency of biochemical steps, but this issue remain poorly studied [282].

Other interesting observations presented in PAPER 2 were the ability of some XRCC1 foci formed outside of the region subjected to visible light to travel through the nucleus, the colocalisation of XRCC1 and Sp100 in a subset of foci and the recruitment of the latter protein to laser induced damage. Interesting problems emerging from these observations are: 1) how are XRCC1 foci present at the site of laser irradiation different from the mobile foci formed outside of this region? 2) how are the foci formed at the site of damage attached, so they display only limited, oscillatory movement? 3) what

triggers the detachment and allows some foci to travel through the nucleus and why this is not observed for foci present at the damage site? 4) do XRCC1 and Sp100 physically interact? 5) what is the role of Sp100 in DNA repair?

Unfortunately, the experiments performed so far do not give many clues regarding these problems. No structural differences were detected between static and mobile XRCC1 foci. Nevertheless, we observed that some foci formed outside of the directly illuminated region were static for a substantial period of time (several minutes) and suddenly, without any exogenous stimulus, became mobile. This suggest that these two foci types might be structurally identical and switch between mobile and static behaviour depending on the presence of some unknown binding sites on proteins or DNA. Alternatively, one can imagine that static XRCC1 foci could represent those trapped between chromatin domains. Occasionally, such a focus would escape into the interchromosomal space and would be allowed to move until being trapped again between other domains. This hypothesis, although quite captivating, does not explain the static behaviour of foci formed at the site of laser irradiation. Among the other proposed problems, the one that could be quite directly addressed is the possible interaction of Sp100 and XRCC1. Some of the possible techniques that could be used for assessing this issue are Forster Resonance Energy Transfer (FRET), Proximity Ligation Assay (PLA) or coimmunoprecipitation.

## 4.8 Other potential applications of inducing local DNA damage by visible laser light in vitro

### 4.8.1 Studies of spatial organization of single and double-strand DNA breaks repair machinery and related research

As mentioned in PAPER 2, the visualization of single and double-strand DNA breaks in the form of foci was so far only possible after inducing a global DNA damage. On the other hand, the formation of SSB and DSB-related foci, i.e. XRCC1 and $\gamma$H2AX respectively, in a small volume of the nucleus after damage induced by focused visible light opens up a possibility to study several aspects of the DDR, which were not accessible before. Preliminary experiments in which we aimed at the simultaneous detection of XRCC1 and $\gamma$H2AX foci have shown, quite surprisingly, that these two entities are spatially distinct, with very little or no colocalisation at all at the site of laser irradiation (Fig. 4.1). Several potential explanations for the observed spatial pattern exist. There is a possibility that SSBs and DSBs are induced in different chromatic regions, but one cannot exclude that separation of these two lesion types is a consequence of chromatin and/or repair machinery reorganization, which occurs within minutes after damage induction. It should be noted that Fig. 4.1 shows the spatial relationship between XRCC1 and $\gamma$H2AX approximately 15 minutes after the insult, since this is the time that elapsed from damage induction to cell fixation, necessary for performing immunofluorescence against $\gamma$H2AX. Visualization of DSBs in the form of $\gamma$H2AX foci is convenient, mainly due to the fact this modification spreads along large chromatin stretches on both sides of the lesion. The signal is thus naturally amplified, which assures an efficient detection with antibodies. Nevertheless, this histone modi-

fication can only be detected in fixed cells which limits the scope of information that can be obtained from these kind of experiments. Thus, establishing a DSB-specific repair factor that would be promptly recruited to these lesions in many copies, just like XRCC1 is recruited to SSBs, would be of great value. In the case of spatial distribution of SSBs and DSBs at the site of local damage, live cell imaging of factors forming foci at these two lesion types would allow to track their positions during the whole repair process. Our experiments have shown that XRCC1 foci formed at the site of laser irradiation do not show substantial mobility, yet it would be interesting to see if the same holds true for DSB-related foci.

Also, if the disappearance of a repair focus from the damage site could be identified with the completion of repair processes (as it is in the case of XRCC1), it would be possible to obtain a set of valuable information regarding the rate of SSB and DSB repair. For example, one could assess the mean time necessary to repair a single SSB or DSB in each phase of the cell cycle or study the influence of the overall number of lesions on the repair rate of an individual break. Since the number of lesions increases with the total dose of light delivered to the damage site, it should also be possible to estimate the maximum number of lesions that are still repairable by an individual cell. Increasing the number of lesions above this threshold should oversaturate the repair capacity of the cell and lead to cell death.

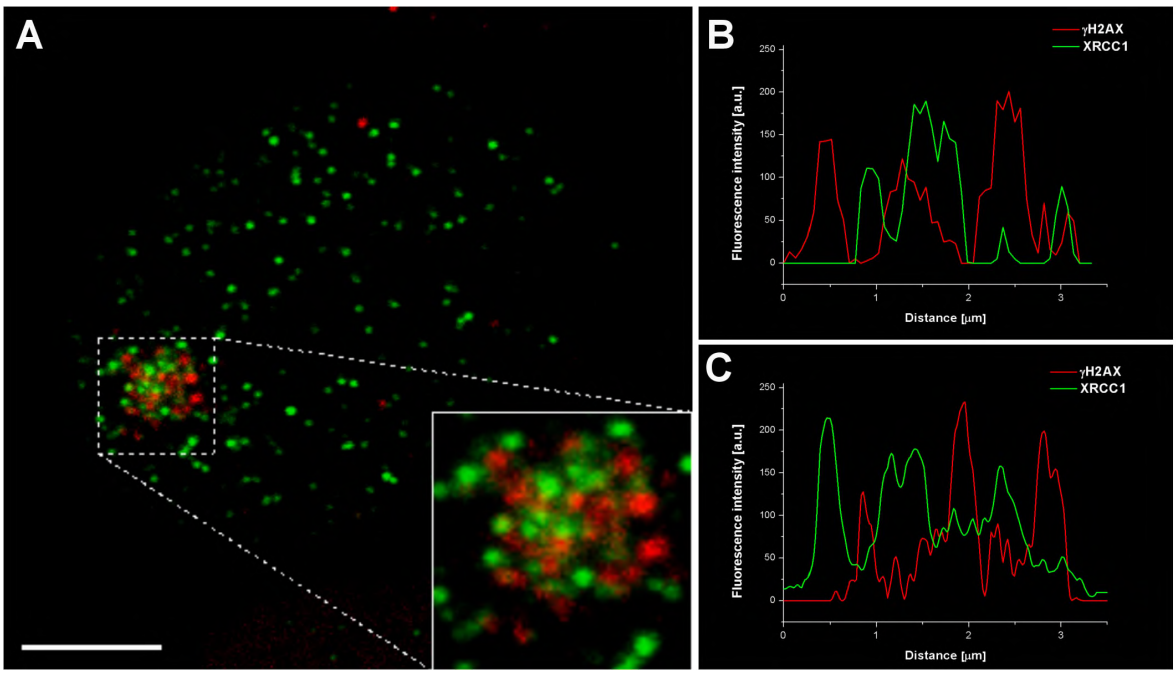


Figure 4.1: **γH2AX and XRCC1 foci are spatially separated at the damage site.** HeLa cells expressing RFP-XRCC1 were locally damaged by blue light. RFP-XRCC1 was rapidly recruited to the irradiated region and soon formed distinct foci (red). Subsequently, the cells were fixed and stained against phosphorylated histone H2AX (green). The confocal image (single slice) (A) and fluorescence intensity profiles (B, C) show that there is little colocalisation between XRCC1 and γH2AX foci at the site of irradiation. Scale bar $-5\ \mu m$ in A, $2\ \mu m$ in inset.

One of the most interesting aspects of the DDR that could be studied if SSB and DSB-related foci were simultaneously observed in living cells, would be the conversion

of SSBs to DSBs. Although it seems that blue laser light is able to induce DSBs directly, it is probable that some SSBs are later converted into DSBs, at least in the S phase of the cell cycle. These studies would allow to elucidate whether this conversion really occurs and eventually, what is the yield of indirectly induced DSBs.

Finally, the spatial distribution of repair foci observed after damage induced by visible laser light might allow to study the choice of repair pathway in each individual foci. Both single and double-strand DNA breaks can be repaired through different repair pathways. If one could observe the recruitment of proteins characteristic for each subpathway of SSBR or DSBR to visible-light generated foci, it would be possible to determine if all lesions are repaired through one subpathway (e.g. only SP for SSBs and NHEJ for DSBs) or there are different subpathways running in neighbouring foci (e.g. NHEJ and HR proteins DSB-related foci).

### 4.8.2 Repair of DNA breaks in eu- and hetereochromatin

Local DNA damage by visible light can be induced in any part of the nucleus by repeatedly scanning a region or by parking the beam for a given time. The latter approach enables to confine the damage to a very small volume and seems suitable for studying the DDR in regions of chromatin which differ in compaction. Initial experiments were performed in mouse 3T3 cells, which contain large and highly condensed chromocenters. Since we used cells stably expressing histone H1-GFP, small lesions were localised precisely in these densely packed regions, and then the recruitment of XRCC1 or phosphorylation of H2AX was followed. The experiments have shown that XRCC1 is promptly recruited to chromocenters, despite the presence of compacted chromatin (Fig. 4.2). However, in most experiments, minutes after induction of the damage additional foci of XRCC1 were formed at the border of eu- and heterochromatin. It is tempting to hypothesize that some of the lesions initially surrounded by heterochromatin are moved to the periphery of the chromocenters, so the repair might proceed at the interface of two differently packed regions.

In the case of $\gamma$H2AX two scenarios were observed. In a subset of cells, phosphorylation was detected inside of the chromocenters (Fig. 4.3) In some cells, though, $\gamma$H2AX was excluded from heterochromatin and was visible around chromocenters (Fig. 4.4). Interestingly, when damage was induced in eu- and heterochromatin with the same dose of light, the area of phosporylation was markedly different, with much smaller foci visible in euchromatin (Fig. 4.3). The simplest explanation of this phenomenon is based on the fact that there are more lesions induced in heterochromatin, due to a higher DNA content. Nevertheless, other hypotheses such as different scattering of light between euchromatin and chromocenters or variations in signalling of DSBs depending on the compaction of chromatin, should also be considered.

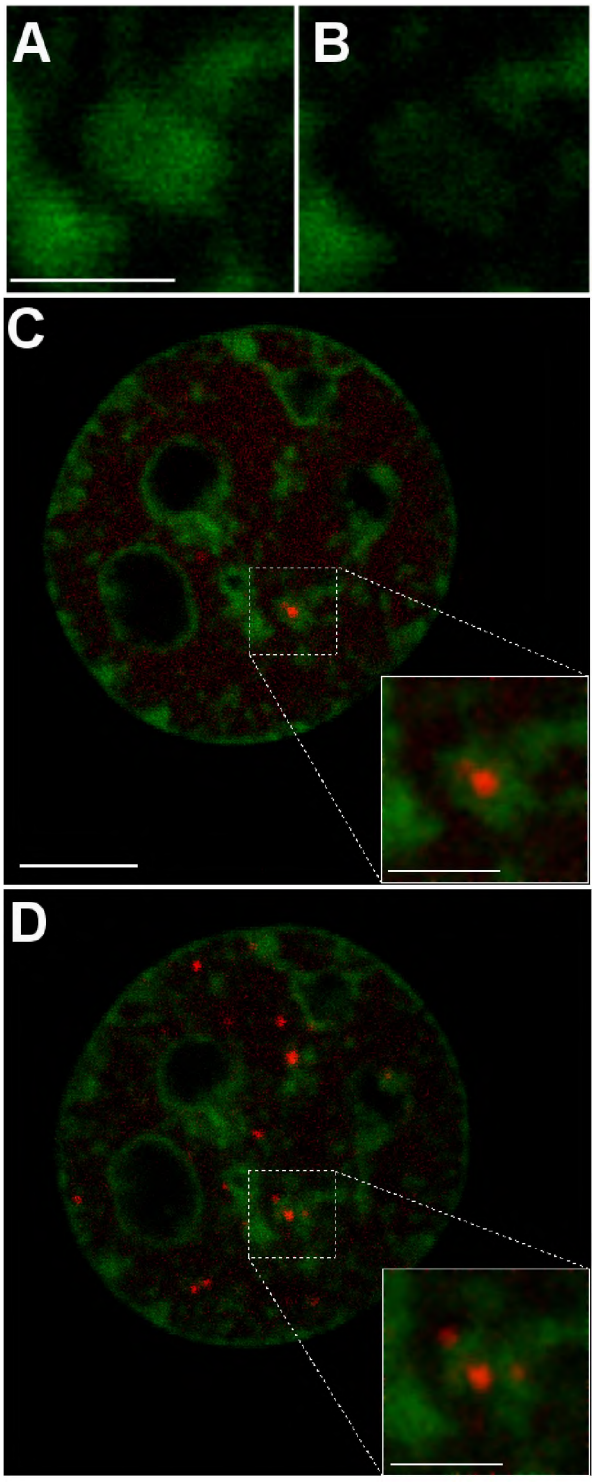


Figure 4.2: **XRCC1 is recruited to visible light induced damage located in heterochromatin.** 3T3 cells coexpressing histone H1-GFP and RFP-XRCC1 were locally damaged by visible light. The damage was induced by parking the laser beam (488 $nm$) at a chromocenter (A), which resulted in the bleaching of H1-GFP (B). RFP-XRCC1 was rapidly recruited to the damage site and formed a focus within the damaged chromocenter (C). Several minutes after damage induction additional XRCC1 foci were formed at the border of eu- and heterochromatin (D). Scale bar $-5$ $\mu m$ in C and D, 2 $\mu m$ in A, B and insets.

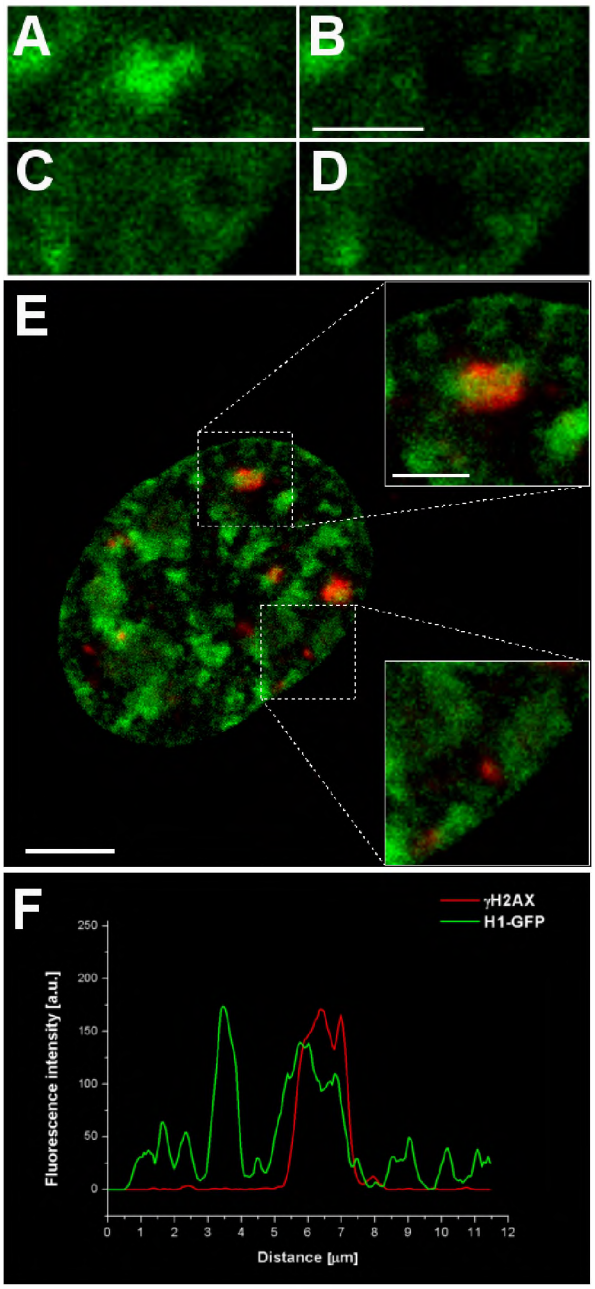


Figure 4.3: **Histone H2AX is phosphorylated in eu- and heterochromatin after damage induced with visible light.** 3T3 cells expressing histone H1-GFP were locally damaged by visible light. The damage was induced by parking the laser beam (488 $nm$) at a chromocenter (A) or in euchromatin (C). Visible light irradiation resulted in the bleaching of H1-GFP (B, D). 15 minutes after damage induction the cells were fixed and stained against $\gamma$H2AX. Phosphorylation of histone H2AX can be seen in eu- and heterochromatin (E, insets), but the size of region in which $\gamma$H2AX is detected is markedly different. The appearance of $\gamma$H2AX in dense chromatin is also presented on a fluorescence line profile (F). Scale bar $-5$ $\mu m$ in E, 2 $\mu m$ in A-E and insets.

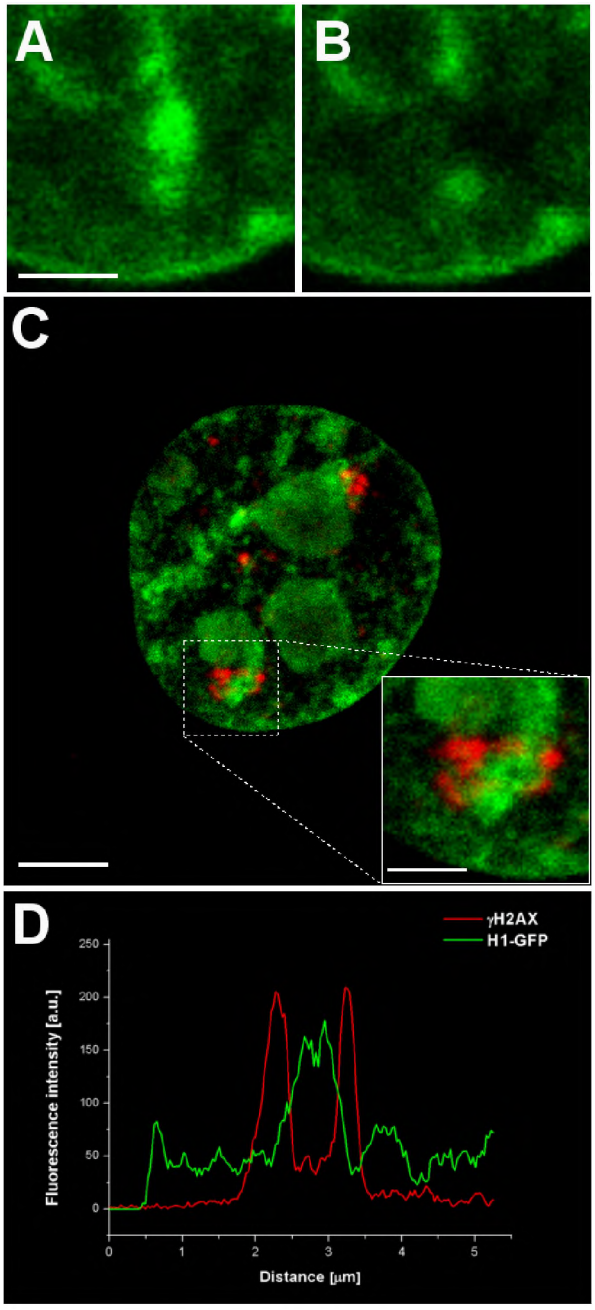


Figure 4.4: **$\gamma$H2AX is excluded from heterochromatin after damage induced within a chromocenter by visible light.** 3T3 cells expressing histone H1-GFP were locally damaged by visible light. The damage was induced by parking the laser beam ($488nm$) at a chromocenter (A), which resulted in the bleaching of H1-GFP (B). 15 minutes after damage induction the cells were fixed and stained against $\gamma$H2AX. Phosphorylation of histone H2AX can be detected mainly at the border of eu- and heterochromatin (C, D). Scale bar $-5\ \mu m$ in C, $2\ \mu m$ in A, B and inset.

These experiments suggest that both single and double-strand DNA breaks can be signalled and probably repaired within densely packed chromatin. Sometimes, however, heterochromatin seems refractory to repair, which is manifested by the exclusion of $\gamma$H2AX from chromocenters and by the formation of additional XRCC1 foci at the periphery of these densely packed regions. Again, further studies are needed to confirm the hypothesis regarding the repair of SSBs in heterochromatin and to show the early events in the repair of DSBs.

In preparation to the above described experiments an optimization of the $\gamma$H2AX staining protocol was done. This allowed to detect weaker phosphorylation events and in turn, to verify the lowest dose of visible light which results in DNA damage. It was found that parking the laser beam for as short as 10 ms, which corresponds to approximately 6 $\mu J$, gives rise to $\gamma$H2AX foci. The recruitment of other repair factors after irradiation with this dose remains to be demonstrated.

Table 4.1: Comparison of methods of local DNA damage induction based on laser microirradiation.

| – | AUTHOR, YEAR | LASER | IRRADIATION | PHOTO-SENSITIZER | TYPES OF DAMAGE / REPAIR FACTORS DETECTED | OTHER INFOR-MATION |
|---|---|---|---|---|---|---|
| 1 | Tashiro, 2000 [283] | 337 $nm$ pulsed (PALM) | 10 $MJ/m^2$ | BrdU for 20 $h$ | Rad51, ssDNA | |
| 2 | Lukas, 2003 [271] | 337 $nm$ $N_2$ 30 $Hz$ pulsed (PALM) | Laser output: 50% | IdU 10 $\mu M$ for 24 $h$ | 40%: BRCA1, no $\gamma$H2AX, 50%: BRCA1, $\gamma$H2AX, Nbs1, 60%: BRCA1, global $\gamma$H2AX | |
| 3 | Lukas, 2004 [272] | 337 $nm$ $N_2$ 30 $Hz$ pulsed (PALM) | Laser output: 50%, irradiation $< 1$ $s$ | BrdU 10 $\mu M$ for 24 $h$ | $\gamma$H2AX, Nbs1, Mdc1 | Cells observed for 48 $h$ after irradiation without morphological effects |
| 4 | Celeste, 2003 [284] | 337.1 $nm$ | As in Rogakou, 1999 | Hoechst 33258 10 $\mu g/ml$ for 20 $min$ | $\gamma$H2AX, Nbs1, 53BP1, Mre11 | |
| 5 | Bekker-Jensen, 2005 [266] | 337 $nm$ (PALM) | Laser output: 55% | BrdU 10 $\mu M$ for 24 $h$ | Mdc1, 53BP1, $\gamma$H2AX | 17% cell death in comparison to 6% in non-irradiated, 21% normal mitosis vs 90%, 62% no cell division. |
| 6 | Bekker-Jensen 2006 [285] | 337 $nm$ (PALM) | As in Lucas, 2003 | – | $\gamma$H2AX, 53BP1, RPA, ATM, Mdc1, Mre11, Rad51, ATR, FANCD2, ssDNA (TUNEL), Nbs1, BRCA1, no Ku70, SMC1 | Comparison to damage induced by IR, comparable to 4-6 $Gy$, High dose (73% – BrdU): reduced Topro staining, RPA not in foci but homogenous, Ku70 and cohesin accumulation. |
| 7 | Mortusewicz, 2005 [128] | 337 $nm$ pulsed $N_2$ | 8 $nJ$/pulse, 30 pulses, 1 $\mu m$ spot | BrdU 10 $\mu g/ml$ for 20 $h$ | $\gamma$H2AX , DNMT1, PCNA | |
| | | 405 $nm$ | Laser set to maximum power, 50 $mW$, at 100% transmission, irradiation for 1 $s$ | BrdU 10 $\mu g/ml$ for 20 $h$ | Thymine dimers, DSBs (data not shown), DNMT1, PCNA, LigIII | |

*continued on next page...*

... continued from previous page

| | | | | | | |
|---|---|---|---|---|---|---|
| 8 | Roukos, 2011 [286] | 355 $nm$ Nd:YAG pulsed 470 $ps$ | 0,2 $mW$ average power 100 $nJ$/pulse, total irradiation $< 1{,}5$ $s$ | – | $\gamma$H2AX, ATM, Mre11, Ku70, PCNA, Cdt1, BRCA1, XRCC1, TFIIH | Damage not interfering with cellular viability, no damage in transmitted light or stained cells – cells visible for 7 $h$, probably no cell division. At higher doses whole nucleus $\gamma$H2AX staining |
| 9 | Kruhlak, 2006 [146] | 364 $nm$ | 0,86 $nJ$/pixel | Hoechst 33342 7,5 $\mu g/ml$ | $\gamma$H2AX, 53BP1 | Calculation of number of DSBs. |
| 10 | Kruhlak, 2007 [287] | 364 $nm$ | 0,86$nJ$/pixel using 50% output, 15,2 $\mu m^3$ | Hoechst 33342 0,8 $\mu l/ml$ for 20 $min$ | $\gamma$H2AX | |
| | | 800 $nm$ Ti:sapphire femtosecond pulsed | 12 $mW$ output at sample, 17,6 $\mu m^2$, irradiation for 60 $ms$ | – | | Similar kinetics after multiphoton and Hoechst sensitised damage. |
| 11 | Lan, 2004 [148] | 365 $nm$ pulsed | Power measurement: 0,19 $\mu J$ 0,49 $\mu J$ 1 $\mu J$/pulse 1 $\mu m$ spot size | – | 1 pulse 0,19 $\mu J$: PAR 1 pulse 0,49 $\mu J$: $\gamma$H2AX 10 pulses 1 $\mu J$: 8-oxoG 0,19 $\mu J$: XRCC1, Pol$\beta$, Lig III, PNCA, CAF1 0,49 $\mu J$: NTH1, OGG1, NEIL1 and 2 | |
| 12 | Rogakou, 1999 [145] | 390 $nm$ | 100% = 20 $\mu J$/pulse 10 pulses/s Maximum rate: 8 $\mu m/s$ Operated at outputs: 1-30% 0,5 $\mu m$ spot size | 0,4 $\mu M$ BrdU for 24 $h$ + Hoechst 33258 for 5 $min$ or Hoechst alone. | BrdU + Hoechst: nearly whole cell $\gamma$H2AX after 1% laser Hoechst: faint $\gamma$H2AX after 1%, significant after 30% | |
| 13 | Bradshaw, 2005 [273] | 390 $nm$ | Power output 75% = 2,5 $\mu W$ 4 $ns$ pulse duration, 2 pulses per $\mu m$ | Hoechst 33258 10 $ng/ml$ for 10 $min$ | $\gamma$H2AX, TRF2, ATM, WRN, BLM, Nbs1, Mre11 | |
| | | 790 $nm$ | Set to 20% power = 7-8 $mW$, 200 $ms$ pulse | Hoechst 33258 10 $ng/ml$ for 10 $min$ | | |

continued on next page...

*... continued from previous page*

| | | | | | | |
|---|---|---|---|---|---|---|
| 14 | Lan, 2005 [262] | 365 $nm$ pulsed | Low dose: 0,75 $\mu J$ High dose: 2,5 $\mu J$ | – | Low dose: PAR, no $\gamma$H2AX, no OGG1, XRCC1, LigIII High dose: PAR, $\gamma$H2AX, OGG1, WRN | Damage enhanced after BrdU |
| | | 405 $nm$ | 1 scan: 1600 $nW$ | – | 1 scan: XRCC1, no $\gamma$H2AX, 100 scans: XRCC1, $\gamma$H2AX , 500 scans: XRCC1, $\gamma$H2AX, OGG1 | Damage enhanced after BrdU |
| 15 | Mortusewicz, 2006 [275] | 405 $nm$ diode laser | Laser set to maximum power, at 100% transmission, irradiation for 1 $s$ | BrdU 10 $\mu g/ml$ for 24-48 $h$ | $\gamma$H2AX, PAR, PCNA, XRCC1, LigI, LigIII, PBD, FEN1, no Ku70, faint LigIV | |
| 16 | Mortusewicz, 2007 [274] | 405 $nm$ diode laser | Laser set to 50% transmission, irradiation for 1 $s$, 1 $\mu m$ spot | BrdU 10 $\mu g/ml$ for 24-48 $h$ or Hoechst 33258 10 $\mu g/ml$ for 10 $min$ | PARP1, PARP2, XRCC1 | Hoechst sensitisation leads to more damage. |
| 17 | Mortusewicz, 2007 [238] | 405 $nm$ diode laser | Laser set to maximum power, at 100% transmission, irradiation for 1 $s$ | BrdU 10 $\mu g/ml$ for 24-48 $h$ | XRCC1, PCNA, $\gamma$H2AX, PAR | |
| 18 | Mortusewicz, 2008 [288] | 405 $nm$ diode laser | Set to 50-80 $\mu W$, measured after objective | BrdU 10 $\mu g/ml$ for 24-48 $h$ | $\gamma$H2AX, PAR, PCNA, PC4, RPA34 | |
| 19 | Godon, 2008 [289] | 405 $nm$ diode laser | Maximum output for 500 $ms$, spot size 176 $nm$ | – | XRCC1, PARP1, PCNA | |
| 20 | Baldeyron, 2011 [290] | 405 $nm$ diode laser | 25 $mW$, laser set to 70% maximum output or 100% for single nuclei imaging | Hoechst 33258 10 $\mu g/ml$ for 5 $min$ | $\gamma$H2AX, HP1$\alpha$, KAP-1, CAF-1, Mdc1, 53BP1 | DAPI used in IF despite Hoechst present for photosensitisation. |
| 21 | Hanssen-Bauer, 2011 [150] | 405 $nm$ diode laser | Measured power: 30 $mW$ 10/60 iterations 150/600 iterations | – | Low dose: Pol$\beta$, PNK, XRCC1, PARP1 High dose: PCNA, FEN1, $\gamma$H2AX (600 it) | |
| 22 | Hanssen-Bauer, 2012 [263] | 405 $nm$ diode laser | 30 $mW$ 60 iterations 1,27 $\mu s$/pixel 600 iterations | – | Low dose: Pol$\beta$, PNKP, no PCNA High dose: PCNA, FEN1, $\gamma$H2AX | |
| 23 | Bolin, 2012 [291] | 405 $nm$ diode laser | Maximum output for 500 $ms$, spot size 176 $nm$ | – | PARP1, XRCC1, PCNA | |
| 24 | Campalans, 2013 [131] | 405 $nm$ diode laser | Laser set to 10% | – | no 8-oxoG, XRCC1 | |
| | | | | Ro 19-8022 5 $\mu m$ for 5 $min$ | 8-oxoG, OGG1, XRCC1 | |

*continued on next page...*

*... continued from previous page*

| | | | | | | |
|---|---|---|---|---|---|---|
| 25 | Wei, 2013 [244] | 405 $nm$ | Final output of 5 $mW$ after passing through the lens, irradiation for 10 $ms$ | – | PAR, XRCC1, LigIII, PCNA, Pol$\beta$, PNK, LigI, APTX | |
| 26 | Abdou, 2015 [292] | 405 $nm$ | 30 $mW$ at 60% 30 iterations | Hoechst, 0,5 $\mu g/ml$ for 20 $min$ | 8-oxoG, XRCC1, OGG1 | |
| | | 750 $nm$ Ti:sapphire | 50 $mW$ laser line at 10%, 10 iterations, 1,2 $\mu m$ region | Hoechst 33258, 1 $\mu g/ml$ for 20 $min$ | XRCC1, no 8-oxodG, PARP1, Lig3, PNKP, OGG1 (faint), $\gamma$H2AX | Huge XRCC1 and $\gamma$H2AX effect. |
| 27 | Berquist, 2010 [130] | 435 $nm$ SRS NL100 | Laser intensity 1,5% (total energy output 10 $nW$) | – | No $\gamma$H2AX foci at this power (not shown), XRCC1 | |
| 28 | Tadokoro, 2012 [264] | 435 $nm$ SRS NL100 | 3% intensity | – | XRCC1, no 53BP1, RECQL5 | |
| 29 | Popuri, 2012 [265] | 435 $nm$ SRS NL100 | 7% or more to induce DBSs 3-4% to induce SSBs | – | Low dose: XRCC1, no 53BP1 High dose: 53BP1, XRCC1, $\gamma$H2AX, RECQL5, BLM, WRN, RECQL4 | |
| 30 | Zarębski, 2009 [129] | 514 $nm$ | 35 $\mu W$, 10 scans, 166 lines/s, 512 × 512 pixels | Ethidium bromide 100 or 200 $nM$ for 20 $min$ | $\gamma$H2AX, XRCC1, 8-oxoG, HP1$\alpha$, HP1$\beta$ no 8-oxoG in low oxygen | |
| 31 | Chen, 2005 [293] | 532 $nm$ pulsed 12$ps$ 76 $MHz$ | – | – | $\gamma$H2AX | The same setup as used for microtubules ablation. |
| 32 | Kim, 2002 [127] | 532 $nm$ pulsed Nd:YAG | 2-3 $\mu J$/pulse 4-6 $ns$ pulse duration 5 $\mu m$ line scanned for 2 $min$ | – | Mre11, Rad50, cohesin, Ku70, ATM, BrdU (TUNEL) | *„Parameters similiar to those used for mitotic chromosome cutting, nuclear body ablation, 2-3 times higher than estimated values of optical water breakdown"* Damage visible in phase contrast Cell viability observed for 30 hours (not shown) |

*continued on next page...*

*... continued from previous page*

| | | | | | | |
|---|---|---|---|---|---|---|
| 33 | Kim, 2005 [270] | 532 $nm$ pulsed Nd:YAG | 2-3 $\mu J$/pulse 4-6 $ns$ pulse duration 5 $\mu m$ line scanned for 2 $min$ | – | $\gamma$H2AX, Ku, Mre11, DNA-PK, Lig IV, Rad51 | *Nd:YAG laser can be focused to 200-300 $nm$ spot, damage most likely caused by ionization (optical breakdown) of the medium (water) and plasma formation, breaks caused by expansion of cavitation bubbles that caused photomechanical pressure.* |
| 34 | Meldrum, 2003 [267] | 750 $nm$ Ti:Sapphire 120 $fs$, 82 $MHz$ | Final power of 10 $mW$ at the stage Peak fluence =190 $GJ/cm^2$ Pixel dwell time 25 $ms$ | – | CPDs | No significant effect on cell viability. |
| 35 | Daddysman, 2011 [268] | 750 $nm$ Ti:Sapphire tunable | 80 $mW$ measured after the objective | – | Minimum dose for CPDs | Cells destroyed or morphological changes. |
| | | 400-525 $nm$ | 14 $mW$ for 425 $nm$, 80 $MHz$ repetition rate | – | CPDs | No morphological changes. |
| | | 488 $nm$ CW | 13 $mW$ | – | no CPDs | No morphological changes, but are for 488 $nm$ pulsed. |
| 36 | Zielińska, 2011 [294] | 768 $nm$ Ti:sapphire | 10 $mW$ power at sample | – | OGG1 | |
| 37 | Träutlein, 2010 [151] | 775 $nm$ tunable femtosecond 230 $fs$ 107 $MHz$ | Peak irradiance 312 $GW/cm^2$, measured af microscope, Pixel dwell time 44,2 $ms$ 10 $\mu m$ lines, 76 pixels 300 $GW$ chosen for experiments | – | XRCC1, 6-4PP, CPD, $\gamma$H2AX | |
| | | 1050 $nm$ tunable 77 $fs$ | 1200 $GW/cm^2$ 900 $GW$ chosen for experiments | – | XRCC1, faint 6-4PP and CPD, $\gamma$H2AX | |

*continued on next page...*

*... continued from previous page*

| | | | | | | |
|---|---|---|---|---|---|---|
| 38 | Mari, 2006 [254] | 800 $nm$ Ti:Sapphire 200 $fs$ 76 $MHz$ | 10 $mW$ output at the sample 86 $ms$ exposure restricted to a 2,5 $\mu m$ circular region | – | $\gamma$H2AX, TUNEL, Ku80, DNA PK, LigIV, XRCC4 | No damage to nucleus seen after DAPI, ToPro3, DRAQ5 or transmitted light, cell membranes intact 2 $h$ af damage (trypan blue) Cells able to divide after damage but with caffeine to overcome G2/M checkpoint. |
| 39 | Gomez-Godinez, 2007 [269] | 800 $nm$ Ti:Sapphire 200 $fs$ 76 $MHz$ | 20 $ms$ exposure at 2,1 or $6{,}1 \times 10^6$ $W/cm^2$ | – | Low dose: $\gamma$H2AX, Nbs1 High dose: Rad50, Nbs1 | Phase-dark line after high dose damage. |
| 40 | Inagaki, 2009 [295] | 800 $nm$ Ti:Sapphire 200 $fs$ 76 $MHz$ | 40 or 75 $mW$ output, 40x40 pixel (4 $\mu m^2$), pixel dwell time 1,6 $\mu s$ 5 iterations | – | 40 $mW$: Rad18, Rad51, Ku86, $\gamma$H2AX, no XRCC1 CPD XPA 75 $mw$: all of the above + PCNA | |
| | | UV laser (as in Dinant, 2007) | Irradiation for 0,49 $s$ | – | Rad18, PCNA | |
| 41 | Dinant, 2007 [147] | 266 $nm$ pulsed diode 7.8 $kHz$ | 2 $mW$ (7.8 $kHz$) | – | None of those below, but at high dose: $\gamma$H2AX, Ku70, TUNEL, CPD, 6-4PP Low dose: only NER factors | Low dose: cells able to go through mitosis (movie). |
| | | 405 $nm$ diode laser | 30 $mW$, damage at 60% max power | Hoechst 33342 0,5 $\mu g/ml$ shortly before irradiation | $\gamma$H2AX, TUNEL, MDC1, Rad54, Ku70, PARP1, CPD, no 6-4PP | 10× higher laser intensity needed to induce damage without Hoechst. |
| | | 800 $nm$ Ti:Sapphire 200 $fs$ 76 $MHz$ | 80 $mW$ maximumu output | – | $\gamma$H2AX, TUNEL, PKcs, Mdc1, Rad54, Ku70, PARP1, CPD, 6-4PP | When dose was lowered, no XPA and no Rad54 detected, so not possible to induce one type of lesion. |

*continued on next page...*

... continued from previous page

| | | | | | | |
|---|---|---|---|---|---|---|
| 42 | Kong, 2009 [132] | 337 $nm$ pulsed $N_2$, 4 $ns$ 6 $Hz$ | 0,04 $\mu J$/pulse Peak irradiance: 0,13 × 1011 $W/cm^2$ Total energy: 0,8 $\mu J$ | – | CPD, 6-4PP, 8-oxoG, PARP1, XRCC1, FEN1, Ku70 (lowe dose +BrdU and high dose no BrdU), 53BP1 (high dose), cohesin (high dose) | Damage visible in phase contrast. |
| | | 405 $nm$ CW diode laser | 1,87 $mW$ Scanning rate 40 $\mu s$/pixel Peak irradiance: 0,56 × $10^2$ $W/cm^2$ Total energy: 75000 $nW$ | – | No Ku70 53BP1 (low dose+BrdU), cohesin | Damage NOT visible in phase contrast. |
| | | 532 $nm$ pulsed Nd:YAG 6 $ns$ 10 $Hz$ | 0,032 $\mu J$/pulse Peak irradiance: 0,27 × $10^{10} W/cm^2$ Total energy: 38 $\mu J$ Scanned for 2 $min$ with 10 $\mu m/s$ | – | CPD, no 6-4PP and no 8-oxoG, PARP1, XRCC1, FEN1, Ku70, 53BP1, cohesin | Damage visible in phase contrast. |
| | | 532 $nm$ Nd:YVO4 12 $ps$ 76 $MHz$ | 0,044 $\mu J$/pulse Peak irradiance: 0,22 × $10^{10} W/cm^2$ Total energy: 2407,7 $\mu J$ | – | CPD, 6-4PP, no 8-oxoG, PARP1, XRCC1, FEN1, Ku70, 53BP1, cohesin | Damage visible in phase contrast. |
| | | 800 $nm$ Ti:Sapphire 200 $fs$, 76 $MHz$ | 0,047 $\mu J$/pulse Peak irradiance: 0,61 × $10^{12} W/cm^2$ Total energy: 4286 $\mu J$ | – | CPD, 6-4PP, no 8-oxoG, PARP1, XRCC1, FEN1, Ku70, 53BP1, cohesin | Damage visible in phase contrast. |

Damage induced in the presence of a photosensiziter.

Information regarding laser power is not sufficient.

Cells viable after damage induction.

Deleterious effects on cell viability.

# Chapter 5

# CONCLUSIONS

The work presented in this doctoral thesis aimed at the development and application of a new method of local DNA damage induction. These goals have been achieved. It was shown that a focused beam of visible laser light, typically used in confocal microscopy, is capable of generating localised DNA lesions in the nuclei of living cells in the absence of exogenous photosensitisers. The mechanism of damage induction remains unknown, but is probably not based on excitation of endogenous, cytosolic photosensitisers. Comparisons with the existing approaches allowing for the induction of local DNA damage proves that the proposed method is advantageous in several aspects. The most important of these are the absence of exogenous photosensitisers and induction of a well-defined, repairable damage. Wide accessibility of the blue laser makes this method immediately available for many researchers. Other methods allowing for localised induction of DNA damage are often poorly characterised with respect to the setup used or types of generated lesions, which hinders comparison between different studies and leads to contradictory results. The major drawback of inducing local DNA damage by blue laser light is the concomitant excitation of the GFP. However, it was shown that this issue does not preclude the use of this method in studying the recruitment of repair proteins to locally inflicted damage and can be easily overcome by choosing appropriate fluorescent tags. The new method has been applied for demonstrating an interesting behaviour of a central BER and SSBR protein, XRCC1, at sites of local DNA damage. It is believed that this observation was possible due to the induction of a low number of DNA breaks by focused visible light. These studies provide important insights into the spatial organization of SSBR and raise intriguing questions regarding the role of nuclear bodies in the DNA repair processes. Although the proposed method might be applied for studying any aspect of the DNA Damage Response, it seems particularly attractive for elucidating the spatial relationship between SSB and DSB repair sites and for studying the repair response in structurally different chromatin regions.

The conducted research underscores a need to perform a comprehensive characterisation of the applied methods at the beginning of every experiment. One should not choose a protocol based solely on the criterion of its previous usage. Unfortunately, in the field of DNA repair, for a long time the only criterion that a particular method was expected to meet was the ability to generate DNA lesions. This approach, although useful at the beginning as it provided basic information regarding the behaviour of repair factors after DNA damage induction, is not sufficient for deciphering the some-

times subtle differences between DNA repair pathways. In recent years the importance of setup and damage characterisation has been appreciated by several researchers and hopefully this will become a normal practice in the nearest future. Taking into account the continuing development of super-resolution imaging techniques, I firmly believe that the methods allowing for local DNA damage induction, including the method proposed in this doctoral thesis, are still to provide many new insights concerning the fascinating processes of DNA Damage Response.

# References


[1] Evans, M. D., Griffiths, H. R. & Lunec, J. in *Mechanisms of Cell Toxicity* (ed.B̃ittar, E. E.) **20**, 25–73 (Elsevier, 1997).

[2] Von Sonntag, C. *Free-Radical-Induced DNA Damage and Its Repair.* (2006). doi:10.1007/3-540-30592-0

[3] Sonntag, C. *The chemical basis of radiation biology.* (1987).

[4] Steenken, S. *Purine bases, nucleosides, and nucleotides: aqueous solution redox chemistry and transformation reactions of their radical cations and e- and OH adducts.* Chem. Rev. **89**, 503–520 (1989).

[5] Vieira, A. J. S. C. & Steenken, S. *Pattern of hydroxy radical reaction with adenine and its nucleosides and nucleotides. Characterization of two types of isomeric hydroxy adduct and their unimolecular transformation reactions.* J. Am. Chem. Soc. **112**, 6986–6994 (1990).

[6] Steenken, S. *Addition-elimination paths in electron-transfer reactions between radicals and molecules. Oxidation of organic molecules by the OH radical.* J. Chem. Soc., Faraday Trans. 1 **83**, 113–124 (1987).

[7] Burrows, C. J. & Muller, J. G. *Oxidative Nucleobase Modifications Leading to Strand Scission.* Chem. Rev. **98**, 1109–1152 (1998).

[8] Ravanat, J. L. & Cadet, J. *Reaction of singlet oxygen with 2'-deoxyguanosine and DNA. Isolation and characterization of the main oxidation products.* Chem. Res. Toxicol. **8**, 379–388 (1995).

[9] Kamiya, H. & Kasai, H. *2-Hydroxyadenine (isoguanine) as oxidative DNA damage: its formation and mutation inducibility.* Nucleic Acids Symp. Ser. 233–234 (1995).

[10] Bruner, S. D., Norman, D. P. & Verdine, G. L. *Structural basis for recognition and repair of the endogenous mutagen 8-oxoguanine in DNA.* Nature **403**, 859–866 (2000).

[11] Kamiya, H. & Kasai, H. *Substitution and deletion mutations induced by 2-hydroxyadenine in Escherichia coli: effects of sequence contexts in leading and lagging strands.* Nucleic Acids Res. **25**, 304–311 (1997).

[12] Ono, T., Negishi, K. & Hayatsu, H. *Spectra of superoxide-induced mutations in the lacI gene of a wild-type and a mutM strain of Escherichia coli K-12.* Mutat. Res. **326**, 175–183 (1995).

[13] Jovanovic, S. V & Simic, M. G. *Mechanism of OH radical reactions with thymine and uracil derivatives.* J. Am. Chem. Soc. **108**, 5968–5972 (1986).

[14] Frenkel, K. et al. *Quantitative determination of the 5-(hydroxymethyl)uracil moiety in the DNA of gamma-irradiated cells.* Biochemistry **24**, 4527–4533 (1985).

[15] Gajewski, E., Rao, G., Nackerdien, Z. & Dizdaroglu, M. *Modification of DNA bases in mammalian chromatin by radiation-generated free radicals.* Biochemistry **29**, 7876–7882 (1990).

[16] Fuciarelli, A. F., Wegher, B. J., Blakely, W. F. & Dizdaroglu, M. *Yields of radiation-induced base products in DNA: effects of DNA conformation and gassing conditions.* Int. J. Radiat. Biol. **58**, 397–415 (1990).

[17] Nackerdien, Z., Olinski, R. & Dizdaroglu, M. *DNA base damage in chromatin of gamma-irradiated cultured human cells.* Free Radic. Res. Commun. **16**, 259–273 (1992).

[18] Pullman, A. & Pullman, B. *Molecular electrostatic potential of the nucleic acids.* Q. Rev. Biophys. **14**, 289–380 (1981).

[19] Boiteux, S. & Laval, J. *Imidazole open ring 7-methylguanine: an inhibitor of DNA synthesis.* Biochem. Biophys. Res. Commun. **110**, 552–558 (1983).

[20] O'Connor, T. R., Boiteux, S. & Laval, J. *Ring-opened 7-methylguanine residues in DNA are a block to in vitro DNA synthesis.* Nucleic Acids Research **16**, 5879–5894 (1988).

[21] Rydberg, B. & Lindahl, T. *Nonenzymatic methylation of DNA by the intracellular methyl group donor S-adenosyl-L-methionine is a potentially mutagenic reaction.* EMBO J. **1**, 211–216 (1982).

[22] Larson, K., Sahm, J., Shenkar, R. & Strauss, B. *Methylation-induced blocks to in vitro DNA replication.* Mutat. Res. **150**, 77–84 (1985).

[23] Loechler, E. L., Green, C. L. & Essigmann, J. M. *In vivo mutagenesis by O6-methylguanine built into a unique site in a viral genome.* Proc. Natl. Acad. Sci. U. S. A. **81**, 6271–6275 (1984).

[24] Holliday, R. & Ho, T. *Gene silencing and endogenous DNA methylation in mammalian cells.* Mutat. Res. **400**, 361–368 (1998).

[25] Chung, F.-L. et al. *Formation of trans-4-hydroxy-2-nonenal- and other enal-derived cyclic DNA adducts from omega-3 and omega-6 polyunsaturated fatty acids and their roles in DNA repair and human p53 gene mutation.* Mutat. Res. **531**, 25–36 (2003).

[26] Chung, F.-L., Chen, H. J. & Nath, R. G. *Lipid peroxidation as a potential endogenous source for the formation of exocyclic DNA adducts.* Carcinogenesis **17**, 2105–2111 (1996).

[27] Akasaka, S. & Guengerich, F. P. *Mutagenicity of site-specifically located 1,N2-ethenoguanine in Chinese hamster ovary cell chromosomal DNA.* Chem. Res. Toxicol. **12**, 501–507 (1999).

[28] Guengerich, F. P. et al. *Formation of etheno adducts and their effects on DNA polymerases.* IARC Sci. Publ. 137–145 (1999).

[29] Bartsch, H. & Nair, J. in (eds. Dansette, P. M. et al.) 675–686 (Springer US, 2001). doi:10.1007/978-1-4615-0667-6_100.

[30] Lindahl, T. *Instability and decay of the primary structure of DNA.* Nature **362**, 709–15 (1993).

[31] Barnes, D. E. & Lindahl, T. *Repair and genetic consequences of endogenous DNA base damage in mammalian cells.* Annu. Rev. Genet. **38**, 445–76 (2004).

[32] Lindahl, T. *The Croonian Lecture, 1996: endogenous damage to DNA.* Philosophical transactions of the Royal Society of London. Series B, Biological sciences **351**, 1529–1538 (1996).

[33] Karran, P. & Lindahl, T. *Hypoxanthine in deoxyribonucleic acid: generation by heat-induced hydrolysis of adenine residues and release in free form by a deoxyribonucleic acid glycosylase from calf thymus.* Biochemistry **19**, 6005–6011 (1980).

[34] Pfeifer, G. P. *Formation and Processing of UV Photoproducts: Effects of DNA Sequence and Chromatin Environment.* Photochem. Photobiol. **65**, 270–283 (1997).

[35] Black, H. S. et al. *Photocarcinogenesis: an overview.* J. Photochem. Photobiol. B. **40**, 29–47 (1997).

[36] Rastogi, R. P., Richa, Kumar, A., Tyagi, M. B. & Sinha, R. P. *Molecular mechanisms of ultraviolet radiation-induced DNA damage and repair.* J. Nucleic Acids **2010**, 592980 (2010).

[37] Monari, A., Dumont, E. & Chatgilialoglu, C. *Radiation-induced and oxidative DNA damages.* (Frontiers Media SA, 2015). doi:10.3389/978-2-88919-660-9.

[38] Vilenchik, M. M. & Knudson, A. G. *Inverse radiation dose-rate effects on somatic and germ-line mutations and DNA damage rates.* Proc. Natl. Acad. Sci. U. S. A. **97**, 5381–6 (2000).

[39] Vilenchik, M. M. & Knudson, A. G. *Endogenous DNA double-strand breaks: production, fidelity of repair, and induction of cancer.* Proc. Natl. Acad. Sci. U. S. A. **100**, 12871–6 (2003).

[40] Milligan, J. R. et al. *DNA repair by thiols in air shows two radicals make a double-strand break.* Radiat. Res. **143**, 273–280 (1995).

[41] Ma, W., Halweg, C. J., Menendez, D. & Resnick, M. A. *Differential effects of poly(ADP-ribose) polymerase inhibition on DNA break repair in human cells are revealed with Epstein-Barr virus.* Proc. Natl. Acad. Sci. U. S. A. **109**, 6590–6595 (2012).

[42] Povirk, L. F. *DNA damage and mutagenesis by radiomimetic DNA-cleaving agents: bleomycin, neocarzinostatin and other enediynes.* Mutat. Res. **355**, 71–89 (1996).

[43] Chen, J. & Stubbe, J. *Bleomycins: towards better therapeutics.* Nat. Rev. Cancer **5**, 102–112 (2005).

[44] Cannan, W. J. & Pederson, D. S. *Mechanisms and Consequences of Double-Strand DNA Break Formation in Chromatin.* J. Cell. Physiol. **231**, 3–14 (2016).

[45] Chiu, S. M., Sokany, N. M., Friedman, L. R. & Oleinick, N. L. *Differential processing of ultraviolet or ionizing radiation-induced DNA-protein cross-links in Chinese hamster cells.* Int. J. Radiat. Biol. Relat. Stud. Phys. Chem. Med. **46**, 681–690 (1984).

[46] Miller, C. A. 3rd, Cohen, M. D. & Costa, M. *Complexing of actin and other nuclear proteins to DNA by cis-diamminedichloroplatinum(II) and chromium compounds.* Carcinogenesis **12**, 269–276 (1991).

[47] Ferraro, A., Grandi, P., Eufemi, M., Altieri, F. & Turano, C. *Crosslinking of nuclear proteins to DNA by cis-diamminedichloroplatinum in intact cells. Involvement of nuclear matrix proteins.* FEBS Lett. **307**, 383–385 (1992).

[48] Samuel, S. K. et al. *In situ cross-linking by cisplatin of nuclear matrix-bound transcription factors to nuclear DNA of human breast cancer cells.* Cancer Res. **58**, 3004–3008 (1998).

[49] Chakrabarti, S. K., Bai, C. & Subramanian, K. S. *DNA-Protein crosslinks induced by nickel compounds in isolated rat renal cortical cells and its antagonism by specific amino acids and magnesium ion.* Toxicol. Appl. Pharmacol. **154**, 245–255 (1999).

[50] Reardon, J. T., Cheng, Y. & Sancar, A. *Repair of DNA–Protein Cross-links in Mammalian Cells.* Cell Cycle **5**, 1366–1370 (2014).

[51] Li, T. K. & Liu, L. F. *Tumor cell death induced by topoisomerase-targeting drugs.* Annu. Rev. Pharmacol. Toxicol. **41**, 53–77 (2001).

[52] Subramanian, D., Rosenstein, B. S. & Muller, M. T. *Ultraviolet-induced DNA damage stimulates topoisomerase I-DNA complex formation in vivo: possible relationship with DNA repair.* Cancer Res. **58**, 976–984 (1998).

[53] Pommier, Y. et al. *Benzo[a]pyrene diol epoxide adducts in DNA are potent suppressors of a normal topoisomerase I cleavage site and powerful inducers of other topoisomerase I cleavages.* Proc. Natl. Acad. Sci. U. S. A. **97**, 2040–2045 (2000).

[54] DeMott, M. S. et al. *Covalent trapping of human DNA polymerase beta by the oxidative DNA lesion 2-deoxyribonolactone.* J. Biol. Chem. **277**, 7637–7640 (2002).

[55] Guan, L. & Greenberg, M. M. *Irreversible inhibition of DNA polymerase beta by an oxidized abasic lesion.* J. Am. Chem. Soc. **132**, 5004–5005 (2010).

[56] Prasad, R. et al. *Suicidal cross-linking of PARP-1 to AP site intermediates in cells undergoing base excision repair.* Nucleic Acids Res. **42**, 6337–51 (2014).

[57] Pinto, A. L. & Lippard, S. J. *Sequence-dependent termination of in vitro DNA synthesis by cis- and trans-diamminedichloroplatinum (II).* Proc. Natl. Acad. Sci. U. S. A. **82**, 4616–4619 (1985).

[58] Briggs, J. A. & Briggs, R. C. *Characterization of chromium effects on a rat liver epithelial cell line and their relevance to in vitro transformation.* Cancer Res. **48**, 6484–6490 (1988).

[59] Voitkun, V., Zhitkovich, A. & Costa, M. *Cr(III)-mediated crosslinks of glutathione or amino acids to the DNA phosphate backbone are mutagenic in human cells.* Nucleic Acids Research **26**, 2024–2030 (1998).

[60] Liu, Y.-R. et al. *Exposure to formaldehyde induces heritable DNA mutations in mice.* J. Toxicol. Environ. Health. A **72**, 767–773 (2009).

[61] Ide, H., Shoulkamy, M. I., Nakano, T., Miyamoto-Matsubara, M. & Salem, A. M. H. *Repair and biochemical effects of DNA-protein crosslinks.* Mutat. Res. **711**, 113–22 (2011).

[62] Hendry, L. B., Mahesh, V. B., Bransome, E. D. & Ewing, D. E. *Small molecule intercalation with double stranded DNA: implications for normal gene regulation and for predicting the biological efficacy and genotoxicity of drugs and other chemicals.* Mutat. Res. **623**, 53–71 (2007).

[63] Raj, A. S. & Heddle, J. A. *Simultaneous detection of chromosomal aberrations and sister-chromatid exchanges: experience with DNA intercalating agents.* Mutat. Res. **78**, 253–260 (1980).

[64] Wilson, W. R., Harris, N. M. & Ferguson, L. R. *Comparison of the mutagenic and clastogenic activity of amsacrine and other DNA-intercalating drugs in cultured V79 Chinese hamster cells.* Cancer Res. **44**, 4420–4431 (1984).

[65] Chen, A. Y., Yu, C., Bodley, A., Peng, L. F. & Liu, L. F. A new mammalian DNA topoisomerase I poison Hoechst 33342: cytotoxicity and drug resistance in human cell cultures. Cancer Res. **53**, 1332–1337 (1993). .

[66] Bailly, C. et al. *Enhanced binding to DNA and topoisomerase I inhibition by an analog of the antitumor antibiotic rebeccamycin containing an amino sugar residue.* Mol. Pharmacol. **55**, 377–385 (1999).

[67] Mišković, K., Bujak, M., Baus Lončar, M. & Glavaš-Obrovac, L. *Antineoplastic DNA-binding compounds: intercalating and minor groove binding drugs.* Arh. Hig. Rada Toksikol. **64**, 593–602 (2013).

[68] Wojcik, K., Zarebski, M., Cossarizza, A. & Dobrucki, J. W. *Daunomycin, an antitumor DNA intercalator, influences histone-DNA interactions.* Cancer Biol. Ther. **14**, 823–832 (2013).

[69] Zhang, X. et al. *New insight into the molecular mechanisms of the biological effects of DNA minor groove binders.* PLoS One **6**, e25822 (2011).

[70] Leitner, F., Paillasson, S., Ronot, X. & Demongeot, J. *Dynamic functional and structural analysis of living cells: new tools for vital staining of nuclear DNA and for characterisation of cell motion.* Acta Biotheor. **43**, 299–317 (1995).

[71] Ihmels, H. *Intercalation of Organic Dye Molecules into Double-Stranded DNA – General Principles and Recent Developments.* 161–204 (2005).

[72] Chaney, S. G. & Sancar, A. *DNA Repair: Enzymatic Mechanisms and Relevance to Drug Response.* JNCI J. Natl. Cancer Inst. **88**, 1346–1360 (1996).

[73] R, S. G. K., Mathew, B. B., Sudhamani, C. N. & Naik, H. S. B. *Mechanism of DNA Binding and Cleavage.* **2**, 1–9 (2014).

[74] Szymkowski, D. E., Yarema, K., Essigmann, J. M., Lippard, S. J. & Wood, R. D. *An intrastrand d(GpG) platinum crosslink in duplex M13 DNA is refractory to repair by human cell extracts.* Proc. Natl. Acad. Sci. U. S. A. **89**, 10772–10776 (1992).

[75] Drabløs, F. et al. *Alkylation damage in DNA and RNA–repair mechanisms and medical significance.* DNA Repair (Amst). **3**, 1389–407 (2004).

[76] Masters, J. R. W. & Köberle, B. *Curing metastatic cancer: lessons from testicular germ-cell tumours.* Nat. Rev. Cancer **3**, 517–25 (2003).

[77] Wyatt, M. D. & Pittman, D. L. *Methylating agents and DNA repair responses: Methylated bases and sources of strand breaks.* Chem. Res. Toxicol. **19**, 1580–1594 (2006).

[78] Bennett, R. A., Swerdlow, P. S. & Povirk, L. F. *Spontaneous cleavage of bleomycin-induced abasic sites in chromatin and their mutagenicity in mammalian shuttle vectors.* Biochemistry **32**, 3188–3195 (1993).

[79] Wu, W., Vanderwall, D. E., Stubbe, J., Kozarich, J. W. & Turner, C. J. *Interaction of Co.cntdot.Bleomycin A2 (Green) with d(CCAGGCCTGG)2: Evidence for Intercalation Using 2D NMR.* J. Am. Chem. Soc. **116**, 10843–10844 (1994).

[80] Abraham, A. T., Zhou, X. & Hecht, S. M. *Metallobleomycin-Mediated Cleavage of DNA Not Involving a Threading-Intercalation Mechanism*. J. Am. Chem. Soc. **123**, 5167–5175 (2001).

[81] Alizadeh, E., Orlando, T. M. & Sanche, L. *Biomolecular damage induced by ionizing radiation: the direct and indirect effects of low-energy electrons on DNA*. Annu. Rev. Phys. Chem. **66**, 379–98 (2015).

[82] Michael, B. D. & O'Neill, P. *Molecular biology. A sting in the tail of electron tracks*. Science **287**, 1603–1604 (2000).

[83] Nguyen, J. et al. *Direct observation of ultrafast-electron-transfer reactions unravels high effectiveness of reductive DNA damage*. Proc. Natl. Acad. Sci. **108**, 11778–11783 (2011).

[84] Han, W. & Yu, K. N. *Ionizing Radiation , DNA Double Strand Break and Mutation*. **4**, 1–13 (2010).

[85] Ward, J. F. *DNA damage produced by ionizing radiation in mammalian cells: identities, mechanisms of formation, and reparability*. Prog. Nucleic Acid Res. Mol. Biol. **35**, 95–125 (1988).

[86] Ward, J. F. *The Yield of DNA Double-strand Breaks Produced Intracellularly by Ionizing Radiation: A Review*. Int. J. Radiat. Biol. **57**, 1141–1150 (1990).

[87] Dextraze, M.-E., Gantchev, T., Girouard, S. & Hunting, D. *DNA interstrand cross-links induced by ionizing radiation: an unsung lesion*. Mutat. Res. **704**, 101–7 (2010).

[88] Elkind, M. M. & Redpath, J. L. in *Radiotherapy, Surgery, and Immunotherapy* (ed. Becker, F. F.) 51–99 (Springer US, 1977). doi:10.1007/978-1-4684-2739-4_3.

[89] Hada, M. & Georgakilas, A. G. *Formation of Clustered DNA Damage after High-LET Irradiation: A Review*. J. Radiat. Res. **49**, 203–210 (2008).

[90] Ward, J. F. *Some biochemical consequences of the spatial distribution of ionizing radiation-produced free radicals*. Radiat. Res. **86**, 185–195 (1981).

[91] Ward, J. F. *Biochemistry of DNA lesions*. Radiat. Res. Suppl. **8**, S103–11 (1985).

[92] Asaithamby, A. & Chen, D. J. *Mechanism of cluster DNA damage repair in response to high-atomic number and energy particles radiation*. Mutat. Res. **711**, 87–99 (2011).

[93] Shikazono, N., Noguchi, M., Fujii, K., Urushibara, A. & Yokoya, A. *The Yield, Processing, and Biological Consequences of Clustered DNA Damage Induced by Ionizing Radiation*. J. Radiat. Res. **50**, 27–36 (2009).

[94] Nikjoo, H., O'Neill, P., Terrissol, M. & Goodhead, D. T. *Quantitative modelling of DNA damage using Monte Carlo track structure method*. Radiat. Environ. Biophys. **38**, 31–38 (1999).

[95] Nikjoo, H., O'Neill, P., Wilson, W. E. & Goodhead, D. T. *Computational approach for determining the spectrum of DNA damage induced by ionizing radiation.* Radiat. Res. **156**, 577–583 (2001).

[96] David-Cordonnier, M.-H., Cunniffe, S. M. T., Hickson, I. D. & O'Neill, P. *Efficiency of incision of an AP site within clustered DNA damage by the major human AP endonuclease.* Biochemistry **41**, 634–642 (2002).

[97] Hoffmann-Dörr, S., Greinert, R., Volkmer, B. & Epe, B. *Visible light ($> 395nm$) causes micronuclei formation in mammalian cells without generation of cyclobutane pyrimidine dimers.* Mutat. Res. **572**, 142–9 (2005).

[98] Ravanat, J.-L., Douki, T. & Cadet, J. *Direct and indirect effects of UV radiation on DNA and its components.* J. Photochem. Photobiol. B Biol. **63**, 88–102 (2001).

[99] Cadet, J., Mouret, S., Ravanat, J.-L. & Douki, T. *Photoinduced damage to cellular DNA: direct and photosensitized reactions.* Photochem. Photobiol. **88**, 1048–65 (2012).

[100] Cadet, J., Douki, T., Ravanat, J.-L. & Di Mascio, P. *Sensitized formation of oxidatively generated damage to cellular DNA by UVA radiation.* Photochem. Photobiol. Sci. **8**, 903–11 (2009).

[101] Limoli, C. L., Giedzinski, E., Bonner, W. M. & Cleaver, J. E. *UV-induced replication arrest in the xeroderma pigmentosum variant leads to DNA double-strand breaks, gamma -H2AX formation, and Mre11 relocalizlocalisation.* Proc. Natl. Acad. Sci. U. S. A. **99**, 233–238 (2002).

[102] Greinert, R. et al. *UVA-induced DNA double-strand breaks result from the repair of clustered oxidative DNA damages.* Nucleic Acids Res. **40**, 10263–10273 (2012).

[103] Banyasz, A. et al. *Base pairing enhances fluorescence and favors cyclobutane dimer formation induced upon absorption of UVA radiation by DNA.* J. Am. Chem. Soc. **133**, 5163–5165 (2011).

[104] Gantt, R. et al. *Fluorescent light-induced DNA crosslinkage and chromatid breaks in mouse cells in culture.* **75**, 3809–3812 (1978).

[105] Parshad, R. et al. *Effect of Intensity and Wavelength of Fluorescent Light on Chromosome Damage in Cultured Mouse Cells.* Photochem. Photobiol. **29**, 971–975 (1979).

[106] Parshad, R., Sanford, K. K., Tarone, R. E., Jones, G. M. & Baeck, A. E. *Increased Susceptibility of Mouse Cells to Fluorescent Light-induced Chromosome Damage after Long-Term Culture and Malignant Transformation.* 929–933 (1979).

[107] Pflaum, M., Kielbassa, C., Garmyn, M. & Epe, B. *Oxidative DNA damage induced by visible light in mammalian cells: extent, inhibition by antioxidants and genotoxic effects.* Mutat. Res. Repair **408**, 137–146 (1998).

[108] Churchill, M. E., Peak, J. G. & Peak, M. J. *Repair of near-visible- and blue-light-induced DNA single-strand breaks by the CHO cell lines AA8 and EM9.* Photochem. Photobiol. **54**, 639–44 (1991).

[109] Pflaum, M., Boiteux, S. & Epe, B. *Visible light generates oxidative DNA base modifications in high excess of strand breaks in mammalian cells.* Carcinogenesis **15**, 297–300 (1994).

[110] Kielbassa, C., Roza, L. & Epe, B. *Wavelength dependence of oxidative DNA damage induced by UV and visible light.* Carcinogenesis **18**, 811–6 (1997).

[111] Rosenstein, B. S. & Ducore, J. M. *Induction of DNA strand breaks in normal human fibroblasts exposed to monochromatic ultraviolet and visible wavelengths in the 240–546 nm range.* Photochem. Photobiol. **38**, 51–55 (1983).

[112] Peak, J. G. & Peak, M. J. *Comparison of initial yields of DNA-to-protein crosslinks and single-strand breaks induced in cultured human cells by far- and near-ultraviolet light, blue light and X-rays.* Mutat. Res. Mol. Mech. Mutagen. **246**, 187–191 (1991).

[113] Koch, C. J. & Giandomenico, A. R. *The alkaline elution technique for measuring DNA single strand breaks: increased reliability and sensitivity.* Anal. Biochem. **220**, 58–65 (1994).

[114] Averbeck, D., Dardalhon, M. & Magana-Schwencke, N. *Repair of furocoumarin-plus-UVA-induced damage and mutagenic consequences in eukaryotic cells.* J. Photochem. Photobiol. B. **6**, 221–236 (1990).

[115] Moysan, A. et al. *Formation of cyclobutane thymine dimers photosensitized by pyridopsoralens: quantitative and qualitative distribution within DNA.* Biochemistry **30**, 7080–7088 (1991).

[116] Lhiaubet-Vallet, V., Cuquerella, M. C., Castell, J. V, Bosca, F. & Miranda, M. A. *Triplet excited fluoroquinolones as mediators for thymine cyclobutane dimer formation in DNA.* J. Phys. Chem. B **111**, 7409–7414 (2007).

[117] Robinson, K. S., Traynor, N. J., Moseley, H., Ferguson, J. & Woods, J. A. *Cyclobutane pyrimidine dimers are photosensitised by carprofen plus UVA in human HaCaT cells.* Toxicol. In Vitro **24**, 1126–1132 (2010).

[118] Steenken, S. & Jovanovic, S. V. *How Easily Oxidizable Is DNA? One-Electron Reduction Potentials of Adenosine and Guanosine Radicals in Aqueous Solution.* J. Am. Chem. Soc. **119**, 617–618 (1997).

[119] Gonzalez, M. M. et al. *Photosensitized cleavage of plasmidic DNA by norharmane, a naturally occurring beta-carboline.* Org. Biomol. Chem. **8**, 2543–2552 (2010).

[120] Foote, C. S. *Definition of type I and type II photosensitized oxidation.* Photochemistry and photobiology **54**, 659 (1991).

[121] Epe, B. et al. *DNA damage induced by furocoumarin hydroperoxides plus UV (360 nm).* Carcinogenesis **14**, 2271–2276 (1993).

[122] Epe, B., Ballmaier, D., Adam, W., Grimm, G. N. & Saha-Moller, C. R. *Photolysis of N-hydroxpyridinethiones: a new source of hydroxyl radicals for the direct damage of cell-free and cellular DNA.* Nucleic Acids Res. **24**, 1625–1631 (1996).

[123] Epe, B. *DNA damage spectra induced by photosensitization.* Photochem. Photobiol. Sci. **11**, 98–106 (2012).

[124] Botta, C., Di Giorgio, C., Sabatier, A.-S. & De Méo, M. *Genotoxicity of visible light (400–800 nm) and photoprotection assessment of ectoin, L-ergothioneine and mannitol and four sunscreens.* J. Photochem. Photobiol. B. **91**, 24–34 (2008).

[125] Omata, Y. et al. *Intra- and extracellular reactive oxygen species generated by blue light.* J. Biomed. Mater. Res. A **77**, 470–7 (2006).

[126] Sideris, E. G., Papageorgiou, G. C., Charalampous, S. C. & Vitsa, E. M. *A spectrum response study on single strand DNA breaks, sister chromatid exchanges, and lethality induced by phototherapy lights.* Pediatr. Res. **15**, 1019–1023 (1981).

[127] Kim, J.-S., Krasieva, T. B., LaMorte, V., Taylor, a M. R. & Yokomori, K. *Specific recruitment of human cohesin to laser-induced DNA damage.* J. Biol. Chem. **277**, 45149–53 (2002).

[128] Mortusewicz, O., Schermelleh, L., Walter, J., Cardoso, M. C. & Leonhardt, H. *Recruitment of DNA methyltransferase I to DNA repair sites.* Proc. Natl. Acad. Sci. U. S. A. **102**, 8905–9 (2005).

[129] Zarebski, M., Wiernasz, E. & Dobrucki, J. *Recruitment of heterochromatin protein 1 to DNA repair sites.* Cytom. Part A **75**, 619–625 (2009).

[130] Berquist, B. R. et al. *Functional capacity of XRCC1 protein variants identified in DNA repair-deficient Chinese hamster ovary cell lines and the human population.* Nucleic Acids Res. **38**, 5023–35 (2010).

[131] Campalans, A., Kortulewski, T., Amouroux, R., Vermeulen, W. & Radicella, J. P. *Distinct spatiotemporal patterns and PARP dependence of XRCC1 recruitment to single-strand break and base excision repair.* Nucleic Acids Res. 1–15 (2013).

[132] Kong, X. et al. *Comparative analysis of different laser systems to study cellular responses to DNA damage in mammalian cells.* Nucleic Acids Res. **37**, (2009).

[133] Heiss, M. et al. *Targeted irradiation of Mammalian cells using a heavy-ion microprobe.* Radiat. Res. **165**, 231–239 (2006).

[134] Asaithamby, A. & Chen, D. J. *Mechanism of cluster DNA damage repair in response to high-atomic number and energy particles radiation.* Mutat. Res. **711**, 87–99 (2011).

[135] Hable, V. et al. *Recruitment Kinetics of DNA Repair Proteins Mdc1 and Rad52 but Not 53BP1 Depend on Damage Complexity.* PLoS One **7**, e41943 (2012).

[136] Asaithamby, A., Hu, B. & Chen, D. J. *Unrepaired clustered DNA lesions induce chromosome breakage in human cells.* Proc. Natl. Acad. Sci. U. S. A. **108**, 8293–8 (2011).

[137] Jakob, B. et al. *DNA double-strand breaks in heterochromatin elicit fast repair protein recruitment, histone H2AX phosphorylation and relocation to euchromatin.* Nucleic Acids Res. **39**, 6489–99 (2011).

[138] Berns, M. W., Olson, R. S. & Rounds, D. E. *In vitro production of chromosomal lesions with an argon laser microbeam.* Nature **221**, 74–75 (1969).

[139] Berns, M. W. & Floyd, A. D. *Chromosomal microdissection by laser. A cytochemical and functional analysis.* Exp. Cell Res. **67**, 305–310 (1971).

[140] Bloom, W. & Leider, R. J. *Optical and electron microscopic changes in ultraviolet-irradiated chromosome segments.* The Journal of Cell Biology **13**, 269–301 (1962).

[141] Cremer, C., Cremer, T., Fukuda, M. & Nakanishi, K. *Detection of laser-UV microirradiation-induced DNA photolesions by immunofluorescent staining.* Hum. Genet. **110**, 107–110 (1980).

[142] Cremer, T., Peterson, S. P. & Cremer, C. of *Chinese Hamster Cells at Wavelength Laser Microirradiation 365 nm: Effects of Psoralen and Caffeine.* **543**, 529–543 (1981).

[143] Cremer, T. et al. *Rabl's Model of the Interphase Chromosome Arrangement Tested in Chinese Hamster Cells by Premature Chromosome Condensation and Laser-UV-Microbeam Experiments.* 46–56 (1982).

[144] Limoli, C. L. & Ward, J. F. *A new method for introducing double-strand breaks into cellular DNA.* Radiat. Res. **134**, 160–169 (1993).

[145] Rogakou, E. P., Boon, C., Redon, C. & Bonner, W. M. *Megabase chromatin domains involved in DNA double-strand breaks in vivo.* J. Cell Biol. **146**, 905–16 (1999).

[146] Kruhlak, M. & Celeste, A. *Changes in chromatin structure and mobility in living cells at sites of DNA double-strand breaks.* J. Cell Biol. **172**, 823–834 (2006).

[147] Dinant, C. et al. *Activation of multiple DNA repair pathways by sub- nuclear damage induction methods.* (2007). doi:10.1242/jcs.004523.

[148] Lan, L. et al. *In situ analysis of repair processes for oxidative DNA damage in mammalian cells.* Proc. Natl. Acad. Sci. U. S. A. **101**, 13738–43 (2004).

[149] Ferrando-May, E. et al. *Highlighting the DNA damage response with ultrashort laser pulses in the near infrared and kinetic modeling.* Front. Genet. **4**, 135 (2013).

[150] Hanssen-Bauer, A. *XRCC1 coordinates disparate responses and multiprotein repair complexes depending on the nature and context of the DNA damage*. Environ. Mol. Mutagen. **635**, (2011).

[151] Träutlein, D., Deibler, M., Leitenstorfer, A. & Ferrando-May, E. *Specific local induction of DNA strand breaks by infrared multi-photon absorption*. Nucleic Acids Res. **38**, e14 (2010).

[152] Soutoglou, E. et al. *Positional stability of single double-strand breaks in mammalian cells*. Nat. Cell Biol. **9**, 675–82 (2007).

[153] Roukos, V. et al. *Spatial dynamics of chromosome translocations in living cells*. Science **341**, 660–664 (2013).

[154] Bulina, M. E. et al. *A genetically encoded photosensitizer*. Nat. Biotechnol. **24**, 95–99 (2006).

[155] Bulina, M. E. et al. *Chromophore-assisted light inactivation (CALI) using the phototoxic fluorescent protein KillerRed*. Nat. Protoc. **1**, 947–953 (2006).

[156] Serebrovskaya, E. O. et al. *Light-induced blockage of cell division with a chromatin-targeted phototoxic fluorescent protein*. Biochem. J. **435**, 65–71 (2011).

[157] Lan, L. et al. *Novel method for site-specific induction of oxidative DNA damage reveals differences in recruitment of repair proteins to heterochromatin and euchromatin*. Nucleic Acids Res. **42**, 2330–45 (2014).

[158] Jansen, R., Embden, J. D. A. van, Gaastra, W. & Schouls, L. M. *Identification of genes that are associated with DNA repeats in prokaryotes*. Mol. Microbiol. **43**, 1565–1575 (2002).

[159] Cong, L. et al. *Multiplex genome engineering using CRISPR/Cas systems*. Science **339**, 819–823 (2013).

[160] Mali, P. et al. *RNA-guided human genome engineering via Cas9*. Science **339**, 823–826 (2013).

[161] Garneau, J. E. et al. *The CRISPR/Cas bacterial immune system cleaves bacteriophage and plasmid DNA*. Nature **468**, 67–71 (2010).

[162] Kusumoto, R. et al. *Diversity of the damage recognition step in the global genomic nucleotide excision repair in vitro*. Mutat. Res. **485**, 219–227 (2001).

[163] Neher, T. M., Rechkunova, N. I., Lavrik, O. I. & Turchi, J. J. *Photo-cross-linking of XPC-Rad23B to cisplatin-damaged DNA reveals contacts with both strands of the DNA duplex and spans the DNA adduct*. Biochemistry **49**, 669–678 (2010).

[164] Lee, Y.-C. et al. *The relationships between XPC binding to conformationally diverse DNA adducts and their excision by the human NER system: is there a correlation?* DNA Repair (Amst). 19, 55–63 (2014).

[165] Gillet, L. C. J. & Scharer, O. D. *Molecular mechanisms of mammalian global genome nucleotide excision repair.* Chem. Rev. **106**, 253–276 (2006).

[166] Hanawalt, P. C. & Spivak, G. *Transcription-coupled DNA repair: two decades of progress and surprises.* Nat. Rev. Mol. Cell Biol. **9**, 958–970 (2008).

[167] Masutani, C. et al. *Purification and cloning of a nucleotide excision repair complex involving the xeroderma pigmentosum group C protein and a human homologue of yeast RAD23.* EMBO J. **13**, 1831–1843 (1994).

[168] Lainé, J.-P. & Egly, J.-M. *Initiation of DNA repair mediated by a stalled RNA polymerase IIO.* The EMBO Journal **25**, 387–397 (2006).

[169] Citterio, E. et al. *Biochemical and biological characterization of wild-type and ATPase-deficient Cockayne syndrome B repair protein.* J. Biol. Chem. **273**, 11844–11851 (1998).

[170] Groisman, R. et al. *The ubiquitin ligase activity in the DDB2 and CSA complexes is differentially regulated by the COP9 signalosome in response to DNA damage.* Cell **113**, 357–367 (2003).

[171] Hasan, S., Hassa, P. O., Imhof, R. & Hottiger, M. O. *Transcription coactivator p300 binds PCNA and may have a role in DNA repair synthesis.* Nature **410**, 387–391 (2001).

[172] Birger, Y. et al. *Chromosomal protein HMGN1 enhances the rate of DNA repair in chromatin.* The EMBO Journal **22**, 1665–1675 (2003).

[173] Nakatsu, Y. et al. *XAB2, a novel tetratricopeptide repeat protein involved in transcription-coupled DNA repair and transcription.* J. Biol. Chem. **275**, 34931–34937 (2000).

[174] Tornaletti, S. *Structural Characterization of RNA Polymerase II Complexes Arrested by a Cyclobutane Pyrimidine Dimer in the Transcribed Strand of Template DNA.* **274**, 24124–24130 (1999).

[175] Oksenych, V., de Jesus, B. B., Zhovmer, A., Egly, J.-M. & Coin, F. *Molecular insights into the recruitment of TFIIH to sites of DNA damage.* EMBO J. **28**, 2971–80 (2009).

[176] Ito, S. et al. *XPG stabilizes TFIIH, allowing transactivation of nuclear receptors: implications for Cockayne syndrome in XP-G/CS patients.* Mol. Cell **26**, 231–243 (2007).

[177] Overmeer, R. M. et al. *Replication protein A safeguards genome integrity by controlling NER incision events.* J. Cell Biol. **192**, 401–415 (2011).

[178] Kelman, Z. *PCNA: structure, functions and interactions.* Oncogene **14**, 629–640 (1997).

[179] Moser, J. et al. *Sealing of chromosomal DNA nicks during nucleotide excision repair requires XRCC1 and DNA ligase III alpha in a cell-cycle-specific manner.* Mol. Cell **27**, 311–323 (2007).

[180] Kunkel, T. A. & Erie, D. A. *Eukaryotic Mismatch Repair in Relation to DNA Replication.* Annu. Rev. Genet. **49**, 291–313 (2015).

[181] Li, G.-M. *Mechanisms and functions of DNA mismatch repair.* Cell Res. **18**, 85–98 (2008).

[182] Fu, D., Calvo, J. A. & Samson, L. D. *Balancing repair and tolerance of DNA damage caused by alkylating agents.* Nat. Rev. Cancer **12**, 104–120 (2012).

[183] Eisen, J. A. *A phylogenomic study of the MutS family of proteins.* Nucleic Acids Res. **26**, 4291–4300 (1998).

[184] Hall, M. C. & Matson, S. W. *The Escherichia coli MutL protein physically interacts with MutH and stimulates the MutH-associated endonuclease activity.* J. Biol. Chem. **274**, 1306–1312 (1999).

[185] Yamaguchi, M., Dao, V. & Modrich, P. *MutS and MutL activate DNA helicase II in a mismatch-dependent manner.* J. Biol. Chem. **273**, 9197–9201 (1998).

[186] Hall, M. C., Jordan, J. R. & Matson, S. W. *Evidence for a physical interaction between the Escherichia coli methyl-directed mismatch repair proteins MutL and UvrD.* The EMBO Journal **17**, 1535–1541 (1998).

[187] López de Saro, F. J. & O'Donnell, M. *Interaction of the $\beta$ sliding clamp with MutS, ligase, and DNA polymerase I.* Proc. Natl. Acad. Sci. **98**, 8376–8380 (2001).

[188] Goellner, E. M., Putnam, C. D. & Kolodner, R. D. *Exonuclease 1-dependent and independent mismatch repair.* DNA Repair (Amst). **32**, 24–32 (2015).

[189] Plotz, G., Raedle, J., Brieger, A., Trojan, J. & Zeuzem, S. *hMutS$\alpha$ forms an ATP-dependent complex with hMutL$\alpha$ and hMutL$\beta$ on DNA.* Nucleic Acids Research **30**, 711–718 (2002).

[190] Plotz, G., Raedle, J., Brieger, A., Trojan, J. & Zeuzem, S. *N-terminus of hMLH1 confers interaction of hMutL$\alpha$ and hMutL$\beta$ with hMutS$\alpha$.* Nucleic Acids Research **31**, 3217–3226 (2003).

[191] Kadyrov, F. A., Dzantiev, L., Constantin, N. & Modrich, P. *Endonucleolytic Function of MutLα in Human Mismatch Repair.* Cell **126**, 297–308 (2016).

[192] Pavlov, Y. I., Mian, I. M. & Kunkel, T. A. *Evidence for Preferential Mismatch Repair of Lagging Strand DNA Replication Errors in Yeast.* Curr. Biol. **13**, 744–748 (2016).

[193] Ghodgaonkar, M. M. et al. *Ribonucleotides Misincorporated into DNA Act as Strand-Discrimination Signals in Eukaryotic Mismatch Repair.* Mol. Cell **50**, 323–332 (2016).

[194] Flores-Rozas, H., Clark, D. & Kolodner, R. D. *Proliferating cell nuclear antigen and Msh2p-Msh6p interact to form an active mispair recognition complex.* Nat. Genet. **26**, 375–378 (2000).

[195] Lee, S. D. & Alani, E. *Analysis of Interactions Between Mismatch Repair Initiation Factors and the Replication Processivity Factor PCNA.* J. Mol. Biol. **355**, 175–184 (2006).

[196] Delacote, F. & Lopez, B. S. *Importance of the cell cycle phase for the choice of the appropriate DSB repair pathway, for genome stability maintenance: the trans-S double-strand break repair model.* Cell Cycle **7**, 33–38 (2008).

[197] Cary, R. B. et al. *DNA looping by Ku abd the DNA-dependent protein kinase.* Proceedings of the National Academy of Sciences of the United States of America **94**, 4267–4272 (1997).

[198] Walker, J. R., Corpina, R. A. & Goldberg, J. *Structure of the Ku heterodimer bound to DNA and its implications for double-strand break repair.* Nature **412**, 607–614 (2001).

[199] Yaneva, M., Kowalewski, T. & Lieber, M. R. *Interaction of DNA-dependent protein kinase with DNA and with Ku: biochemical and atomic-force microscopy studies.* The EMBO Journal **16**, 5098–5112 (1997).

[200] Ma, Y., Pannicke, U., Schwarz, K. & Lieber, M. R. *Hairpin opening and overhang processing by an Artemis/DNA-dependent protein kinase complex in nonhomologous end joining and V(D)J recombination.* Cell **108**, 781–794 (2002).

[201] Grawunder, U. et al. *Activity of DNA ligase IV stimulated by complex formation with XRCC4 protein in mammalian cells.* Nature **388**, 492–495 (1997).

[202] Boboila, C., Alt, F. W. & Schwer, B. *Classical and alternative end-joining pathways for repair of lymphocyte-specific and general DNA double-strand breaks.* Adv. Immunol. **116**, 1–49 (2012).

[203] Wang, M. et al. *PARP-1 and Ku compete for repair of DNA double strand breaks by distinct NHEJ pathways.* Nucleic Acids Research **34**, 6170–6182 (2006).

[204] Zhong, Q., Chen, C.-F., Chen, P.-L. & Lee, W.-H. *BRCA1 facilitates microhomology-mediated end joining of DNA double strand breaks.* J. Biol. Chem. **277**, 28641–28647 (2002).

[205] Lee-Theilen, M., Matthews, A. J., Kelly, D., Zheng, S. & Chaudhuri, J. *CtIP promotes microhomology-mediated alternative end joining during class-switch recombination.* Nat. Struct. Mol. Biol. **18**, 75–79 (2011).

[206] Xie, A., Kwok, A. & Scully, R. *Role of mammalian Mre11 in classical and alternative nonhomologous end joining.* Nat. Struct. Mol. Biol. **16**, 814–818 (2009).

[207] Liang, L. et al. *Human DNA ligases I and III, but not ligase IV, are required for microhomology-mediated end joining of DNA double-strand breaks.* Nucleic Acids Research **36**, 3297–3310 (2008).

[208] Paul, K. et al. *DNA ligases I and III cooperate in alternative non-homologous end-joining in vertebrates.* PLoS One **8**, e59505 (2013).

[209] Lamarche, B. J., Orazio, N. I. & Weitzman, M. D. *The MRN complex in double-strand break repair and telomere maintenance.* FEBS Lett. **584**, 3682–95 (2010).

[210] Hopfner, K.-P. et al. *The Rad50 zinc-hook is a structure joining Mre11 complexes in DNA recombination and repair.* Nature **418**, 562–566 (2002).

[211] Lee, J.-H. & Paull, T. T. *Direct activation of the ATM protein kinase by the Mre11/Rad50/Nbs1 complex.* Science **304**, 93–96 (2004).

[212] Matsuoka, S. et al. *ATM and ATR substrate analysis reveals extensive protein networks responsive to DNA damage.* Science **316**, 1160–1166 (2007).

[213] Savic, V. et al. *Formation of dynamic gamma-H2AX domains along broken DNA strands is distinctly regulated by ATM and MDC1 and dependent upon H2AX densities in chromatin.* Mol. Cell **34**, 298–310 (2009).

[214] Van Attikum, H. & Gasser, S. M. *Crosstalk between histone modifications during the DNA damage response.* Trends Cell Biol. **19**, 207–217 (2016).

[215] Chapman, J. R. & Jackson, S. P. *Phospho-dependent interactions between Nbs1 and MDC1 mediate chromatin retention of the MRN complex at sites of DNA damage.* EMBO Rep. **9**, 795–801 (2008).

[216] Sartori, A. a et al. *Human CtIP promotes DNA end resection.* Nature **450**, 509–14 (2007).

[217] Nimonkar, A. V et al. *BLM-DNA2-RPA-MRN and EXO1-BLM-RPA-MRN constitute two DNA end resection machineries for human DNA break repair.* Genes Dev. **25**, 350–362 (2011).

[218] Shibata, A. et al. *DNA double-strand break repair pathway choice is directed by distinct MRE11 nuclease activities.* Mol. Cell **53**, 7–18 (2014).

[219] San Filippo, J., Sung, P. & Klein, H. *Mechanism of eukaryotic homologous recombination.* Annu. Rev. Biochem. **77**, 229–257 (2008).

[220] Wong, A. K., Pero, R., Ormonde, P. A., Tavtigian, S. V & Bartel, P. L. *RAD51 interacts with the evolutionarily conserved BRC motifs in the human breast cancer susceptibility gene brca2.* J. Biol. Chem. **272**, 31941–31944 (1997).

[221] Xu, D. et al. *RMI, a new OB-fold complex essential for Bloom syndrome protein to maintain genome stability.* Genes Dev. **22**, 2843–2855 (2008).

[222] Brandsma, I. & Gent, D. C. *Pathway choice in DNA double strand break repair: observations of a balancing act.* Genome Integr. **3**, 9 (2012).

[223] Hegde, M. L., Hazra, T. K. & Mitra, S. *Early Steps in the DNA Base Excision/Single-Strand Interruption Repair Pathway in Mammalian Cells.* Cell research **18**, 27–47 (2008).

[224] Wood, R. D., Mitchell, M., Sgouros, J. & Lindahl, T. *Human DNA repair genes.* Science **291**, 1284–1289 (2001).

[225] Dianov, G., Price, A. & Lindahl, T. *Generation of single-nucleotide repair patches following excision of uracil residues from DNA.* Mol. Cell. Biol. **12**, 1605–1612 (1992).

[226] Frosina, G. et al. *Two pathways for base excision repair in mammalian cells.* J. Biol. Chem. **271**, 9573–9578 (1996).

[227] Klungland, A. & Lindahl, T. *Second pathway for completion of human DNA base excision-repair: reconstitution with purified proteins and requirement for DNase IV (FEN1).* EMBO J. **16**, 3341–3348 (1997).

[228] Podlutsky, A. J., Dianova, I. I., Podust, V. N., Bohr, V. A. & Dianov, G. L. *Human DNA polymerase beta initiates DNA synthesis during long-patch repair of reduced AP sites in DNA.* EMBO J. **20**, 1477–1482 (2001).

[229] Cappelli, E. et al. *Involvement of XRCC1 and DNA ligase III gene products in DNA base excision repair.* J. Biol. Chem. **272**, 23970–23975 (1997).

[230] Sleeth, K. M., Robson, R. L. & Dianov, G. L. *Exchangeability of mammalian DNA ligases between base excision repair pathways.* Biochemistry **43**, 12924–12930 (2004).

[231] Almeida, K. H. & Sobol, R. W. *A unified view of base excision repair: lesion-dependent protein complexes regulated by post-translational modification.* DNA Repair (Amst). **6**, 695–711 (2007).

[232] Pogozelski†, W. K. & and Thomas D. Tullius*, ‡ *Oxidative Strand Scission of Nucleic Acids: Routes Initiated by Hydrogen Abstraction from the Sugar Moiety.* Chem. Rev. **98**, 1089–1108 (1998).

[233] Demple, B. & DeMott, M. S. *Dynamics and diversions in base excision DNA repair of oxidized abasic lesions.* Oncogene **21**, 8926–8934 (2002).

[234] Caldecott, K. W. *Protein ADP-ribosylation and the cellular response to DNA strand breaks.* DNA Repair (Amst). **19**, 108–13 (2014).

[235] Davidovic, L., Vodenicharov, M., Affar, E. B. & Poirier, G. G. *Importance of poly(ADP-ribose) glycohydrolase in the control of poly(ADP-ribose) metabolism.* Exp. Cell Res. **268**, 7–13 (2001).

[236] Masson, M. et al. *XRCC1 is specifically associated with poly(ADP-ribose) polymerase and negatively regulates its activity following DNA damage.* Mol. Cell. Biol. **18**, 3563–3571 (1998).

[237] El-Khamisy, S. F. *A requirement for PARP-1 for the assembly or stability of XRCC1 nuclear foci at sites of oxidative DNA damage.* Nucleic Acids Res. **31**, 5526–5533 (2003).

[238] Mortusewicz, O. & Leonhardt, H. *XRCC1 and PCNA are loading platforms with distinct kinetic properties and different capacities to respond to multiple DNA lesions.* BMC Mol. Biol. **8**, 81 (2007).

[239] Thompson, L. H. & West, M. G. *XRCC1 keeps DNA from getting stranded.* Mutat. Res. **459**, 1–18 (2000).

[240] Caldecott, K. W. *XRCC1 and DNA strand break repair.* DNA Repair (Amst). **2**, 955–969 (2003).

[241] Caldecott, K. W. *Mammalian single-strand break repair: mechanisms and links with chromatin.* DNA Repair (Amst). **6**, 443–53 (2007).

[242] Tomas, M. et al. *Imaging of the DNA damage-induced dynamics of nuclear proteins via nonlinear photoperturbation.* J. Biophotonics **6**, 645–55 (2013).

[243] Campalans, A., Kortulewski, T., Amouroux, R., Vermeulen, W. & Radicella, J. P. *Distinct spatiotemporal patterns and PARP dependence of XRCC1 recruitment to single-strand break and base excision repair.* 1–15 (2013).

[244] Wei, L. et al. *Damage response of XRCC1 at sites of DNA single strand breaks is regulated by phosphorylation and ubiquitylation after degradation of poly(ADP-ribose).* J. Cell Sci. **126**, 4414–23 (2013).

[245] Kvam, E. & Tyrrell, R. M. *Induction of oxidative DNA base damage in human skin cells by UV and near visible radiation.* **18**, 2379–2384 (1997).

[246] Yan, S.-J., Lim, S. J., Shi, S., Dutta, P. & Li, W. X. *Unphosphorylated STAT and heterochromatin protect genome stability.* FASEB J. **25**, 232–41 (2011).

[247] Eichler, M., Lavi, R., Shainberg, A. & Lubart, R. *Flavins are Source of Visible-Light-Induced Free Radical Formation in Cells.* **319**, 314–319 (2005).

[248] Giancaspero, T. A. et al. *FAD synthesis and degradation in the nucleus create a local flavin cofactor pool.* J. Biol. Chem. **288**, 29069–80 (2013).

[249] Gudkov, S. V. et al. *Generation of reactive oxygen species in water under exposure to visible or infrared irradiation at absorption bands of molecular oxygen.* Biophysics (Oxf). **57**, 1–8 (2012).

[250] Mori, T. et al. *Simultaneous establishment of monoclonal antibodies specific for either cyclobutane pyrimidine dimer or (6-4)photoproduct from the same mouse immunized with ultraviolet-irradiated DNA.* Photochem. Photobiol. **54**, 225–232 (1991).

[251] Matsunaga, T., Hatakeyama, Y., Ohta, M., Mori, T. & Nikaido, O. *Establishment and characterization of a monoclonal antibody recognizing the Dewar isomers of (6-4)photoproducts. Photochem.* Photobiol. **57**, 934–940 (1993).

[252] Ide, H., Kow, Y. W., Chen, B. X., Erlanger, B. F. & Wallace, S. S. *Antibodies to oxidative DNA damage: characterization of antibodies to 8-oxopurines.* Cell Biol. Toxicol. **13**, 405–417 (1997).

[253] Gavrieli, Y., Sherman, Y. & Ben-Sasson, S. *Identification of programmed cell death in situ via specific labeling of nuclear DNA fragmentation.* The Journal of Cell Biology **119**, 493–501 (1992).

[254] Mari, P.-O. et al. *Dynamic assembly of end-joining complexes requires interaction between Ku70/80 and XRCC4.* Proc. Natl. Acad. Sci. U. S. A. **103**, 18597–602 (2006).

[255] Huda, N. et al. *Recruitment of TRF2 to laser-induced DNA damage sites.* Free Radic. Biol. Med. **53**, 1192–7 (2012).

[256] Rogakou, E. P., Pilch, D. R., Orr, A. H., Ivanova, V. S. & Bonner, W. M. *DNA Double-stranded Breaks Induce Histone H2AX Phosphorylation on Serine 139*.* **273**, 5858–5868 (1998).

[257] Cleaver, J. E., Feeney, L. & Revet, I. *Phosphorylated H2Ax is not an unambiguous marker for DNA double-strand breaks.* Cell Cycle **10**, 3223–4 (2011).

[258] Lu, C. et al. *Serum starvation induces H2AX phosphorylation to regulate apoptosis via p38 MAPK pathway.* FEBS Lett. **582**, 2703–2708 (2008).

[259] McManus, K. & Hendzel, M. *ATM-dependent DNA damage-independent mitotic phosphorylation of H2AX in normally growing mammalian cells.* Mol. Biol. Cell **16**, 5013–5025 (2005).

[260] Martín, M., Terradas, M., Hernández, L. & Genescà, A. *$\gamma$H2AX foci on apparently intact mitotic chromosomes: not signatures of misrejoining events but signals of unresolved DNA damage.* Cell Cycle **13**, 3026–36 (2014).

[261] Soutoglou, E. & Misteli, T. *Activation of the cellular DNA damage response in the absence of DNA lesions.* Science **320**, 1507–10 (2008).

[262] Lan, L. et al. *Accumulation of Werner protein at DNA double-strand breaks in human cells.* J. Cell Sci. **118**, 4153–62 (2005).

[263] Hanssen-Bauer, A. et al. *The region of XRCC1 which harbours the three most common nonsynonymous polymorphic variants, is essential for the scaffolding function of XRCC1.* DNA Repair (Amst). **11**, 357–66 (2012).

[264] Tadokoro, T. et al. *Human RECQL5 participates in the removal of endogenous DNA damage.* Mol. Biol. Cell **23**, 4273–85 (2012).

[265] Popuri, V. et al. *Recruitment and retention dynamics of RECQL5 at DNA double strand break sites.* DNA Repair (Amst). **11**, 624–35 (2012).

[266] Bekker-Jensen, S., Lukas, C., Melander, F., Bartek, J. & Lukas, J. *Dynamic assembly and sustained retention of 53BP1 at the sites of DNA damage are controlled by Mdc1/NFBD1.* J. Cell Biol. **170**, 201–11 (2005).

[267] Meldrum, R. A, Botchway, S. W., Wharton, C. W. & Hirst, G. J. *Nanoscale spatial induction of ultraviolet photoproducts in cellular DNA by three-photon near-infrared absorption.* EMBO Rep. **4**, 1144–9 (2003).

[268] Daddysman, M. K. & Fecko, C. J. *DNA multiphoton absorption generates localized damage for studying repair dynamics in live cells. Biophys.* J. **101**, 2294–303 (2011).

[269] Gomez-Godinez, V., Wakida, N. M., Dvornikov, A. S., Yokomori, K. & Berns, M. W. *Recruitment of DNA damage recognition and repair pathway proteins following near-IR femtosecond laser irradiation of cells.* **12**, 1–3 (2007).

[270] Kim, J.-S. et al. *Independent and sequential recruitment of NHEJ and HR factors to DNA damage sites in mammalian cells.* J. Cell Biol. **170**, 341–7 (2005).

[271] Lukas, C., Falck, J., Bartkova, J., Bartek, J. & Lukas, J. *Distinct spatiotemporal dynamics of mammalian checkpoint regulators induced by DNA damage.* Nat. Cell Biol. **5**, 255–60 (2003).

[272] Lukas, C. et al. *Mdc1 couples DNA double-strand break recognition by Nbs1 with its H2AX-dependent chromatin retention.* EMBO J. **23**, 2674–83 (2004).

[273] Bradshaw, P. S., Stavropoulos, D. J. & Meyn, M. S. *Human telomeric protein TRF2 associates with genomic double-strand breaks as an early response to DNA damage.* Nat. Genet. **37**, 193–7 (2005).

[274] Mortusewicz, O., Amé, J.-C., Schreiber, V. & Leonhardt, H. *Feedback-regulated poly(ADP-ribosyl)ation by PARP-1 is required for rapid response to DNA damage in living cells.* Nucleic Acids Res. **35**, 7665–75 (2007).

[275] Mortusewicz, O., Rothbauer, U., Cardoso, M. C. & Leonhardt, H. *Differential recruitment of DNA Ligase I and III to DNA repair sites.* Nucleic Acids Res. **34**, 3523–32 (2006).

[276] Haywood, R. *Relevance of Sunscreen Application Method, Visible Light and Sunlight Intensity to Free-radical Protection: A Study of ex vivo Human Skin.* Photochem. Photobiol. **82**, 1123 (2006).

[277] Maisels, M. J., Ch, B., Mcdonagh, A. F. & Ph, D. *Phototherapy for Neonatal Jaundice.* (2008).

[278] Christensen, J. E., Reitan, J. O. N. B. & Kinn, G. *Single-strand breaks in the DNA of human cells exposed to visible light from phototherapy in the presence and absence of bilirubin.* J. Photochem. Photobiol B. **7**, 337–346 (1990).

[279] Aycicek, A., Kocyigit, A., Erel, O. & Senturk, H. *Phototherapy causes DNA damage in peripheral mononuclear leukocytes in term infants.* J. Pediatr. (Rio. J). **84**, 141–146 (2008).

[280] Kahveci, H. et al. *Phototherapy causes a transient DNA damage in jaundiced newborns.* Drug Chem. Toxicol. **36**, 88–92 (2013).

[281] Ramy, N. et al. *Jaundice, phototherapy and DNA damage in full-term neonates.* J. Perinatol. **36**, 132–6 (2016).

[282] Lisby, M. & Rothstein, R. *Choreography of recombination proteins during the DNA damage response.* DNA Repair (Amst). **8**, 1068–76 (2009).

[283] Tashiro, S., Walter, J., Shinohara, a, Kamada, N. & Cremer, T. *Rad51 accumulation at sites of DNA damage and in postreplicative chromatin.* J. Cell Biol. **150**, 283–91 (2000).

[284] Celeste, A. et al. *Histone H2AX phosphorylation is dispensable for the initial recognition of DNA breaks.* Nat. Cell Biol. **5**, 675–9 (2003).

[285] Bekker-Jensen, S. et al. *Spatial organization of the mammalian genome surveillance machinery in response to DNA strand breaks.* J. Cell Biol. **173**, 195–206 (2006).

[286] Roukos, V. et al. *Dynamic recruitment of licensing factor Cdt1 to sites of DNA damage.* J. Cell Sci. **124**, 422–34 (2011).

[287] Kruhlak, M. et al. *The ATM repair pathway inhibits RNA polymerase I transcription in response to chromosome breaks.* Nature **447**, 730–4 (2007).

[288] Mortusewicz, O. et al. *Recruitment of RNA polymerase II cofactor PC4 to DNA damage sites.* J. Cell Biol. **183**, 769–76 (2008).

[289] Godon, C. et al. *PARP inhibition versus PARP-1 silencing: different outcomes in terms of single-strand break repair and radiation susceptibility.* Nucleic Acids Res. **36**, 4454–64 (2008).

[290] Baldeyron, C., Soria, G., Roche, D., Cook, A. J. L. & Almouzni, G. *HP1$\alpha$ recruitment to DNA damage by p150CAF-1 promotes homologous recombination repair.* J. Cell Biol. **193**, 81–95 (2011).

[291] Bolin, C. et al. *The impact of cyclin-dependent kinase 5 depletion on poly(ADP-ribose) polymerase activity and responses to radiation.* Cell. Mol. Life Sci. **69**, 951–62 (2012).

[292] Abdou, I., Poirier, G. G., Hendzel, M. J. & Weinfeld, M. *DNA ligase III acts as a DNA strand break sensor in the cellular orchestration of DNA strand break repair.* Nucleic Acids Res. **43**, 875–92 (2015).

[293] Chen, B. P. C. et al. *Cell cycle dependence of DNA-dependent protein kinase phosphorylation in response to DNA double strand breaks.* J. Biol. Chem. **280**, 14709–15 (2005).

[294] Zielinska, A., Davies, O. T., Meldrum, R. a & Hodges, N. J. *Direct visualization of repair of oxidative damage by OGG1 in the nuclei of live cells*. J. Biochem. Mol. Toxicol. **25**, 1–7 (2011).

[295] Inagaki, A. et al. *Dynamic localization of human RAD18 during the cell cycle and a functional connection with DNA double-strand break repair*. DNA Repair (Amst). **8**, 190–201 (2009).